Green-light-sensitive BODIPY photoprotecting groups for amines

Supporting information

Kaja Sitkowska[a,b] Ben. L. Feringa[a]* Wiktor Szymański[a,c]*

[a] Centre for Systems Chemistry, Stratingh Institute for Chemistry,

University of Groningen, Nijenborgh 4, 9747 AG, Groningen, The Netherlands.

[b] University of Warsaw, Faculty of Chemistry, Pasteura 1, 02-093 Warsaw, Poland

[c] Department of Radiology, University of Groningen, University Medical Center

Groningen, Hanzeplein 1, 9713 GZ, Groningen, The Netherlands.

Contents

1. Synthesis optimization tables

1.1. Hydrolysis of Acetoxy BODIPY **1**

Figure S1. Hydrolysis of BODIPY 1

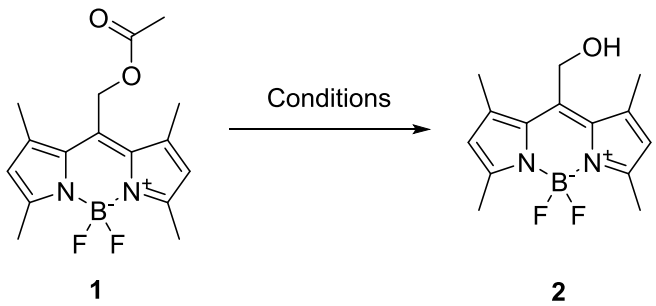

Table S1. Hydrolysis of BODIPY 1

nr	Reagents	Temp. [°C]	Yield
1	LiOH, THF, H_2O	23	Decomposition
2	LiOH, THF, H_2O + sonication	23	Decomposition
3	K_2CO_3, MeOH	23	64% in 2 d
4	NaOH, MeOH, H_2O	23	73% in 2h
5	BF_3xEt_2O, AcCN	0 to 23	No reaction
6	TBAH, NaOH, THF	23	No reaction
7	HCl, acetone	40	Decomposition
8	Sm, I_2, MeOH/THF	23	< 20% (3 d)

1.2. Formation of carbonates

Figure S2. Carbonate formation reaction.

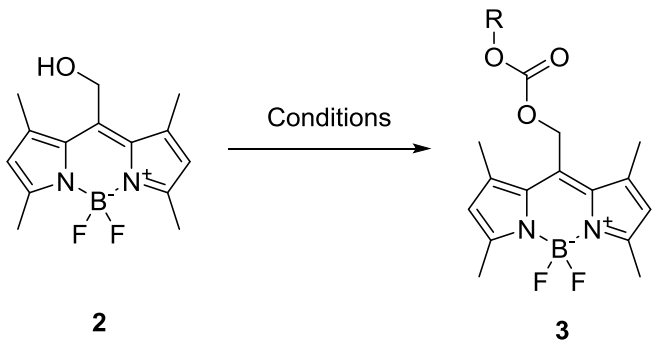

Table S2. Carbonate formation reaction.

nr	Base	Base eq.	R	Cl eq.	Additives	Time	Yield	Other
1	DIPEA	1	$PhNO_2$	1	DMAP cat.	24h	0, considerable decomposition	-
2	NaH	1	Me	1	-	24h	<20%	NaH in mineral oil
3	NaH	1	Me	1	DMAP cat.	24h	<20%	NaH in mineral oil
4	-	1	Me	1	-	24h	0	-
5	NaH	1	Me	1	Et_3N cat.	24h	0	-
6	NaH	1	Me	1	-	24h	<20%	-
7	LDA	1	Me	1	-	5 min	0, instant decomposition	0°C
8	n-BuLi	1	Me	1	-	5 min	0, instant decomposition	0°C
9	t-BuLi	1	Me	1	-	5 min	0, instant decomposition	0°C
10	NaH	1	Me	1	-	24h	0	0°C
11	t-BuOK	1	Me	1	-	24h	0	-
12	LDA	1	$PhNO_2$	1	-	5 min	0, instant decomposition	0°C
13	n-BuLi	1	$PhNO_2$	1	-	5 min	0, instant decomposition	0°C
14	t-BuLi	1	$PhNO_2$	1	-	5 min	0, instant decomposition	0°C
15	NaH	1	$PhNO_2$	1	-	24h	0, decomposition	0°C
16	LDA	1	Me	1	-	5 min	0, instant decomposition	-78°C

17	n-BuLi	1	Me	1	-	5 min	0, instant decomposition	-78°C
18	t-BuLi	1	Me	1	-	5 min	0, instant decomposition	-78°C
19	NaH	1	Me	1	-	24h	0	-78°C
20	t-BuOK	1	Me	1	-	24h	0	-78°C
21	LDA	1	$PhNO_2$	1	-	24h	0, decomposition	-78°C
22	n-BuLi	1	$PhNO_2$	1	-	24h	0, decomposition	-78°C
23	t-BuLi	1	$PhNO_2$	1	-	24h	0, decomposition	-78°C
24	NaH	1	$PhNO_2$	1	-	24h	0, decomposition	-78°C
25	NaH	1	Me	1.2	-	5 min	40%	mixed in an open vial, NaH in mineral oil
26	NaH	1	$PhNO_2$	1.2	-	5 min	0, decomposition	mixed in an open vial, NaH in mineral oil
27	NaH	1.2	Bz	1.6	DMAP cat. after 3h	24h	<20%	-
28	NaH	1.2	Ph	1.6	DMAP cat. after 3h	24h	<20%	-
29	NaH	1.2	PhCl	1.6	DMAP cat. after 3h	24h	<20%	-
30	NaH	1.2	PhMe	1.6	DMAP cat. after 3h	24h	<20%	-
31	NaH	1.2	1ClEt	1.6	DMAP cat. after 3h	24h	<20%	-
32	NaH	1.2	$PhNO_2$	1.6	DMAP cat. after 3h	24h	<20%	-
33	NaH	1.2	Me	1.6	DMAP cat. after 3h	24h	<20%	-
34	NaH	1.2	Me	1.6	DMAP cat. after 3h	24h	<20%	-
35	-	-	Me	1.6	DMAP cat. after 3h	24h	0	-
36	NaH	1	Me	1.1	-	5 min	16%	bigger scale
37	NaH	1.2	Me	1.6	-	5 min	<20%	quick addition

38	-	-	Me	1.1	DMAP 1 eq.	2 d	trace amounts of product	-
39	-	-	Me	1.1	DMAP 0.1 eq., DIPEA 1 eq.	3 d	trace amounts of product	-
40	NaH	1.1	Me	1.1	DMAP 1 eq.	4 d	trace amounts of product	-
41	NaH	1.1	Me	1.1	DMAP 0.1 eq., DIPEA 1 eq.	5 d	trace amounts of product	-
42	-	-	$PhNO_2$	4	DMAP 4 eq.	3h	37%	added **2** in last step,
43	-	-	$PhNO_2$	4	DMAP 4 eq. C=1M	3h	62%	added **2** in last step, 0°C
44	DIPEA	5	$PhNO_2$	4	pyridine 4 eq. C=1M	3h	79%	Suspension of chloroformate/ pyridine added to BOH at 0°C

1.3. Halogenation of carbonates

Figure S3. Halogenation of carbonates

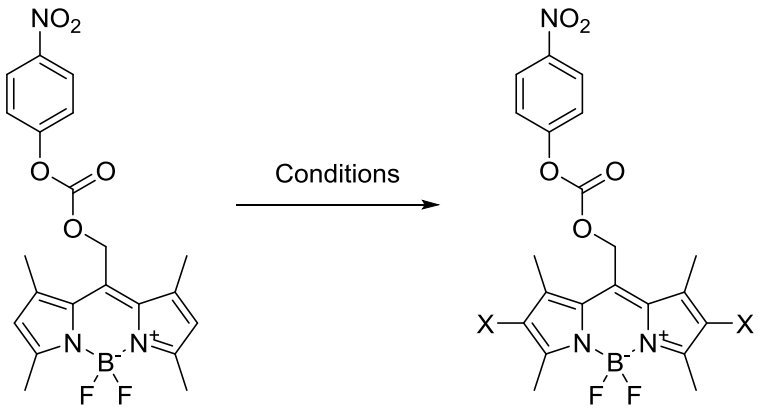

3 **4**, **5**, **6**

Table S3. Halogenation of carbonates

Nr	Solvent	Time	Temp. [°C]	Yield [%]	Reagent	Other	X
1	THF	2 h	-78	90	NBS 2.5 eq.	-	Br
2	THF	2 h	0	90	NBS 2.5 eq.	-	Br
3	THF	2 h	23	90	NBS 2.5 eq.	-	Br
4	THF	2 h	-78	80	NBS 2.5 eq.	-	Br
5	THF	2 h	0	80	NBS 2.5 eq.	-	Br
6	THF	2 h	23	80	NBS 2.5 eq.	-	Br
7	DCM	2 h	23	75	NBS 2.5 eq.	-	Br
8	THF	overnight	23	N.A.	NCS 2.5 eq.	-	Cl
9	THF	overnight	23	N.A.	NCS 5 eq.	-	Cl
10	THF	overnight	23	N.A.	NCS 6 eq.	-	Cl
11	THF	overnight	23	90	NCS 10 eq.	-	Cl
12	THF	overnight	23	N.A.	NIS 2.5 eq.	-	I
13	THF	overnight	23	N.A.	NIS 5 eq.	-	I
14	THF	overnight	23	N.A.	NIS 6 eq.	-	I
15	THF	overnight	23	80	NIS 10 eq.	-	I
16	THF	overnight	0	55	ICl 3 eq.	-	I
17	DCM	overnight	0	45	ICl 3 eq.	-	I
18	THF	overnight	0	92	ICl 3 eq., ZnO 3.6 eq.	-	I
19	DCM	overnight	0	90	ICl 3 eq., ZnO 3.6 eq.	-	I
20	THF	5 min	0	95	ICl 3 eq., ZnO 3.6 eq.	-	I
21	THF	10 min	23	96	NBS 5 eq.	-	Br
22	THF	3 d	23	85	NCS 5 eq. x2	-	Cl

23	THF	overnight	23	0	NCS 5 eq.	65°C for 20 min	Cl
24	THF	overnight	23	0	NCS 5 eq.	30 min UV	Cl

1.4. Formation of carbamates

Figure S4. Formation of carbamates.

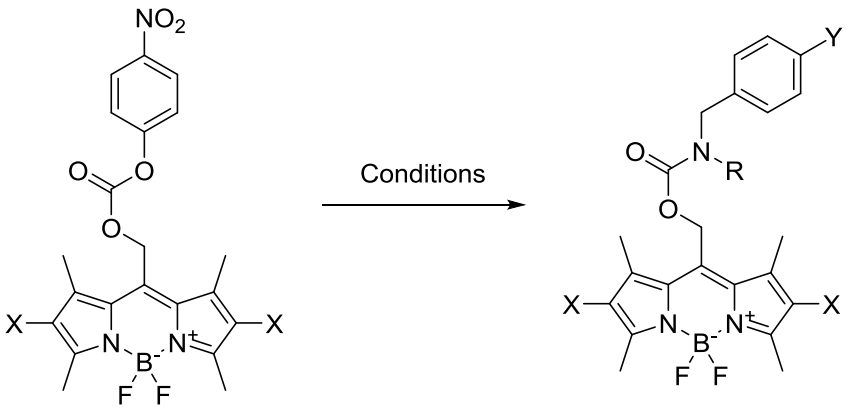

4, 5, 6 **7 - 14**

Table S4. Formation of carbamates.

Nr	Solvent	Time	Yield [%]	Base	Other reagents	X,Y,R
1	THF	overnight	70	pyridine 1 eq.	-	H, F, H
2	THF	overnight	20	pyridine 0.25 eq.	-	Br, F, H
3	THF	overnight	10	pyridine 0.25 eq.	-	H, F, H
4	DCM	overnight	20	pyridine 1 eq.	HOBt 1eq.	Br, F, Me
5	THF	overnight	30	pyridine 1 eq.	HOBt 1eq.	Br, F, Me
6	THF	overnight	30	pyridine 1 eq.	DMAP 1 eq.	Br, F, Me
7	THF	overnight	30	pyridine 1 eq.	COMU 1 eq.	Br, F, Me
8	THF	overnight	30	pyridine 1 eq.	HATU 1 eq.	Br, F, Me
9	THF	overnight	30	pyridine 1 eq.	EDCI 1 eq.	Br, F, Me
10	THF	overnight	30	pyridine 1 eq.	-	Br, F, Me
11	DCM	overnight	20	pyridine 1 eq.	EDCI 1 eq.	Br, H, H
12	toluene	overnight	0	pyridine 1 eq.	-	Br, H, H
13	DCM	overnight	0	pyridine 1 eq.	$Yb(SO_3CF_3)3$ 0.25 eq.	I, F, Me
14	DMSO	1 h	0	pyridine 1 eq.	-	I, F, Me
15	DMF	1 h	0	pyridine 1 eq.	-	I, F, Me
16	MeOH	1 h	10	pyridine 1 eq.	-	I, F, Me
17	tHF	2 h	60	pyridine 1 eq.	-	I, F, H
18	THF	3 h	85	pyridine 1 eq.	-	H, F, H
19	THF	4 h	80	pyridine 1 eq.	-	H,F, Me
20	THF	4 h	30	pyridine 1 eq.	-	Br, F, Me

2. Studies on the deprotection of compounds **7**-**14** in aqueous media

2.1. UV-VIS studies

Samples of compounds **7**-**14,** 20 µM in 20% DMSO / 5 mM phosphate buffer pH = 7.5 were irradiated with light of λ = 530 nm for 10 min. UV-Vis spectra were recorded every 30 s. Half – lives of the compounds were calculated by monoexponential fitting.

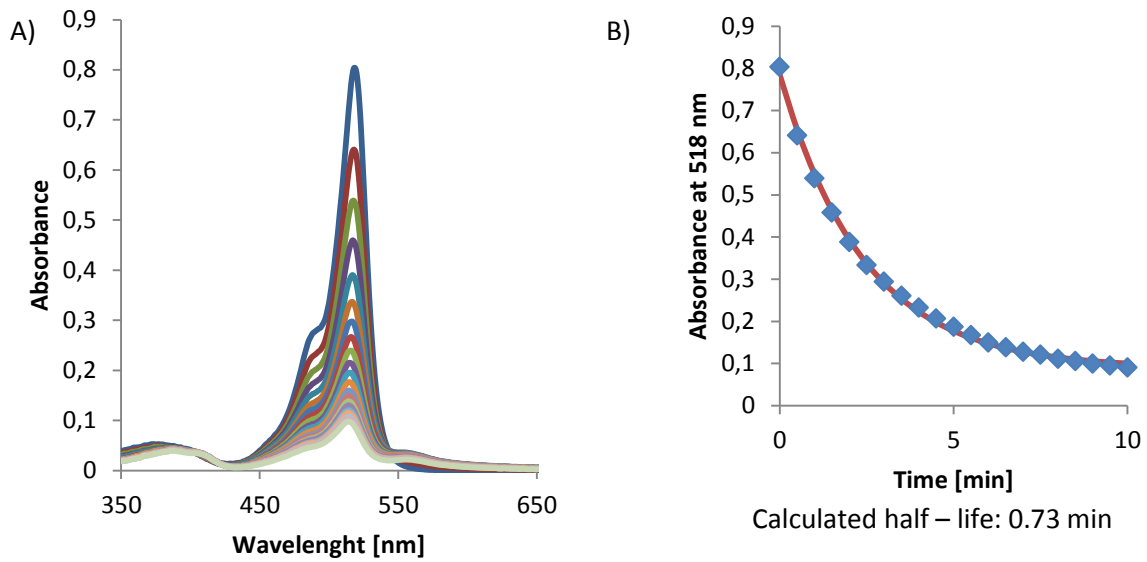

Figure S5. UV-VIS spectra of photodeprotection of compound **7** (20 µmol in 20% DMSO / 5 mmol phosphate buffer pH = 7.5) using λ = 530 nm: A) spectra (measured every 30 s), B) absorbance at 518 nm with monoexponential fitting.

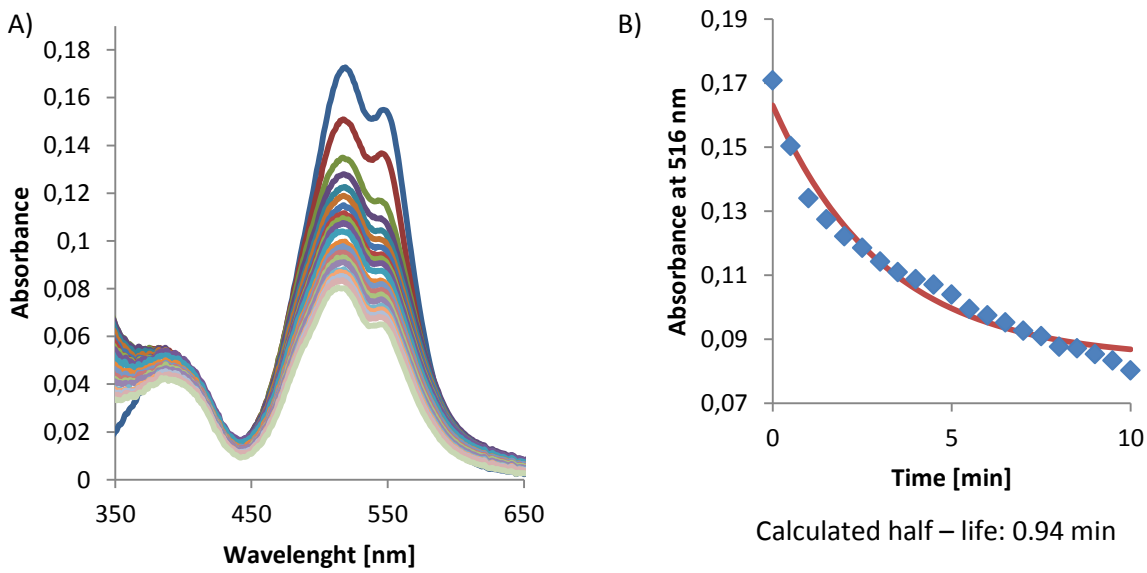

Figure S6. UV-VIS spectra of photodeprotection of compound **8** (20 µmol in 20% DMSO / 5 mmol phosphate buffer pH = 7.5) using λ = 530 nm: A) spectra (measured every 30 s), B) absorbance at 516 nm with monoexponential fitting.

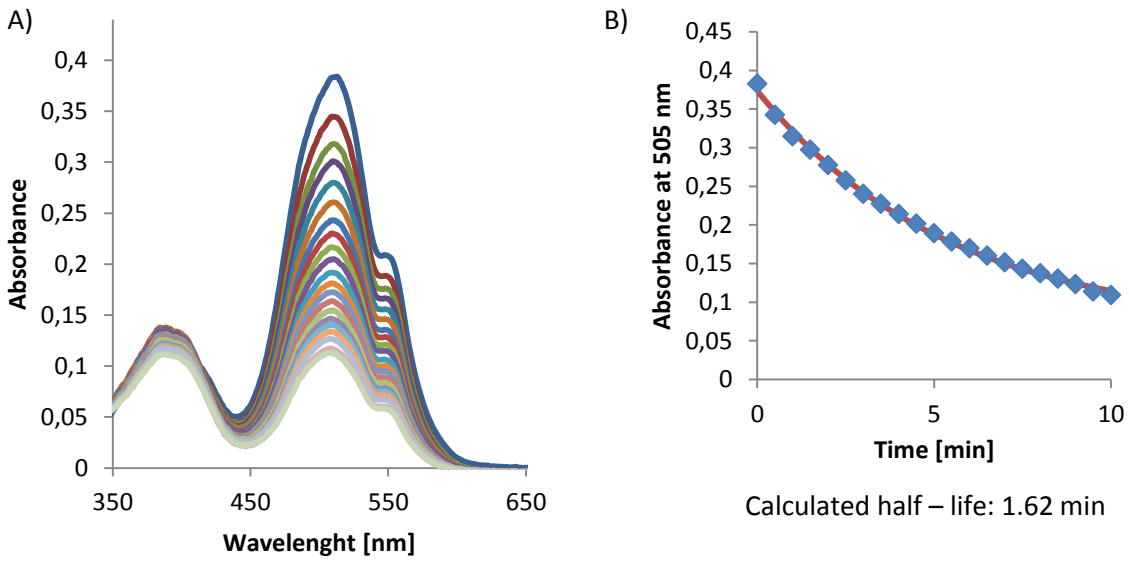

Figure S7. UV-VIS spectra of photodeprotection of compound **9** (20 µmol in 20% DMSO / 5 mmol phosphate buffer pH = 7.5) using λ = 530 nm: A) spectra (measured every 30 s), B) absorbance at 505 nm with monoexponential fitting.

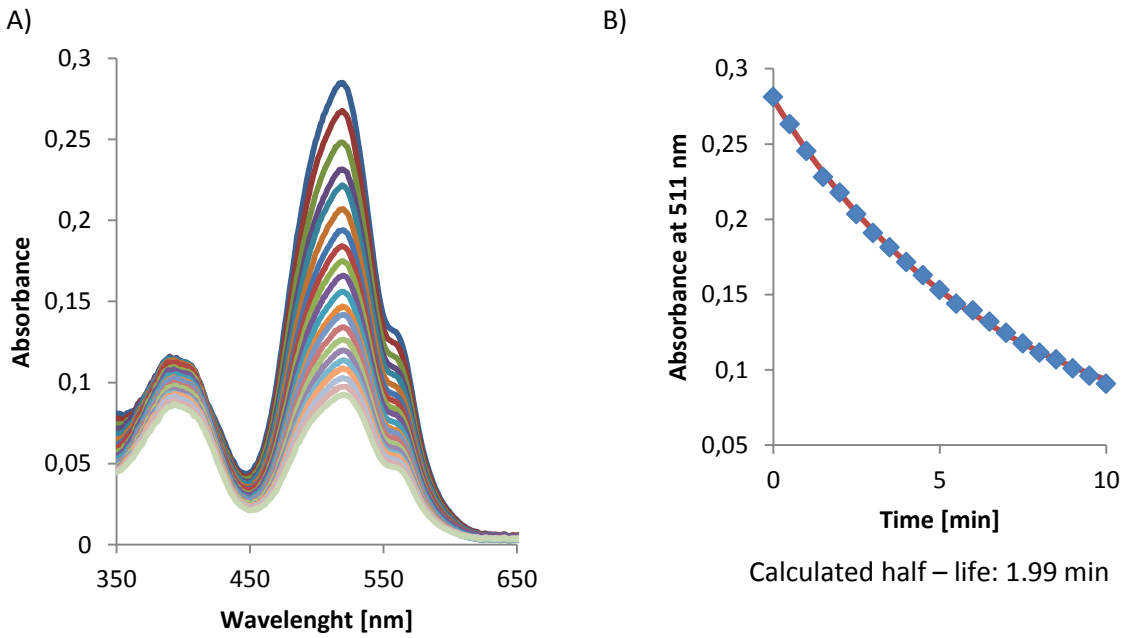

Figure S8. UV-VIS spectra of photodeprotection of compound **10** (20 µmol in 20% DMSO / 5 mmol phosphate buffer pH = 7.5) using λ = 530 nm: A) spectra (measured every 30 s), B) absorbance at 505 nm with monoexponential fitting.

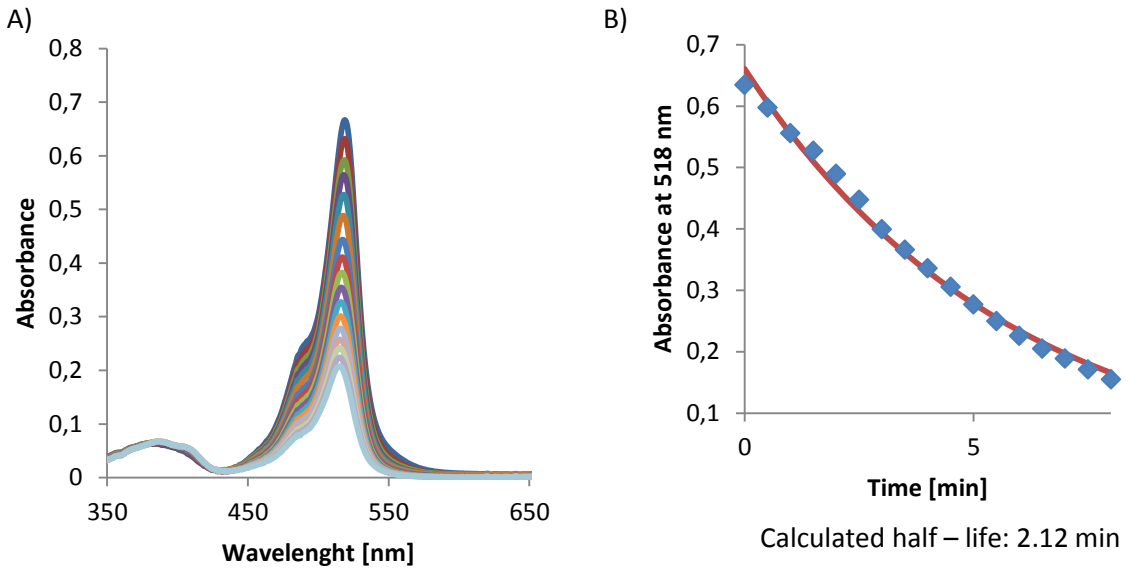

Figure S9. UV-VIS spectra of photodeprotection of compound **11** (20 µmol in 20% DMSO / 5 mmol phosphate buffer pH = 7.5) using λ = 530 nm: A) spectra (measured every 30 s), B) absorbance at 505 nm with monoexponential fitting.

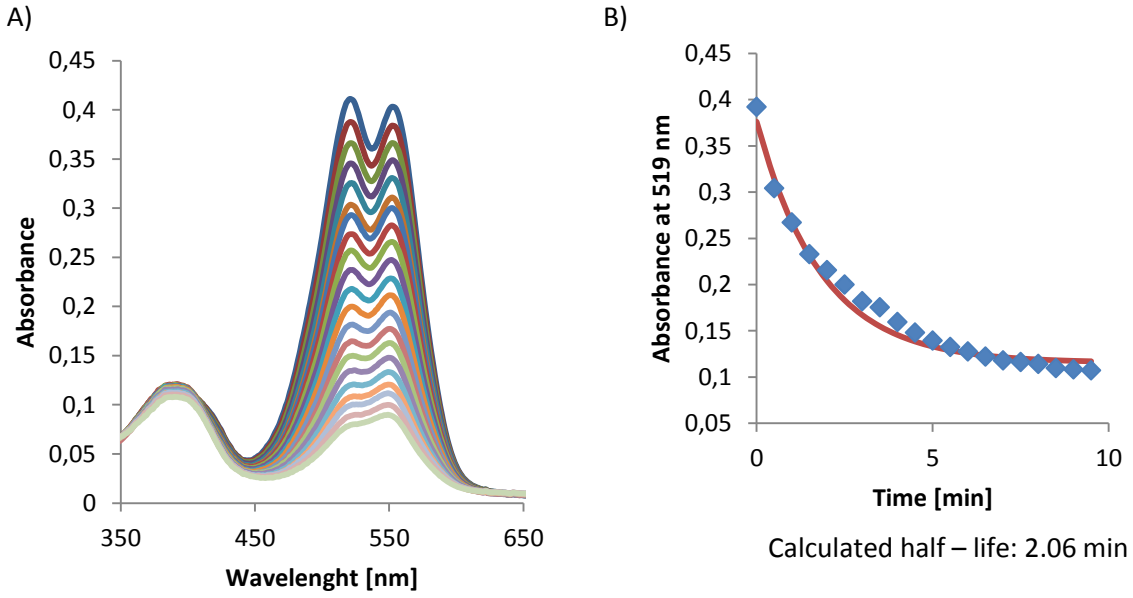

Figure S10. UV-VIS spectra of photodeprotection of compound **12** (20 µmol in 20% DMSO / 5 mmol phosphate buffer pH = 7.5) using λ = 530 nm: A) spectra (measured every 30 s), B) absorbance at 505 nm with monoexponential fitting.

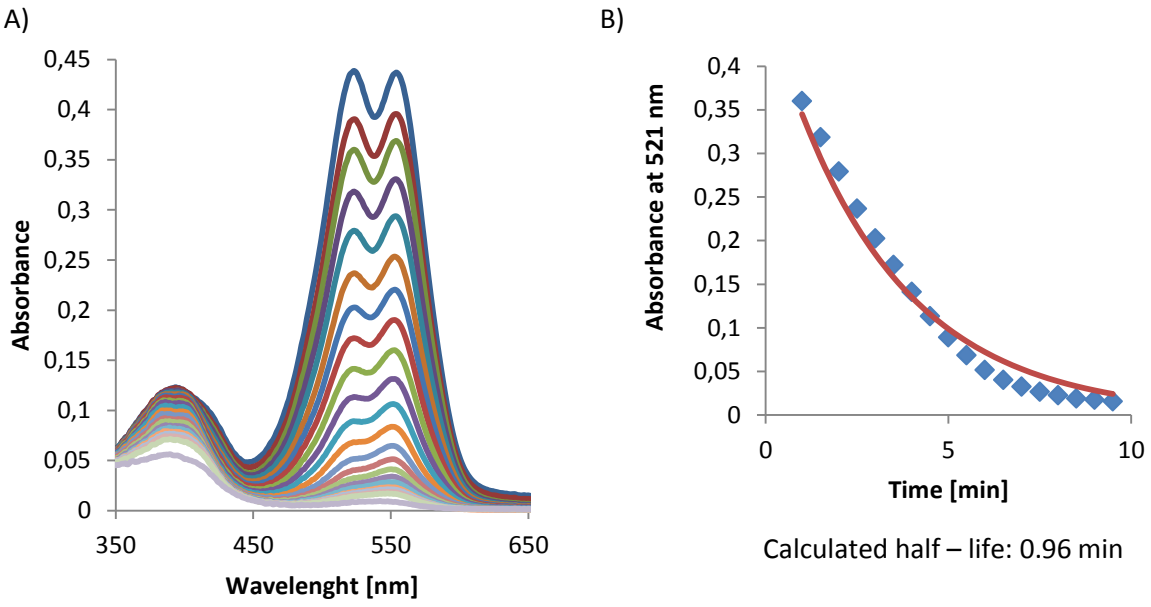

Figure S11. UV-VIS spectra of photodeprotection of compound **13** (20 µmol in 20% DMSO / 5 mmol phosphate buffer pH = 7.5) using λ = 530 nm: A) spectra (measured every 30 s), B) absorbance at 505 nm with monoexponential fitting.

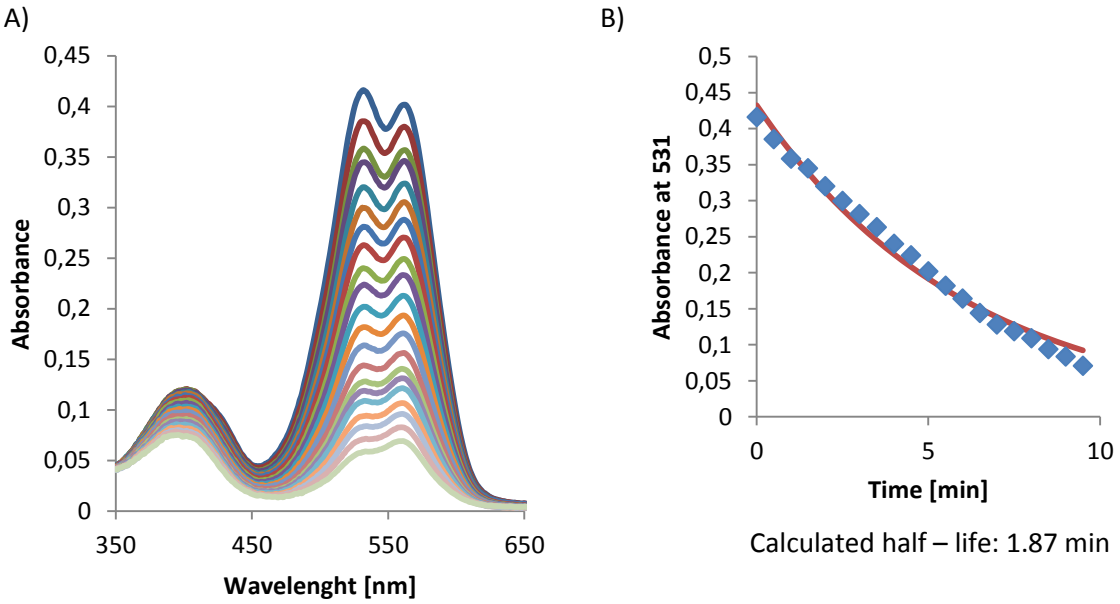

Figure S12. UV-VIS spectra of photodeprotection of compound **14** (20 µmol in 20% DMSO / 5 mmol phosphate buffer pH = 7.5) using λ = 530 nm: A) spectra (measured every 30 s), B) absorbance at 505 nm with monoexponential fitting.

For determining the extinction coefficient, samples of compounds **7**-**14,** 20, 10, 5, 2.5 and 1.25 µM in 20% DMSO in 5 mM phosphate buffer pH = 7.5 were prepared and UV-VIS spectra were taken. The coefficients were obtained using Lambert-Beer law.

(5,5-difluoro-1,3,7,9-tetramethyl-5H-4λ^4,5λ^4-dipyrrolo[1,2-c:2',1'-f][1,3,2]diazaborinin-10-yl)methyl (4-fluorophenyl)carbamate (**7**)

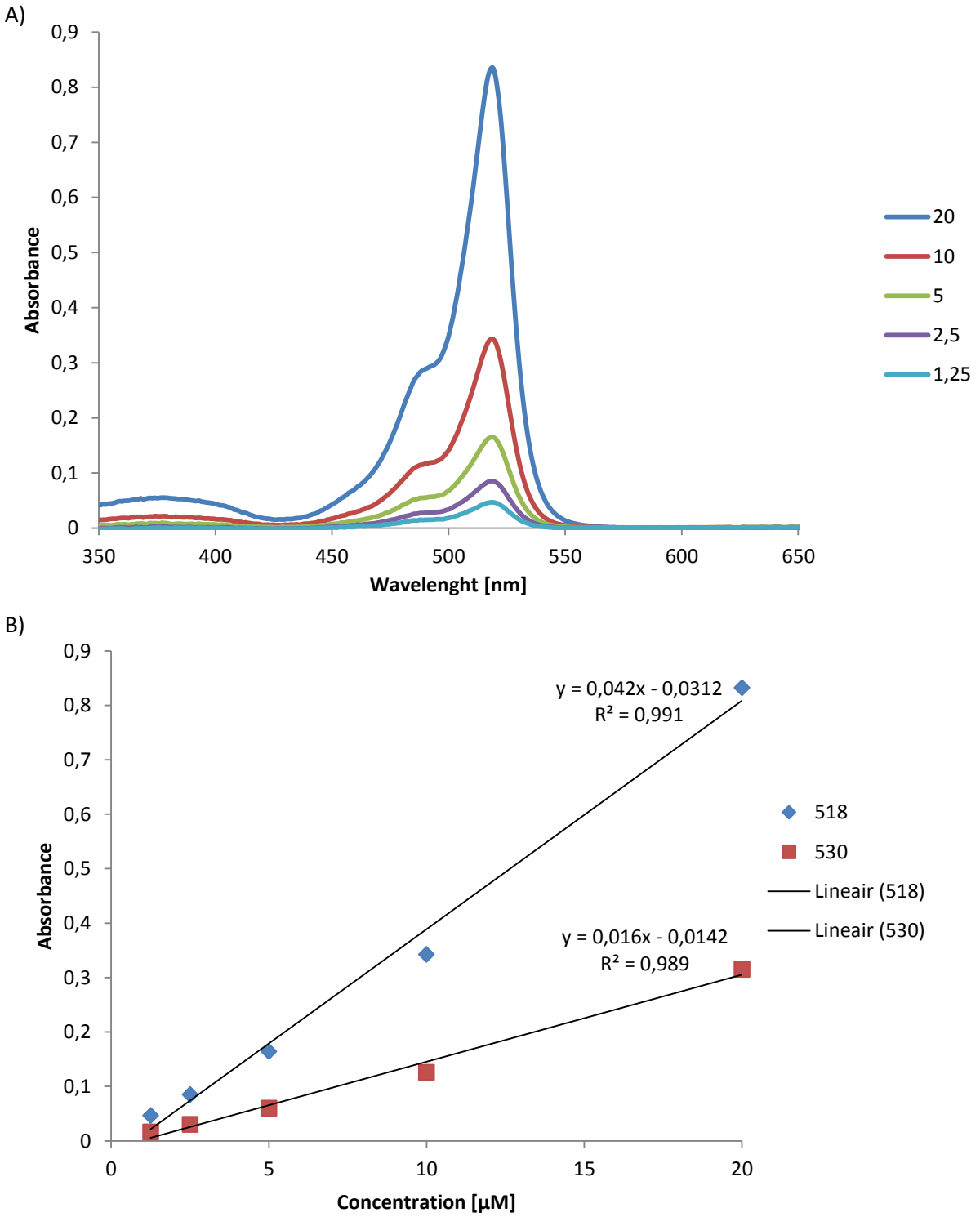

Figure S13. A) UV-VIS spectra of compound **7** in different concentrations (legend in µM); B) linear dependence of Absorbance of the compound of its concentration at λ_{max} and λ = 530 nm

(2,8-dichloro-5,5-difluoro-1,3,7,9-tetramethyl-5H-4λ^4,5λ^4-dipyrrolo[1,2-c:2',1'-f][1,3,2]diazaborinin-10-yl)methyl (4-fluorobenzyl)carbamate (**8**)

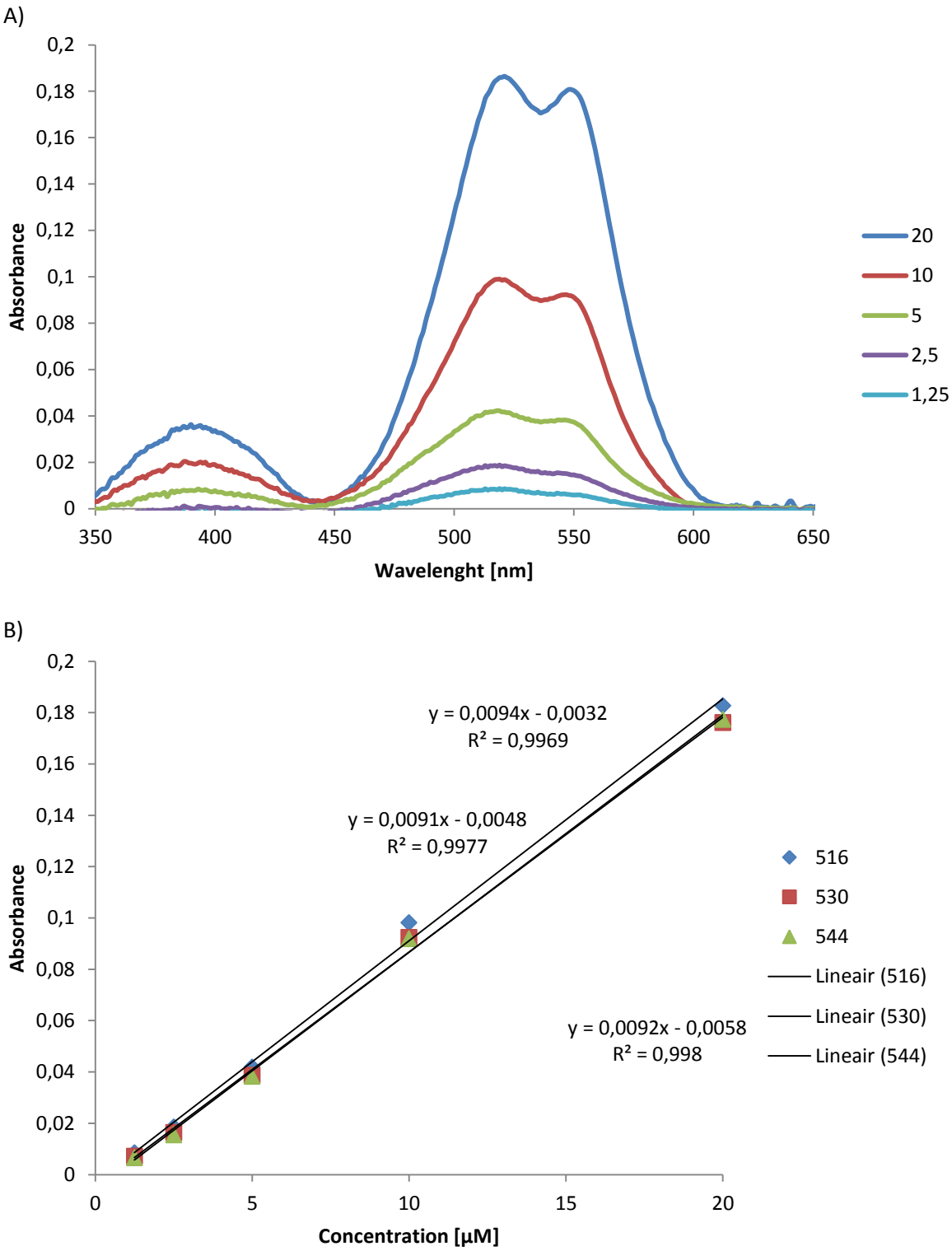

Figure S14. A) UV-VIS spectra of compound **8** in different concentrations (legend in µM); B) linear dependence of Absorbance of the compound of its concentration at λ_{max} and λ = 530 nm

(2,8-dibromo-5,5-difluoro-1,3,7,9-tetramethyl-5H-4λ^4,5λ^4-dipyrrolo[1,2-c:2',1'-f][1,3,2]diazaborinin-10-yl)methyl (4-fluorobenzyl)carbamate (**9**)

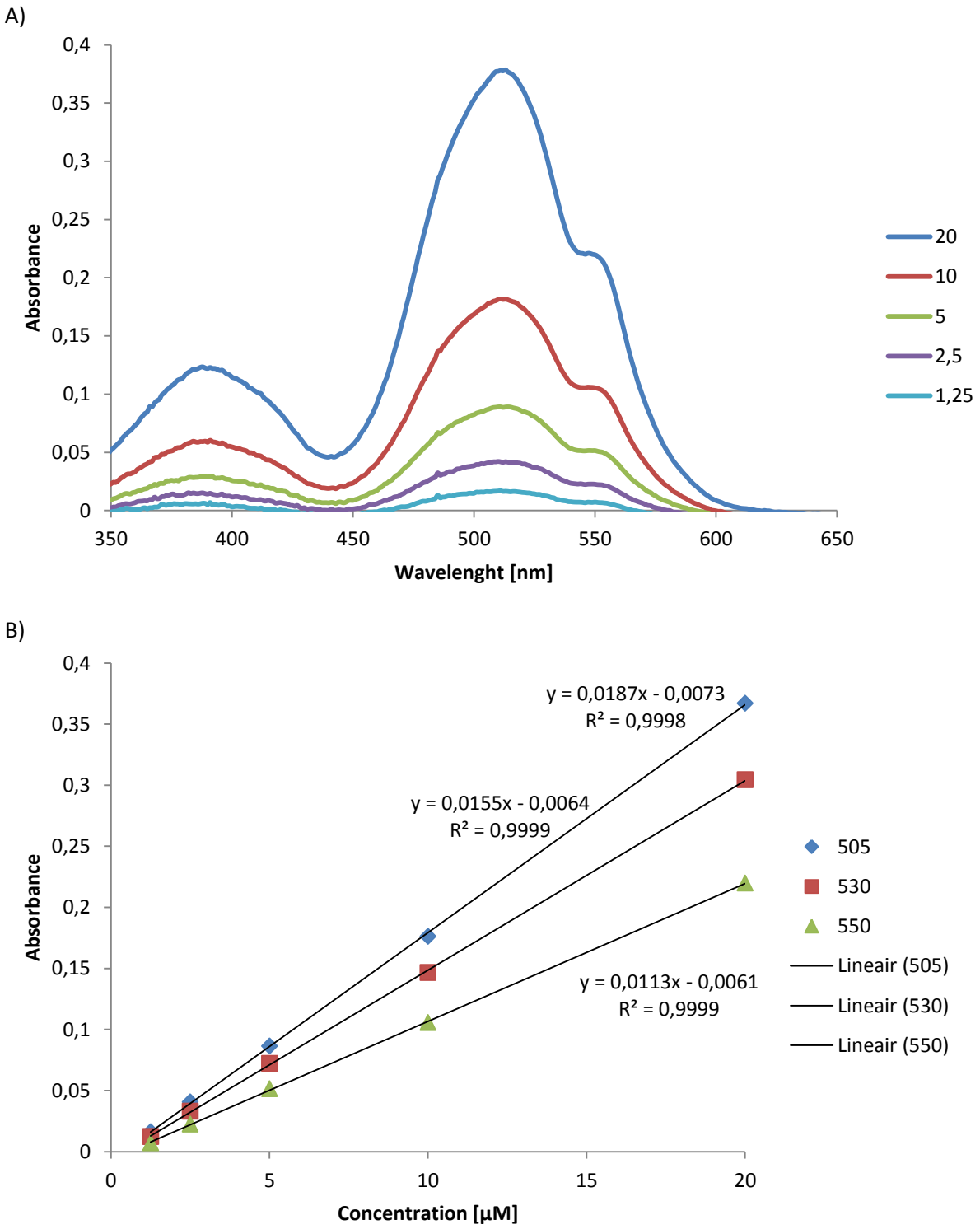

Figure S15. A) UV-VIS spectra of compound **9** in different concentrations (legend in µM); B) linear dependence of Absorbance of the compound of its concentration at λ_{max} and λ = 530 nm

(2,8-diiodo-5,5-difluoro-1,3,7,9-tetramethyl-5H-4λ^4,5λ^4-dipyrrolo[1,2-c:2',1'-f][1,3,2]diazaborinin-10-yl)methyl (4-fluorobenzyl)carbamate (**10**)

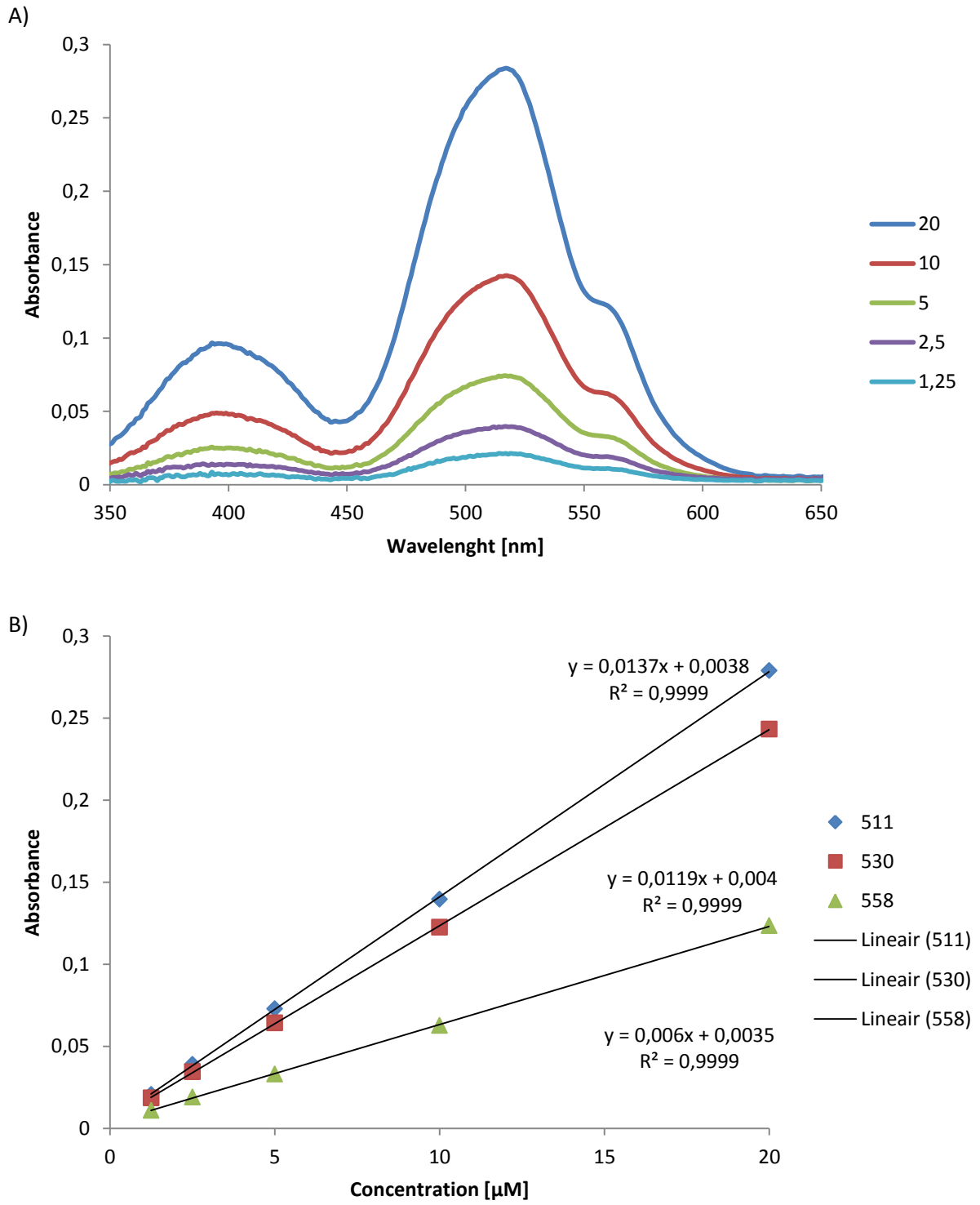

Figure S16. A) UV-VIS spectra of compound **10** in different concentrations (legend in µM); B) linear dependence of Absorbance of the compound of its concentration at λ_{max} and λ = 530 nm

(5,5-difluoro-1,3,7,9-tetramethyl-5H-4λ^4,5λ^4-dipyrrolo[1,2-c:2',1'-f][1,3,2]diazaborinin-10-yl)methyl (4-fluorobenzyl)(methyl)carbamate (**11**)

A)

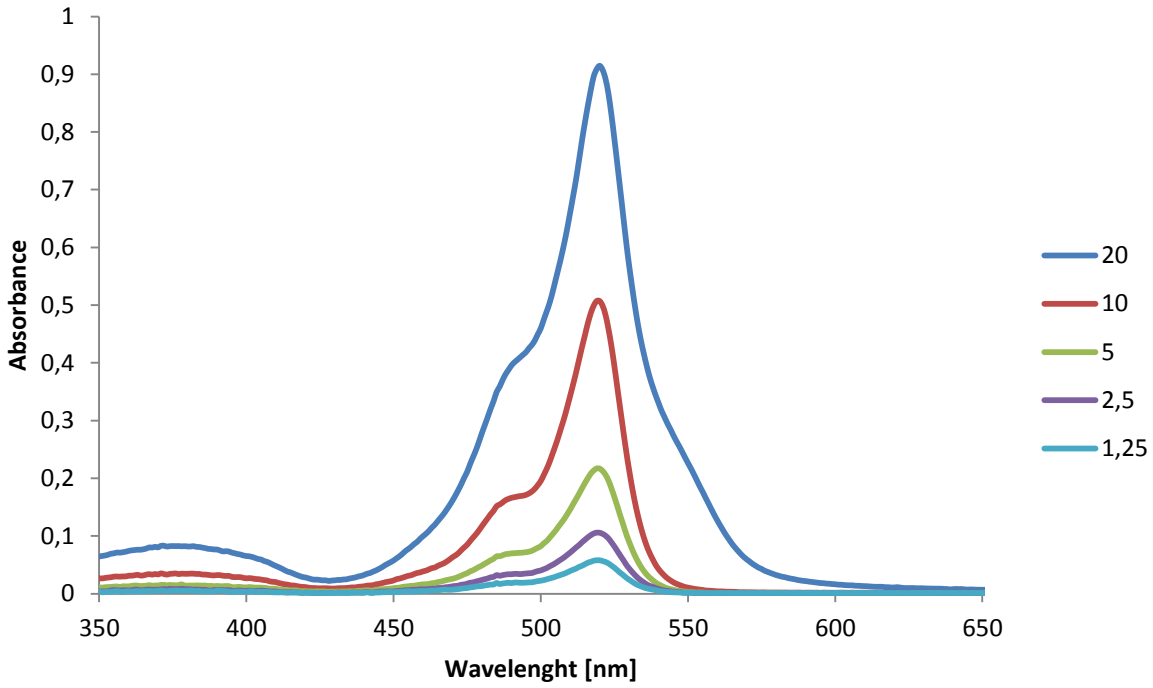

B)

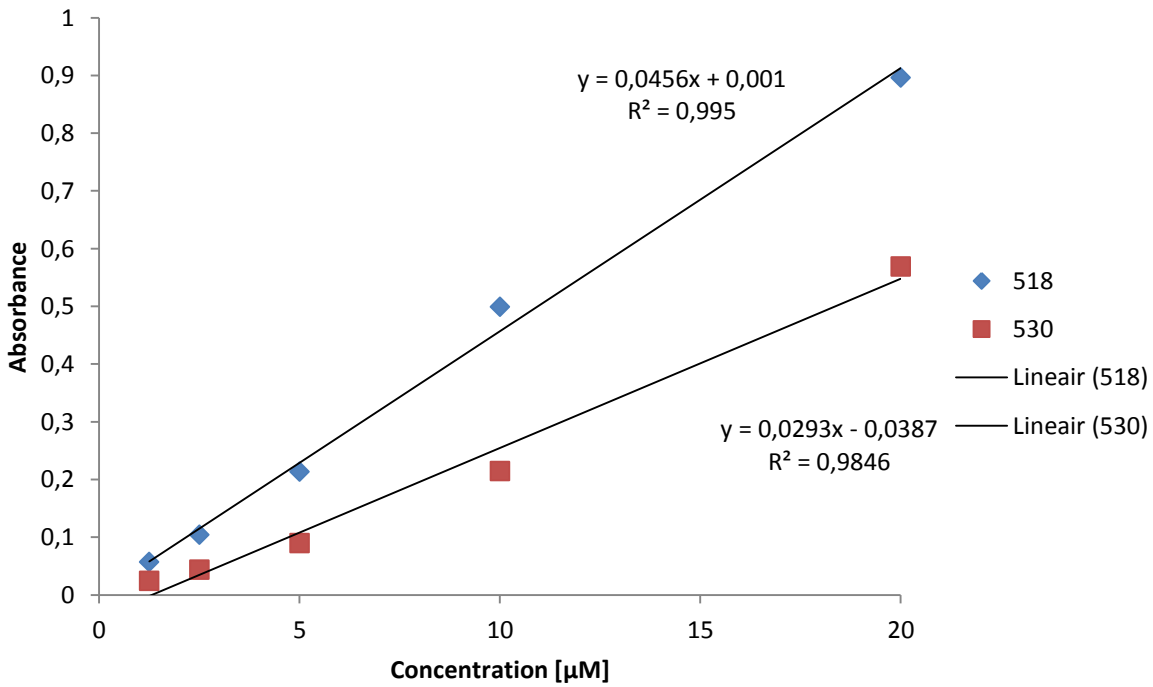

Figure S17. A) UV-VIS spectra of compound **11** in different concentrations (legend in µM); B) linear dependence of Absorbance of the compound of its concentration at λ_{max} and λ = 530 nm

(2,8-dichloro-5,5-difluoro-1,3,7,9-tetramethyl-5H-4λ^4,5λ^4-dipyrrolo[1,2-c:2',1'-f][1,3,2]diazaborinin-10-yl)methyl (4-fluorobenzyl)(methyl)carbamate (**12**)

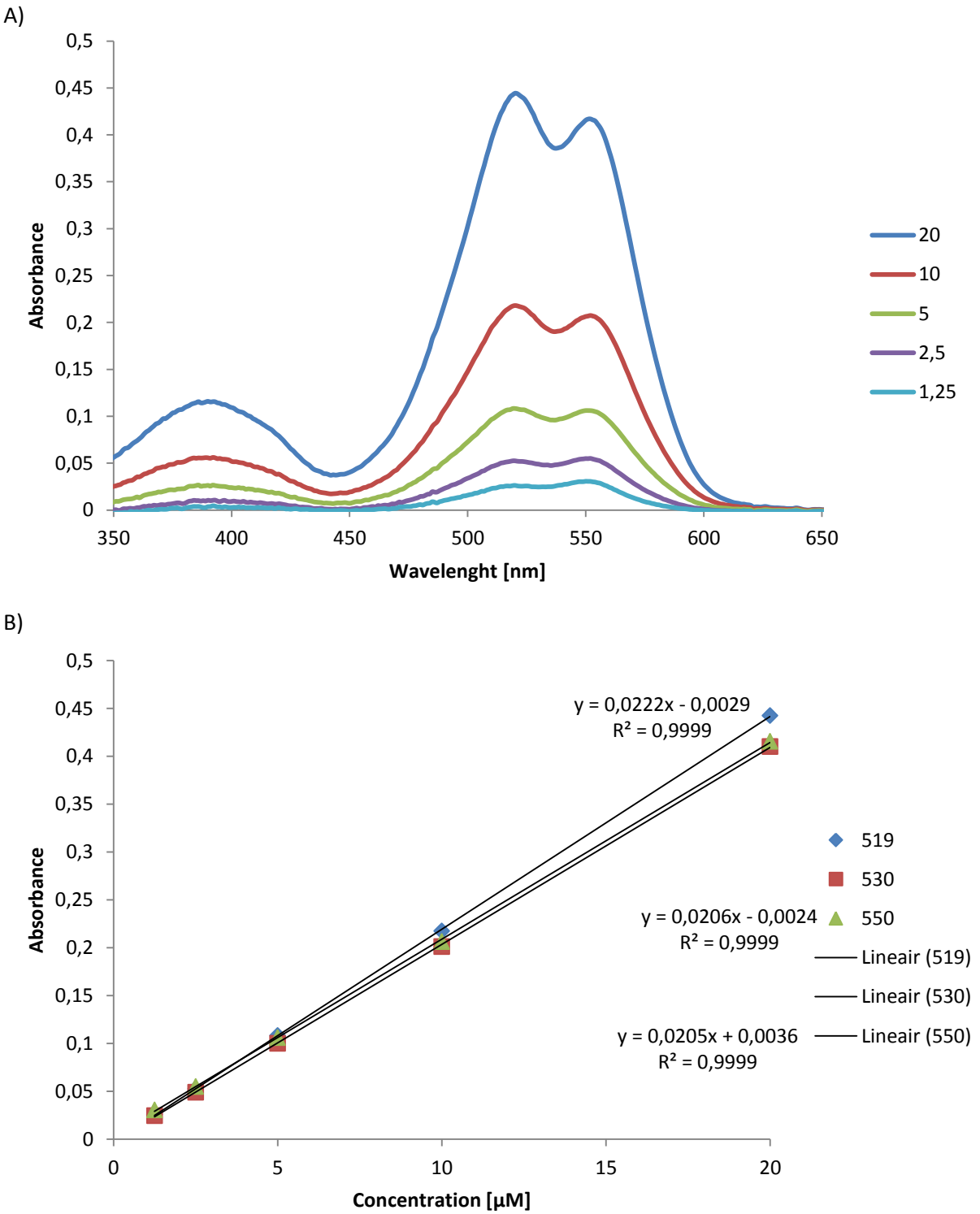

Figure S18. A) UV-VIS spectra of compound **12** in different concentrations (legend in µM); B) linear dependence of Absorbance of the compound of its concentration at λ_{max} and λ = 530 nm

(2,8-dichloro-5,5-difluoro-1,3,7,9-tetramethyl-5H-4λ^4,5λ^4-dipyrrolo[1,2-c:2',1'-f][1,3,2]diazaborinin-10-yl)methyl (4-fluorobenzyl)(methyl)carbamate (**13**)

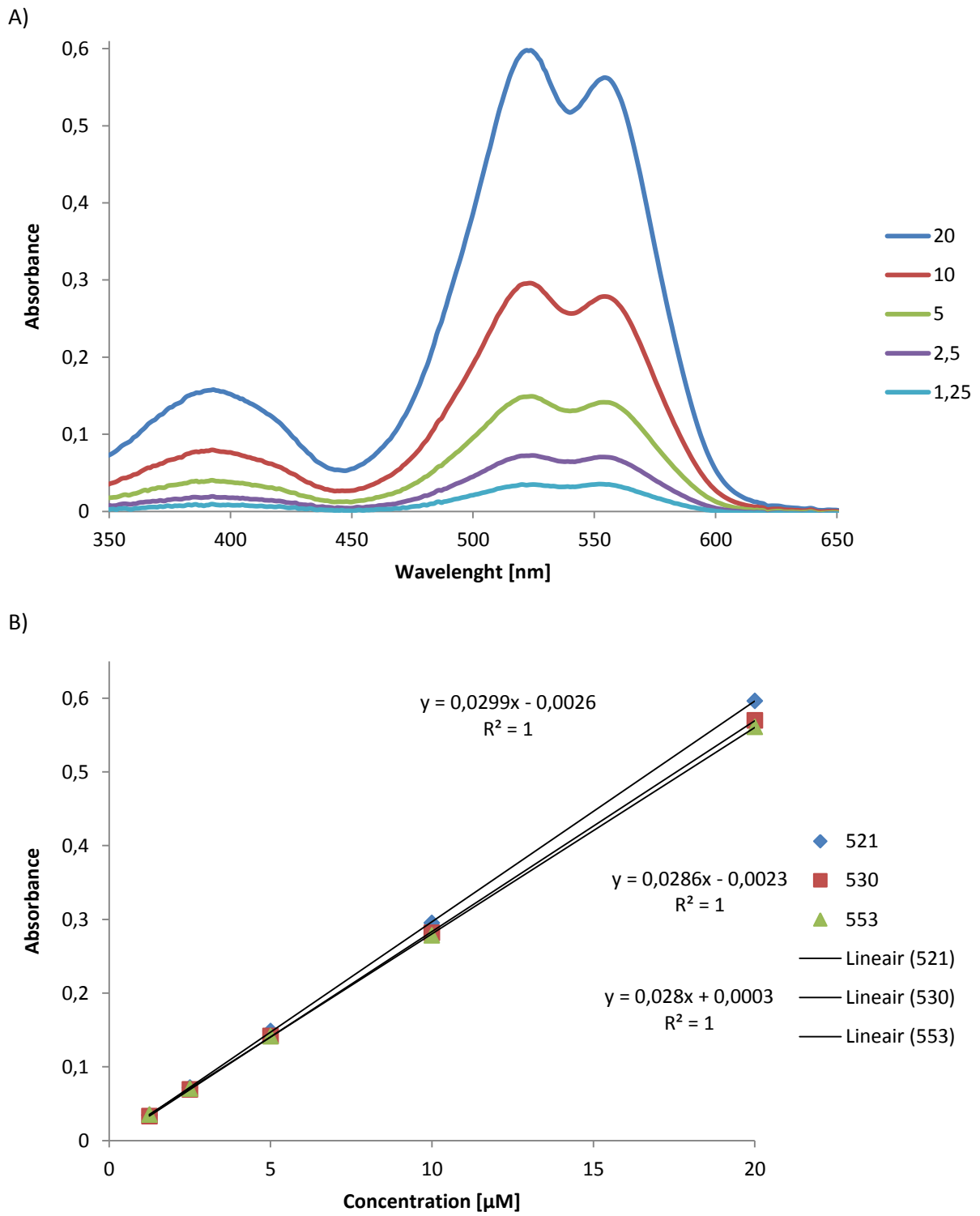

Figure S19. A) UV-VIS spectra of compound **13** in different concentrations (legend in µM); B) linear dependence of Absorbance of the compound of its concentration at λ_{max} and λ = 530 nm

(2,8-dichloro-5,5-difluoro-1,3,7,9-tetramethyl-5H-4λ^4,5λ^4-dipyrrolo[1,2-c:2',1'-f][1,3,2]diazaborinin-10-yl)methyl (4-fluorobenzyl)(methyl)carbamate (**14**)

A)

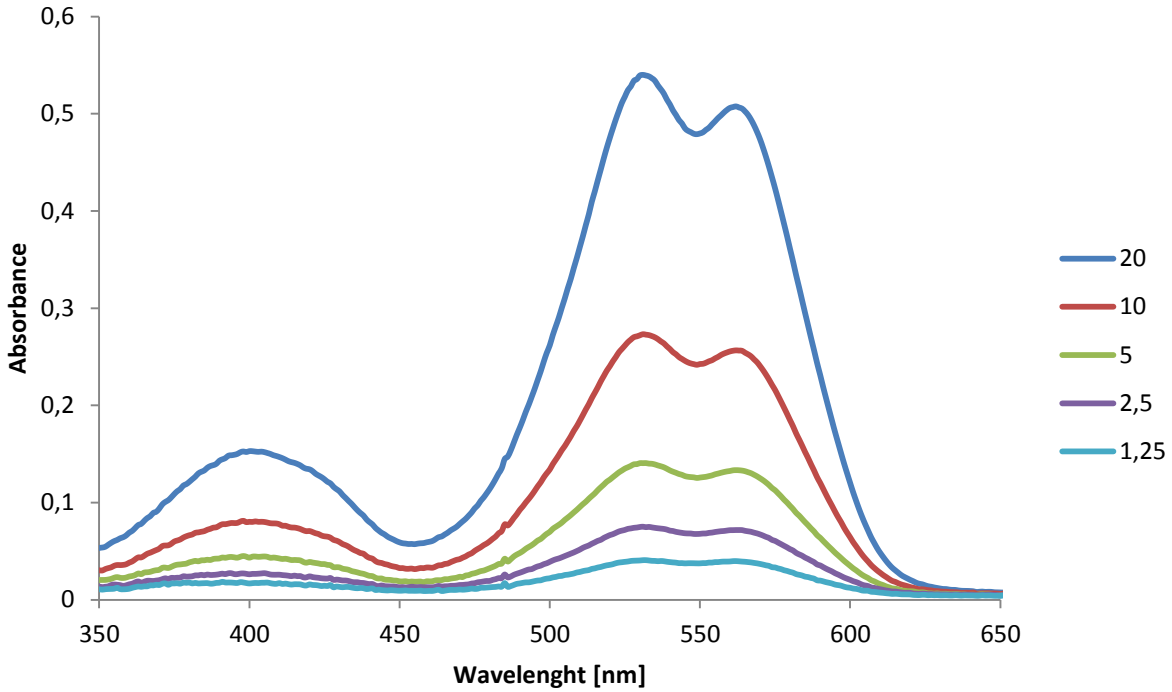

B)

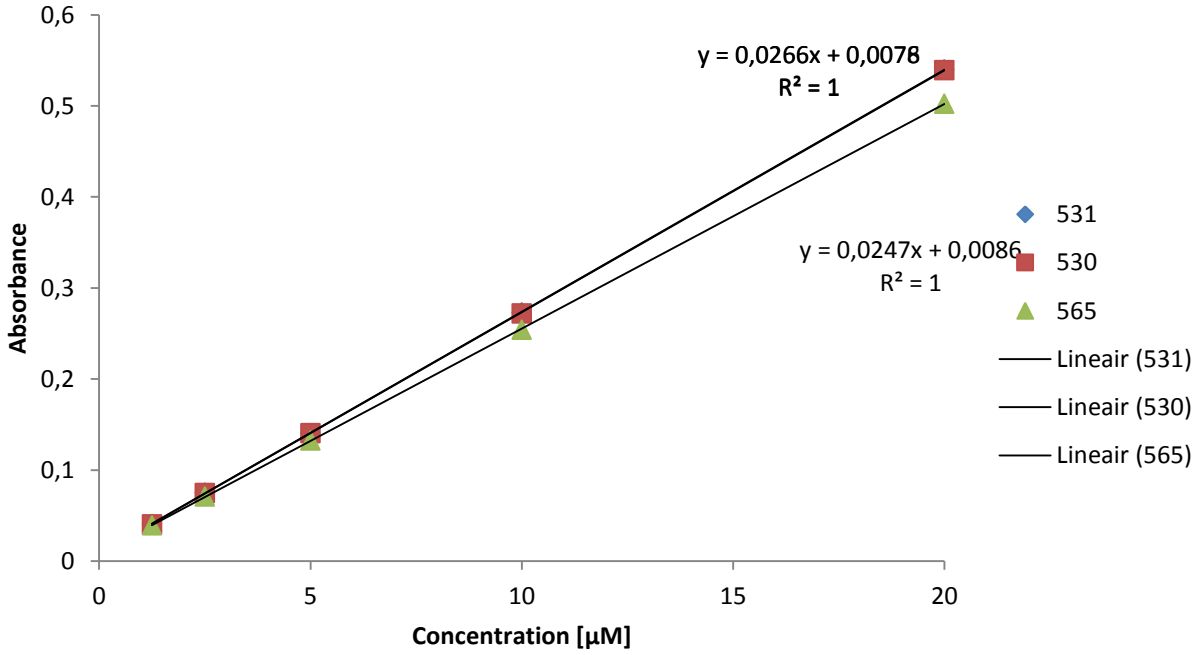

Figure S20. A) UV-VIS spectra of compound 14 in different concentrations (legend in µM); B) linear dependence of Absorbance of the compound of its concentration at λ_{max} and λ = 530 nm

2.2. UPLC measurements

UPLC traces were measured on Thermo Fisher Scientific LC/MS: UPLC model Vanquish, MS model LTQ with an iontrap and HESI (Heated ESI) ionisation source with positive and negative mode. The chromatograms are measured at λ_{obs}=520 nm.

For each of compounds **7** – **14**, two 0.125 mM in 25% DMSO / 5 mM phosphate buffer pH = 7.5 samples were made. After UPLC traces were taken from all of them, one set was irradiated for 1 h and the other stored in room temperature in the dark. After this time, the UPLC traces were taken again in the same order as before. Then, the non-irradiated samples were stored at room temperature in the dark overnight and the UPLC traces were taken again.

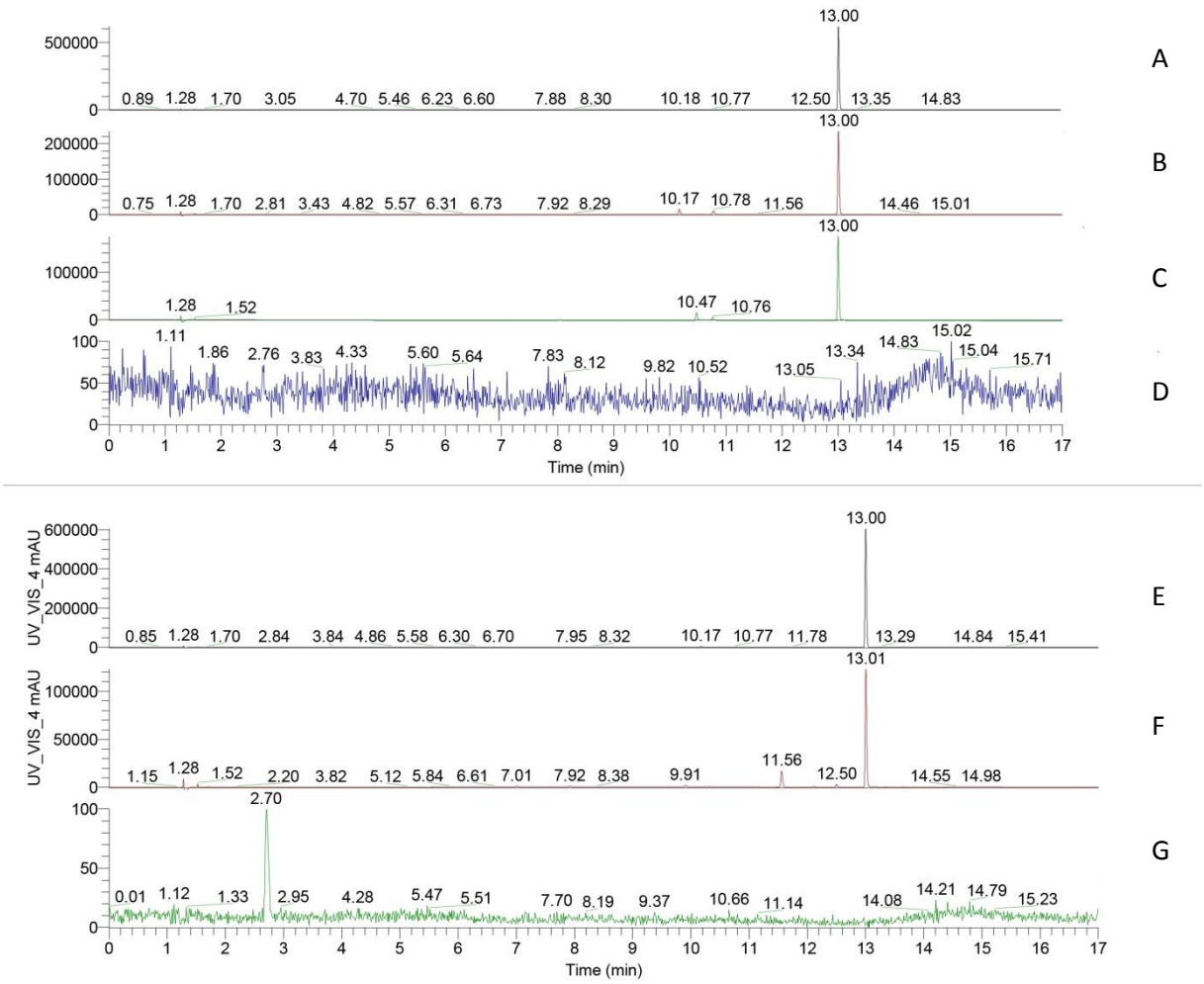

Figure S21. UPLC trace for compound **7**, 0.125 mM in 25% DMSO / 5 mM phosphate buffer, pH=7.5. λ_{obs}=520 nm. A-D: stability study; A) freshly prepared sample, B) sample after 3h at rt, C) sample after one day at rt, D) MS chromatogram with selected mass of the uncaged amine in the sample after one day at rt, presenting no spontaneous hydrolysis to the product. E-G: photodeprotection study; E) freshly prepared sample, F) sample after irradiation with λ_{irr}=530 nm for 1 h, G) MS chromatogram with selected mass of the uncaged amine in the sample after irradiation, presenting the formation of the product.

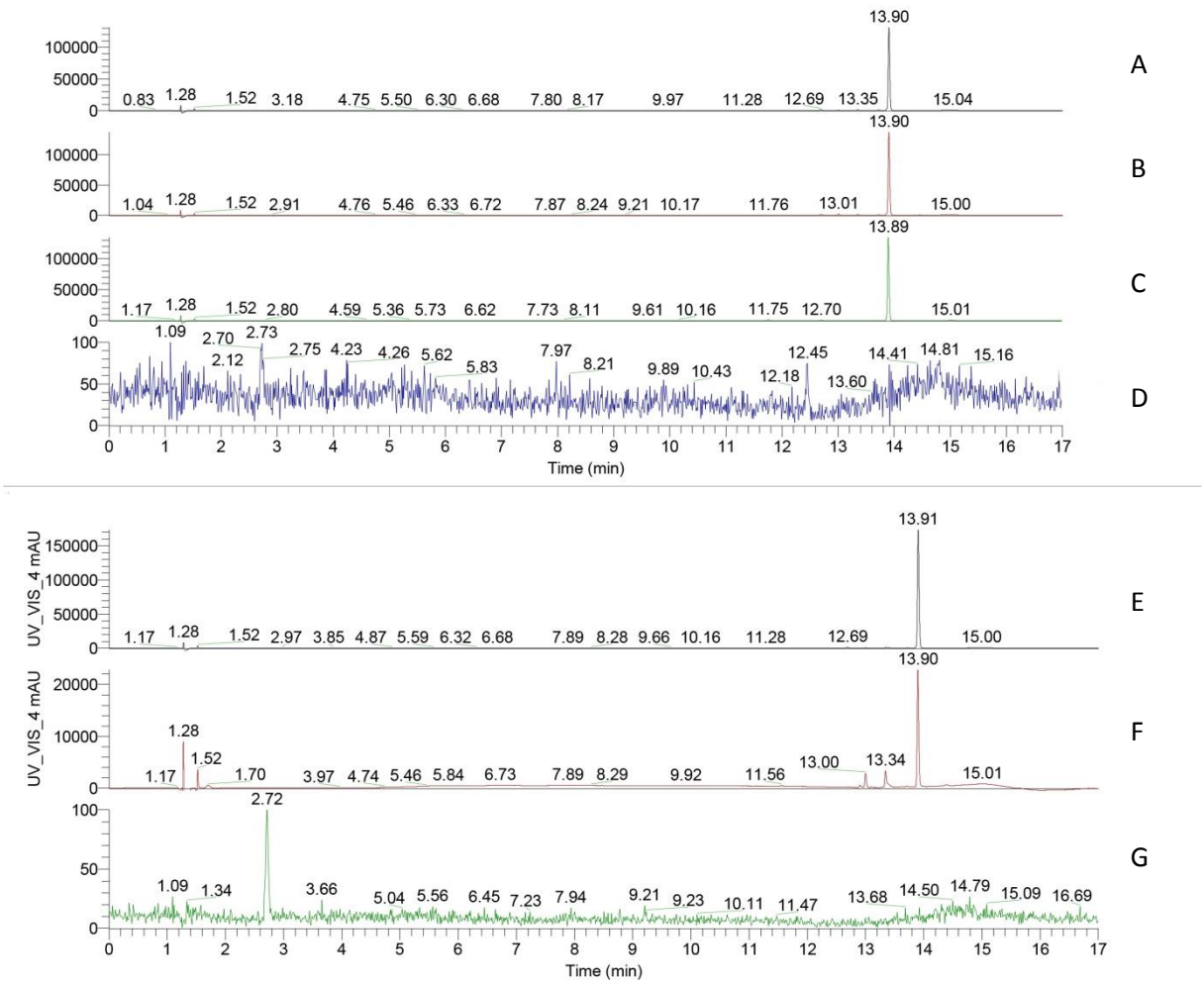

Figure S22. UPLC trace for compound **8**, 0.125 mM in 25% DMSO / 5 mM phosphate buffer, pH=7.5. λ_{obs}=520 nm. A-D: stability study; A) freshly prepared sample, B) sample after 3h at rt, C) sample after one day at rt, D) MS chromatogram with selected mass of the uncaged amine in the sample after one day at rt, presenting no spontaneous hydrolysis to the product. E-G: photodeprotection study; E) freshly prepared sample, F) sample after irradiation with λ_{irr}=530 nm for 1 h, G) MS chromatogram with selected mass of the uncaged amine in the sample after irradiation, presenting the formation of the product.

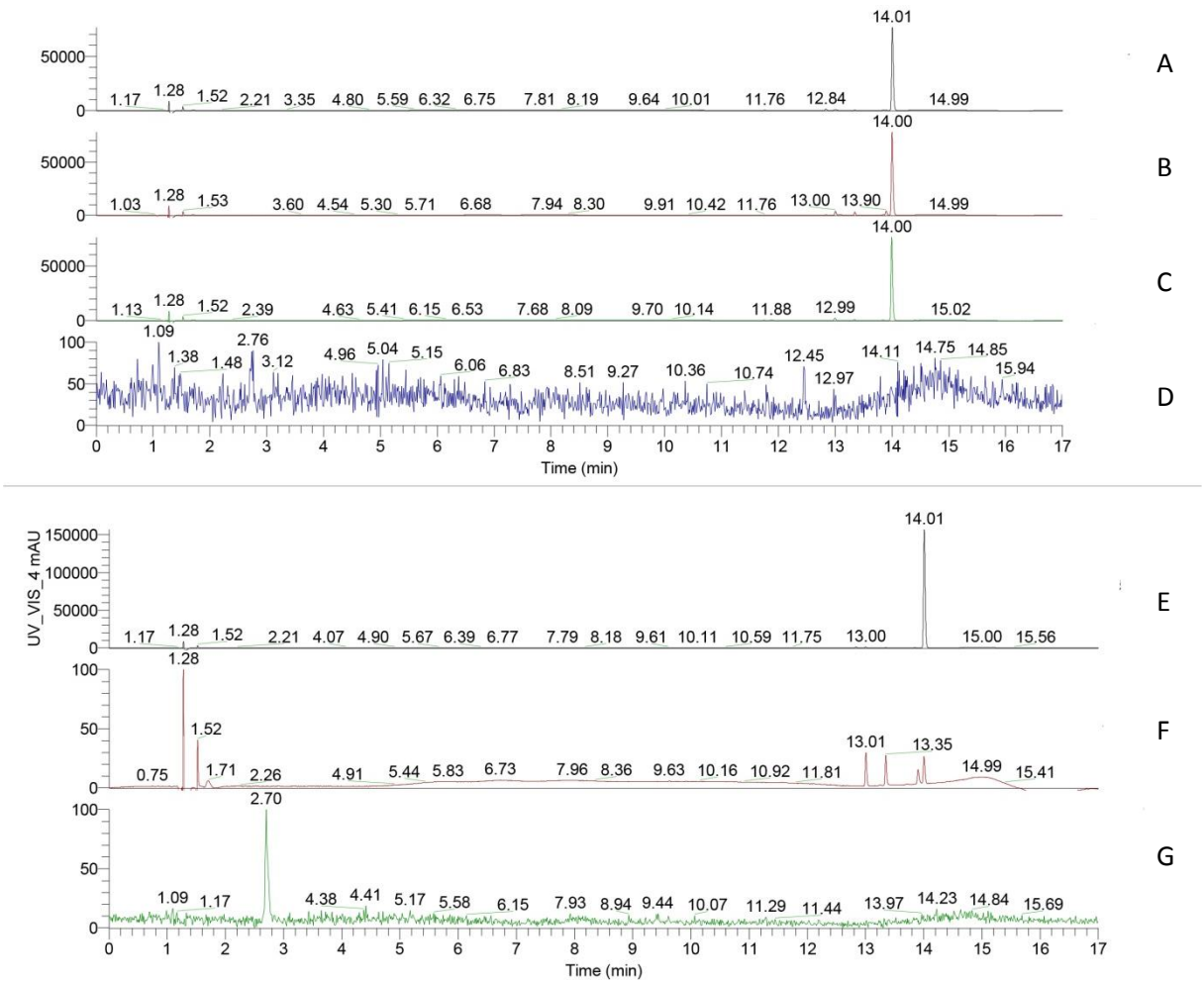

Figure S23. UPLC trace for compound **9**, 0.125 mM in 25% DMSO / 5 mM phosphate buffer, pH=7.5. λ_{obs}=520 nm. A-D: stability study; A) freshly prepared sample, B) sample after 3h at rt, C) sample after one day at rt, D) MS chromatogram with selected mass of the uncaged amine in the sample after one day at rt, presenting no spontaneous hydrolysis to the product. E-G: photodeprotection study; E) freshly prepared sample, F) sample after irradiation with λ_{irr}=530 nm for 1 h, G) MS chromatogram with selected mass of the uncaged amine in the sample after irradiation, presenting the formation of the product.

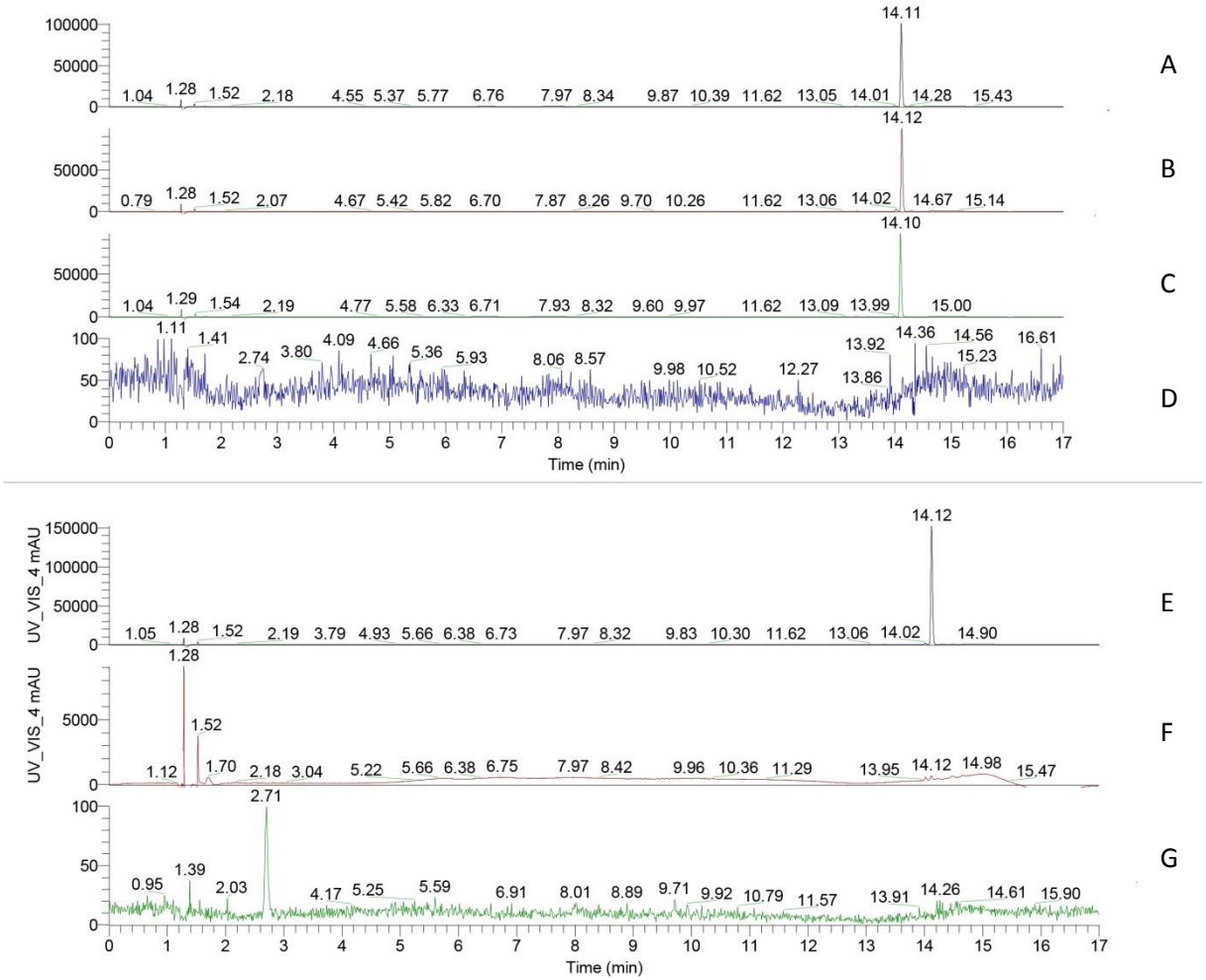

Figure S24. UPLC trace for compound **10**, 0.125 mM in 25% DMSO / 5 mM phosphate buffer, pH=7.5. λ_{obs}=520 nm. A-D: stability study; A) freshly prepared sample, B) sample after 3h at rt, C) sample after one day at rt, D) MS chromatogram with selected mass of the uncaged amine in the sample after one day at rt, presenting no spontaneous hydrolysis to the product. E-G: photodeprotection study; E) freshly prepared sample, F) sample after irradiation with λ_{irr}=530 nm for 1 h, G) MS chromatogram with selected mass of the uncaged amine in the sample after irradiation, presenting the formation of the product.

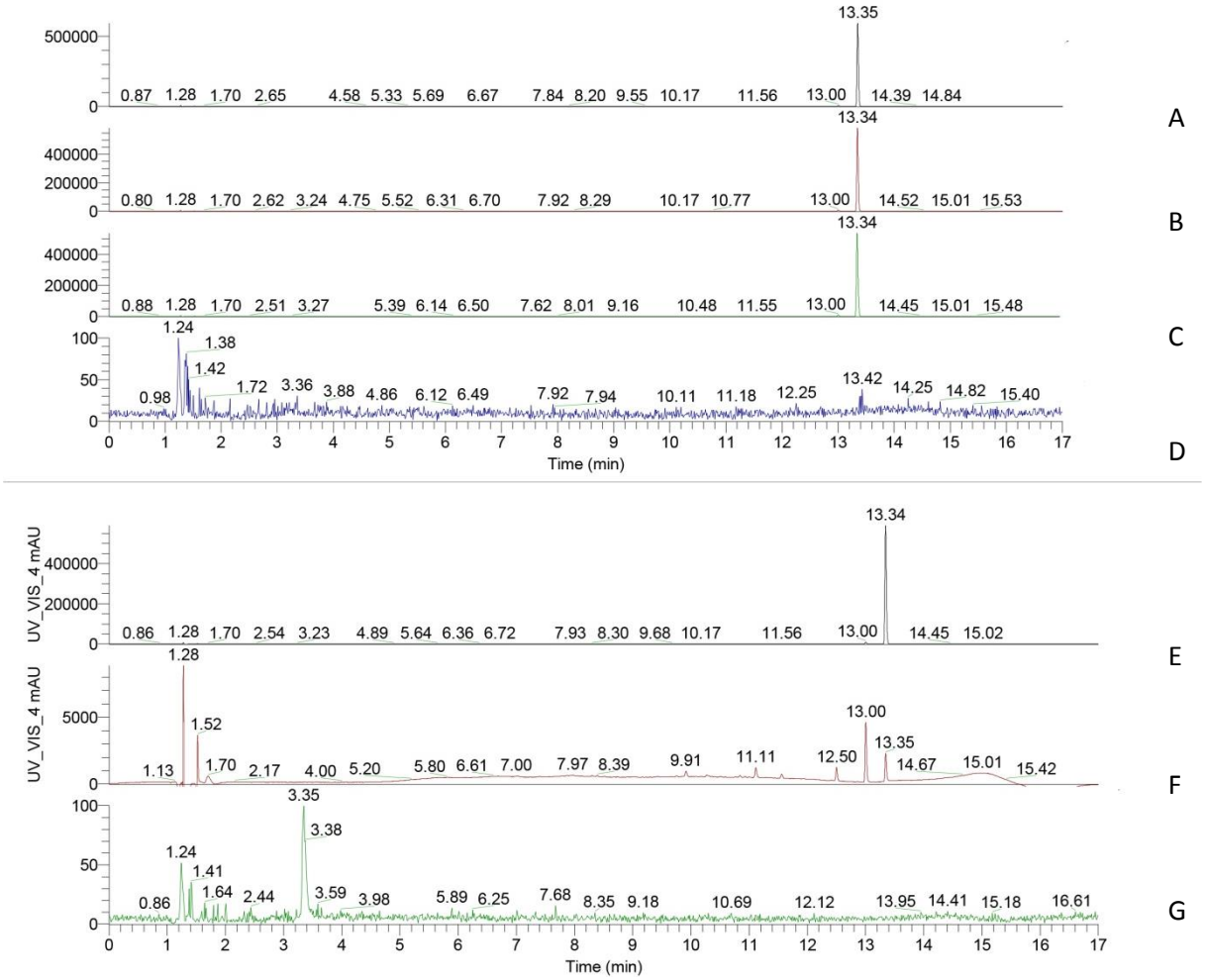

Figure S25. UPLC trace for compound **11**, 0.125 mM in 25% DMSO / 5 mM phosphate buffer, pH=7.5. λ_{obs}=520 nm. A-D: stability study; A) freshly prepared sample, B) sample after 3h at rt, C) sample after one day at rt, D) MS chromatogram with selected mass of the uncaged amine in the sample after one day at rt, presenting no spontaneous hydrolysis to the product. E-G: photodeprotection study; E) freshly prepared sample, F) sample after irradiation with λ_{irr}=530 nm for 1 h, G) MS chromatogram with selected mass of the uncaged amine in the sample after irradiation, presenting the formation of the product.

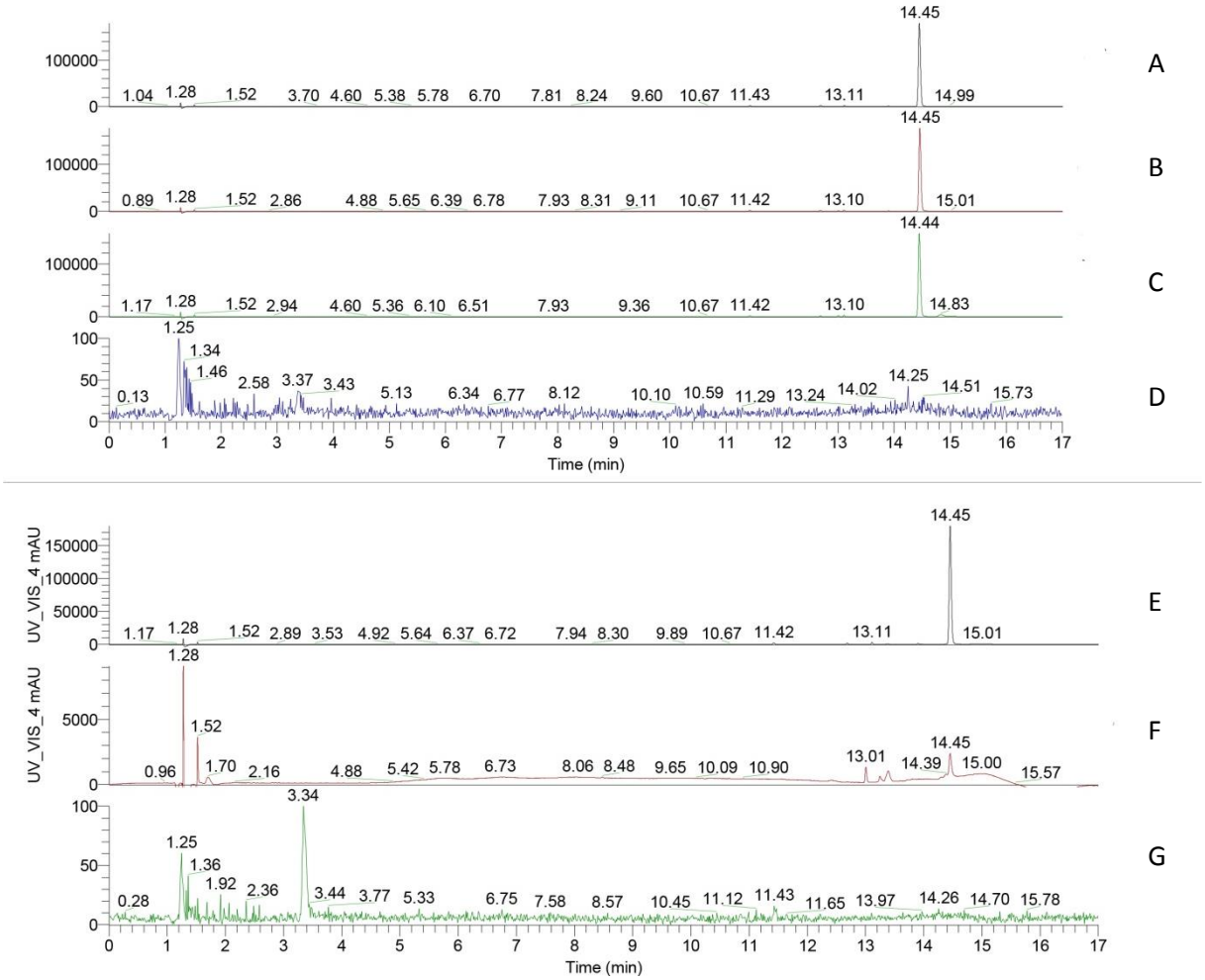

Figure S26. UPLC trace for compound **12**, 0.125 mM in 25% DMSO / 5 mM phosphate buffer, pH=7.5. λ_{obs}=520 nm. A-D: stability study; A) freshly prepared sample, B) sample after 3h at rt, C) sample after one day at rt, D) MS chromatogram with selected mass of the uncaged amine in the sample after one day at rt, presenting no spontaneous hydrolysis to the product. E-G: photodeprotection study; E) freshly prepared sample, F) sample after irradiation with λ_{irr}=530 nm for 1 h, G) MS chromatogram with selected mass of the uncaged amine in the sample after irradiation, presenting the formation of the product.

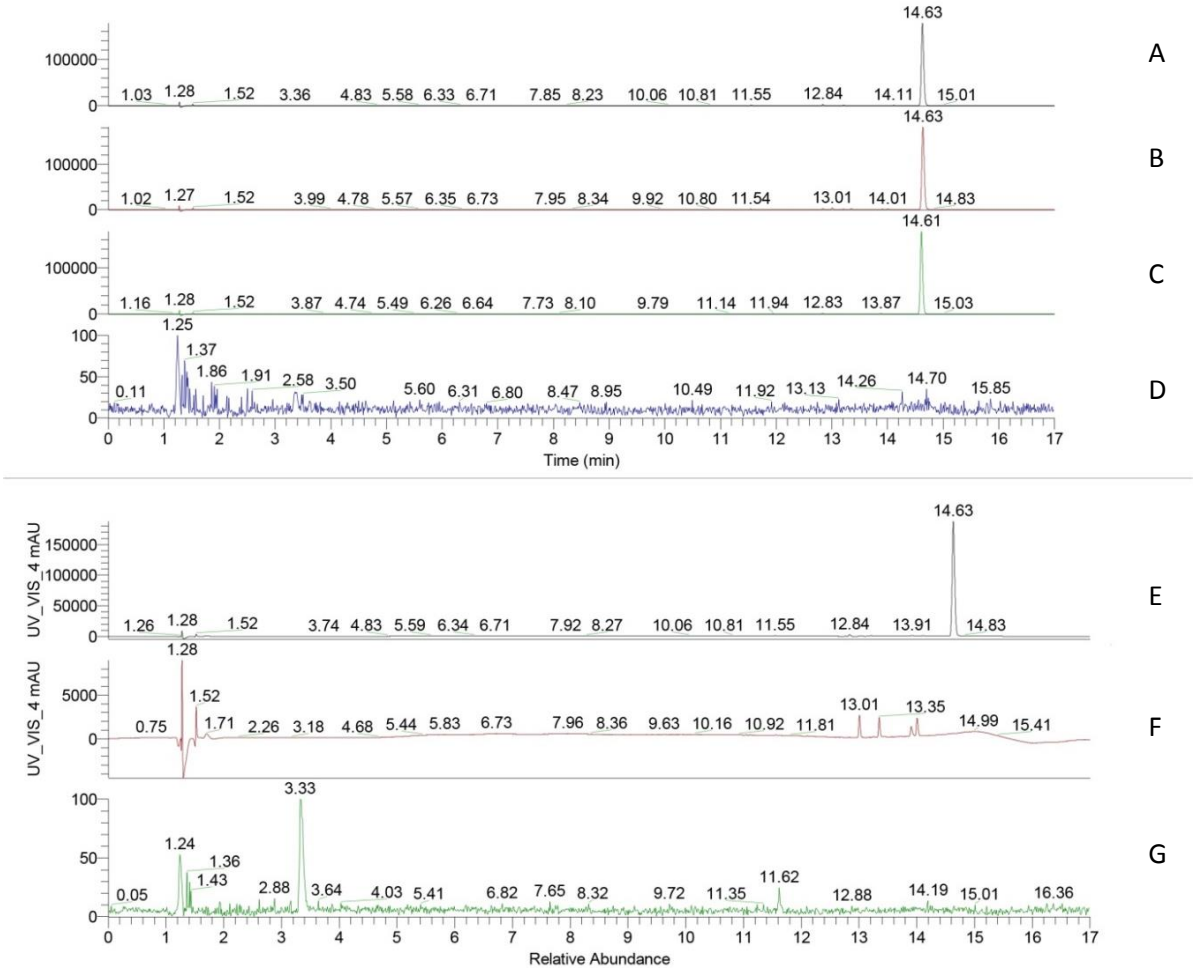

Figure S27. UPLC trace for compound **13**, 0.125 mM in 25% DMSO / 5 mM phosphate buffer, pH=7.5. λ_{obs}=520 nm. A-D: stability study; A) freshly prepared sample, B) sample after 3h at rt, C) sample after one day at rt, D) MS chromatogram with selected mass of the uncaged amine in the sample after one day at rt, presenting no spontaneous hydrolysis to the product. E-G: photodeprotection study; E) freshly prepared sample, F) sample after irradiation with λ_{irr}=530 nm for 1 h, G) MS chromatogram with selected mass of the uncaged amine in the sample after irradiation, presenting the formation of the product.

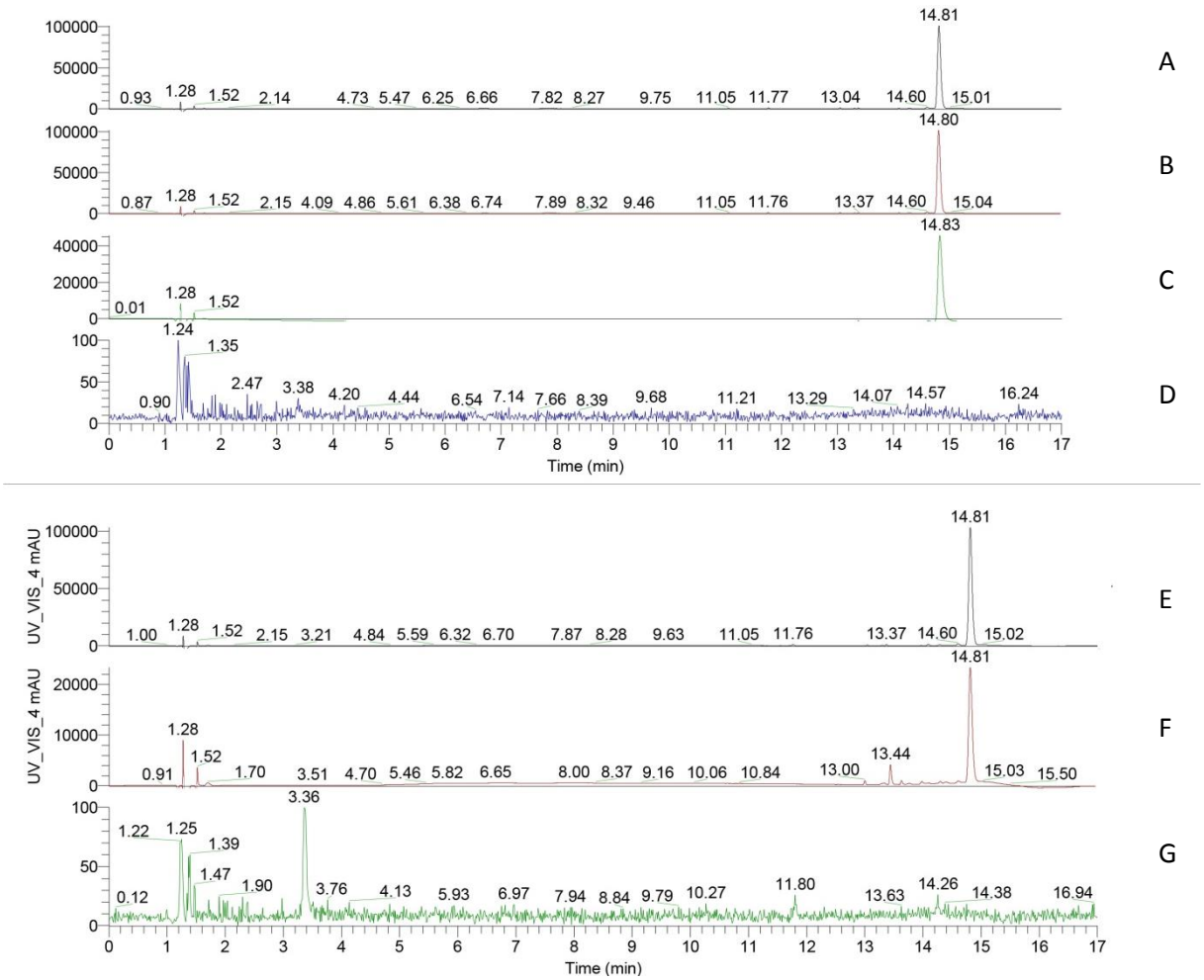

Figure S28. UPLC trace for compound **14**, 0.125 mM in 25% DMSO / 5 mM phosphate buffer, pH=7.5. λ_{obs}=520 nm. A-D: stability study; A) freshly prepared sample, B) sample after 3h at rt, C) sample after one day at rt, D) MS chromatogram with selected mass of the uncaged amine in the sample after one day at rt, presenting no spontaneous hydrolysis to the product. E-G: photodeprotection study; E) freshly prepared sample, F) sample after irradiation with λ_{irr}=530 nm for 1 h, G) MS chromatogram with selected mass of the uncaged amine in the sample after irradiation, presenting the formation of the product.

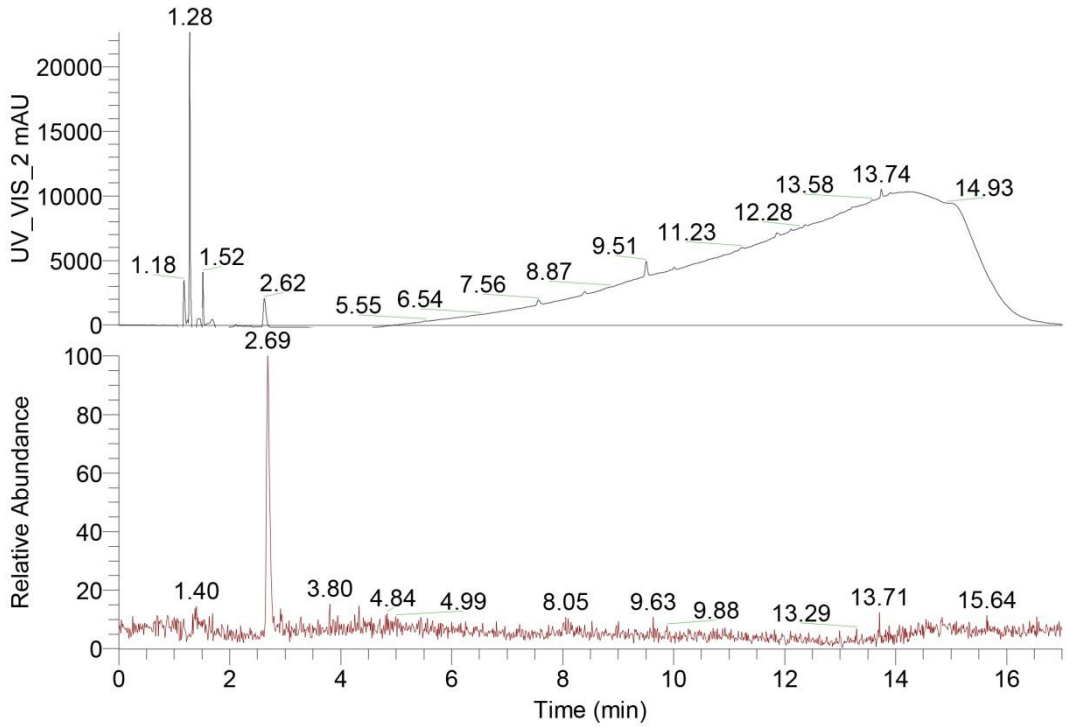

Figure S29. UPLC trace for 4-Fluorobenzylamine, 0.125 mM in 25% DMSO / 5 mM phosphate buffer, pH=7.5.: A) λ_{obs}=254 nm, B) Relative abundance for mass range 125-127 (m/z).

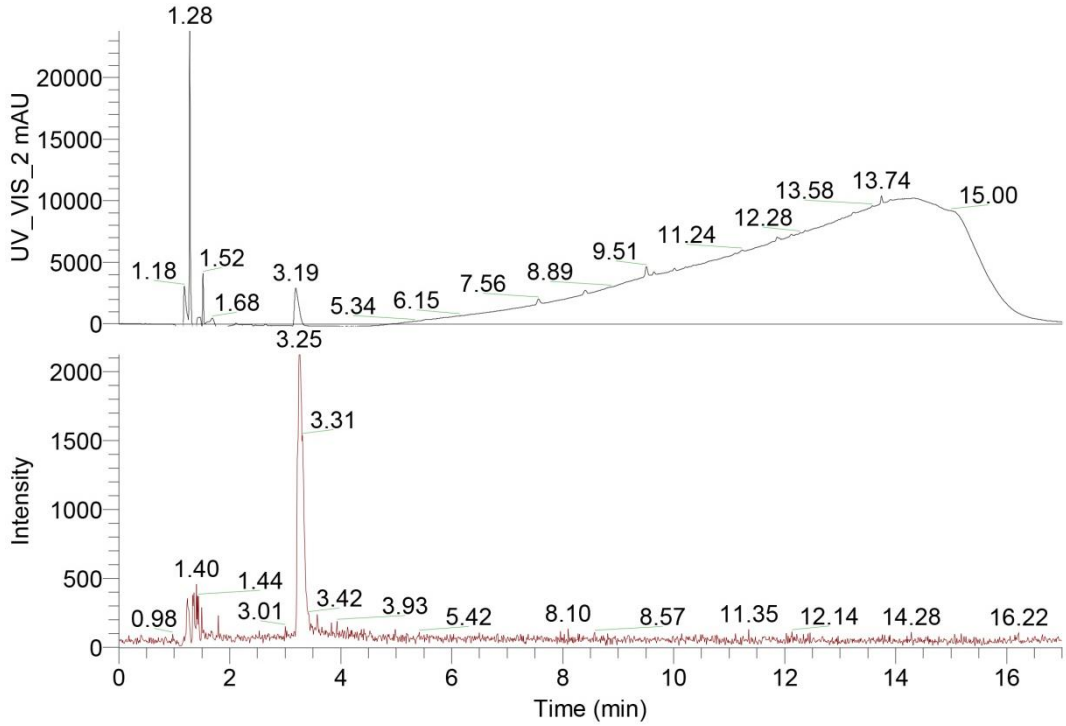

Figure S30. UPLC trace for 4-fluoro-*N*-methylbenzylamine, 0.125 mM in 25% DMSO / 5 mM phosphate buffer, pH=7.5.: A) λ_{obs}=254 nm, B) Relative abundance for mass range 139-141 (m/z).

2.3. ^{19}F NMR analysis

Samples of compounds **9** and **13** in (0.18 mM in d6-DMSO) were prepared and irradiated with λ=530 nm light for 2 h. ^{19}F NMR spectra were taken each h. After irradiation, 10% mol of 2mM solution of appropriate fluoroamines were added to the samples and ^{19}F NMR was taken again.

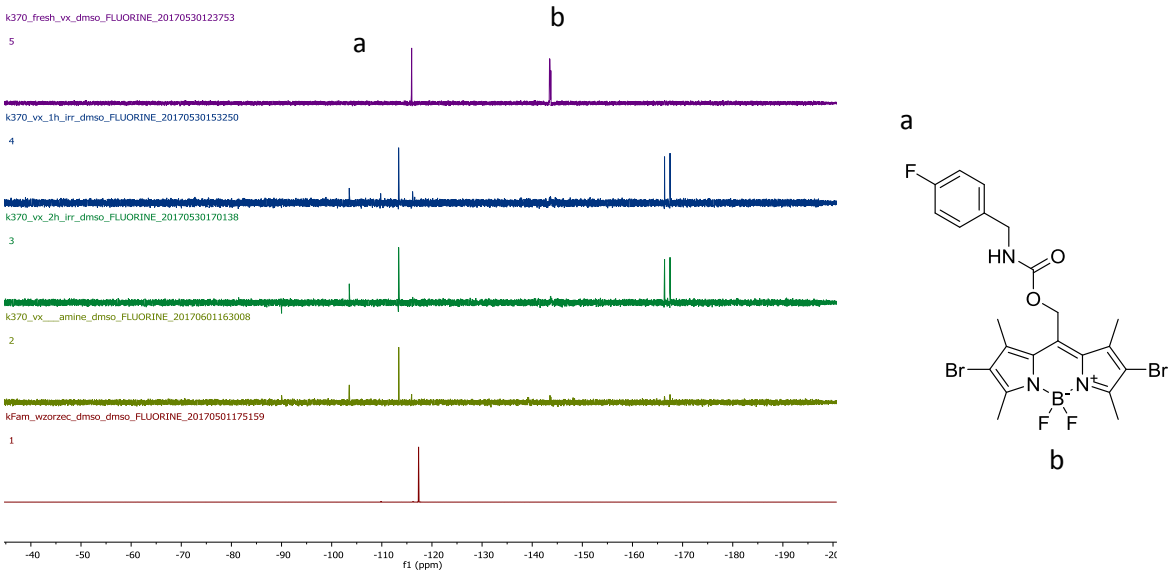

Figure S31. ^{19}F NMR spectra of compound **9**: 5. Fresh sample, 4. After 1 h of irradiation, 3. After 2 h of irradiation, 2. After addition of 10% mol of amine, 1. Amine standard.

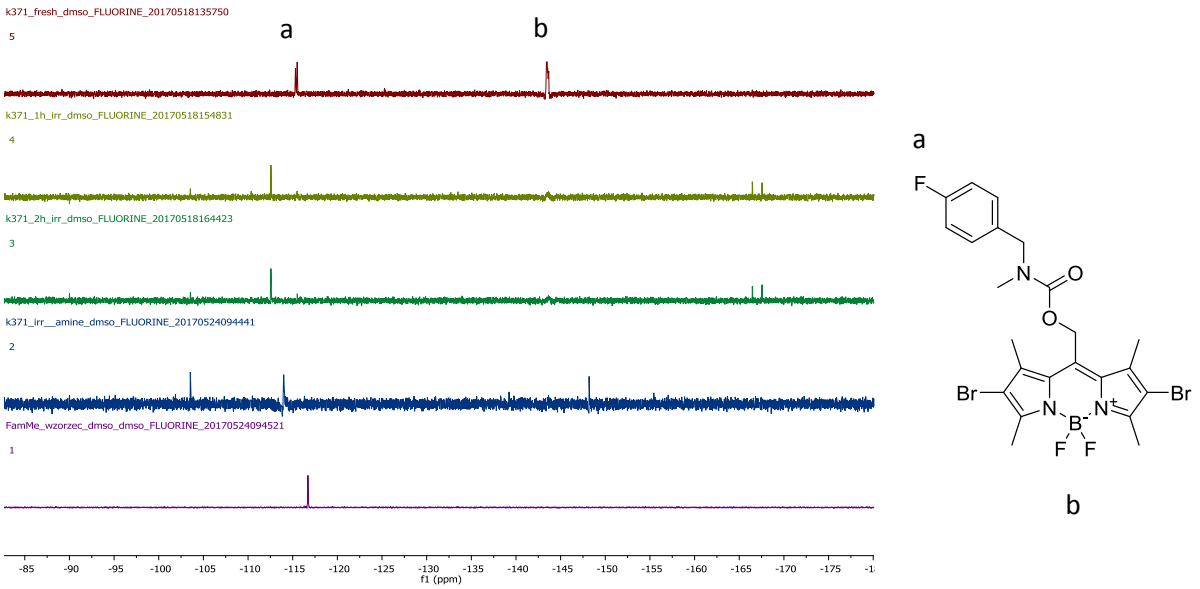

Figure S32. ^{19}F NMR spectra of compound **13**: 5. Fresh sample, 4. After 1 h of irradiation, 3. After 2 h of irradiation, 2. After addition of 10% mol of amine, 1. Amine standard.

3. NMR characterization of compounds

(5,5-difluoro-1,3,7,9-tetramethyl-5H-4l4,5l4-dipyrrolo[1,2-c:2',1'-f][1,3,2]diazaborinin-10-yl)methyl acetate (**1**) (according to a literature procedure [1])

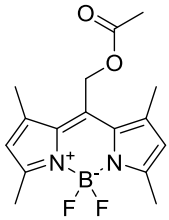

^{1}H NMR

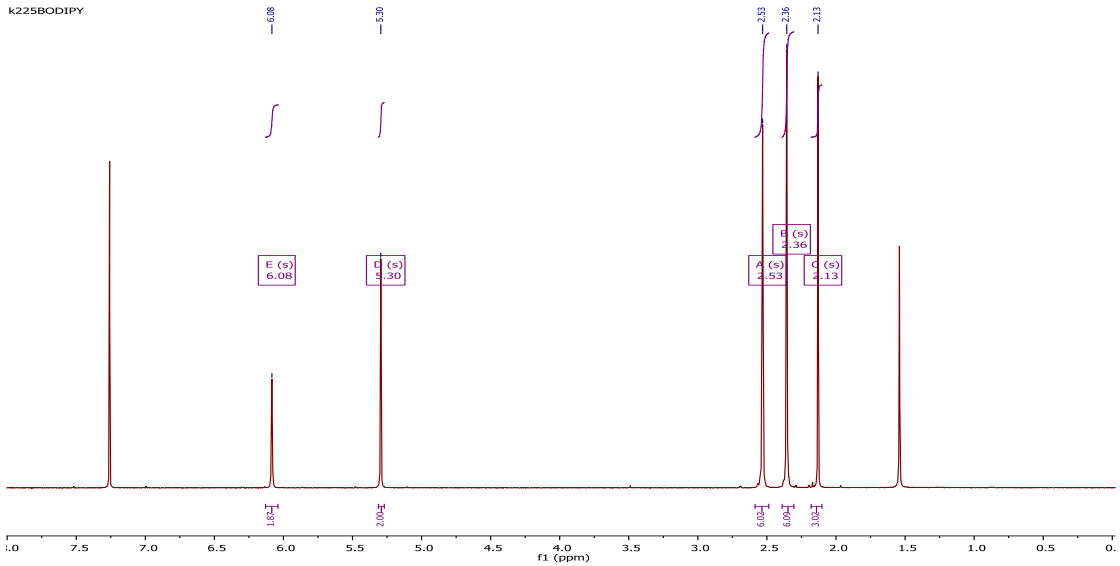

^{19}F NMR

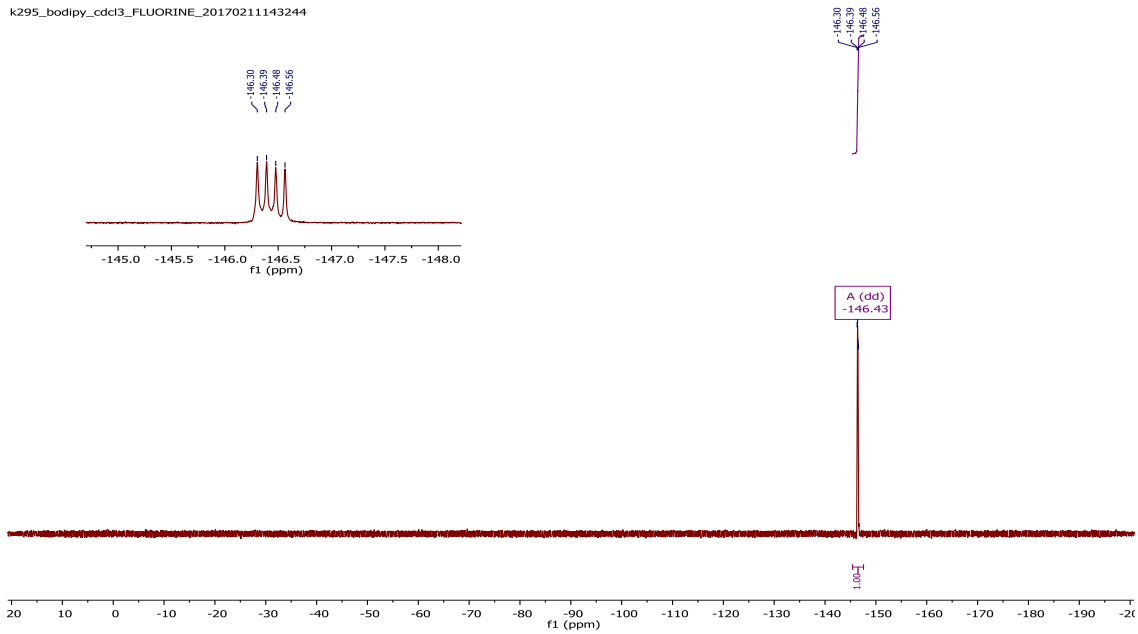

5,5-difluoro-1,3,7,9-tetramethyl-5H-4l4,5l4-dipyrrolo[1,2-c:2',1'-f][1,3,2]diazaborinin-10-yl)methanol (**2**) (according to a literature procedure [2])

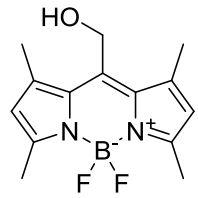

^{1}H NMR

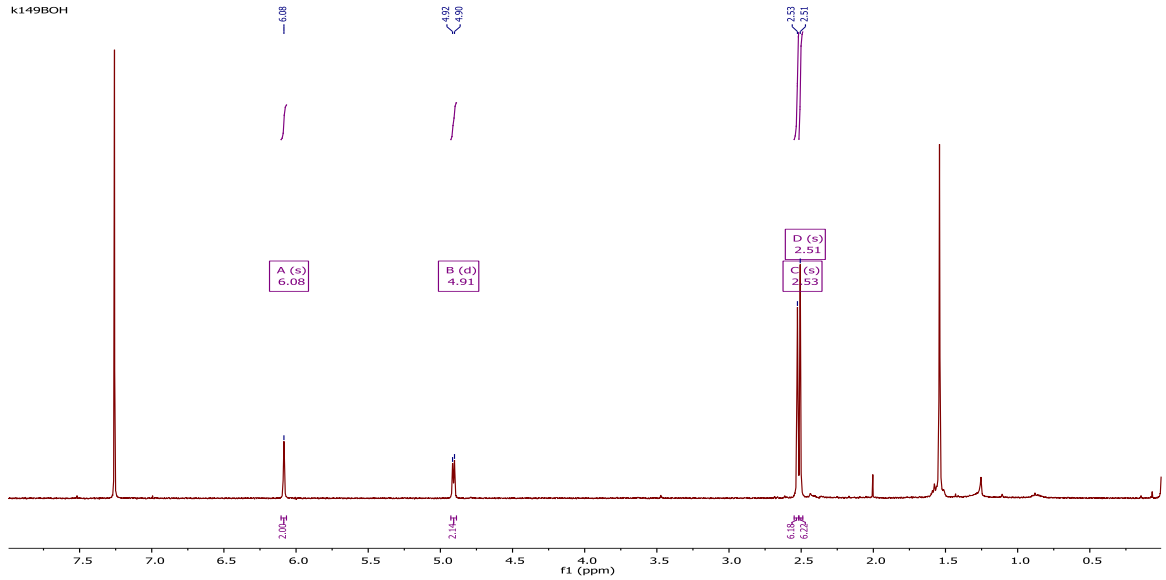

^{19}F NMR

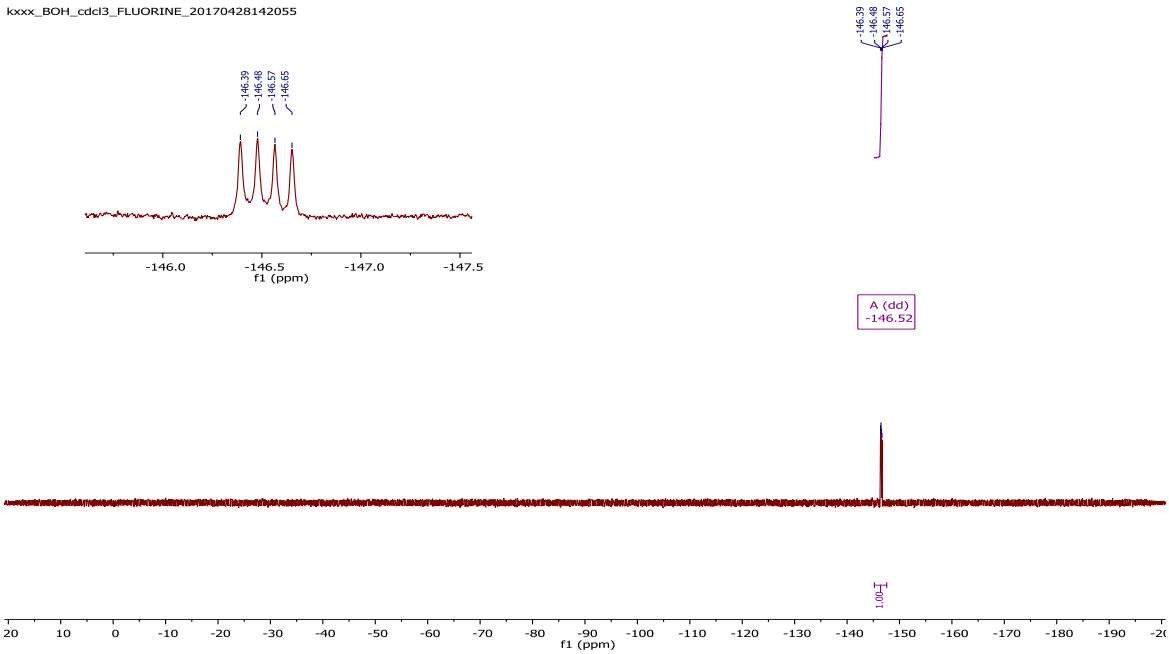

(5,5-difluoro-1,3,7,9-tetramethyl-5H-4l4,5l4-dipyrrolo[1,2-c:2',1'-f][1,3,2]diazaborinin-10-yl)methyl (4-nitrophenyl) carbonate (**3**)

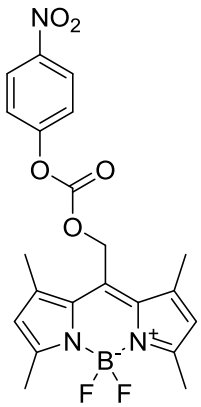

^{1}H NMR

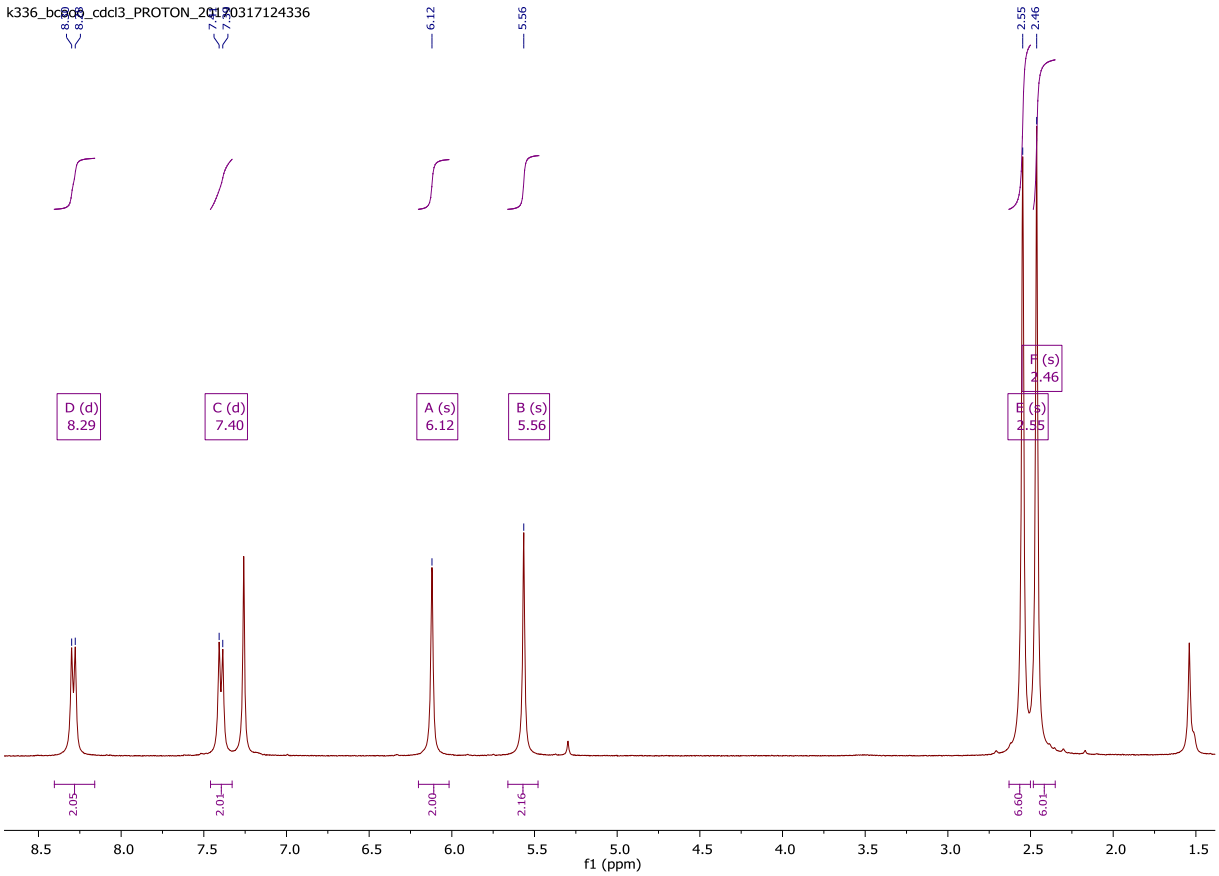

^{19}F NMR

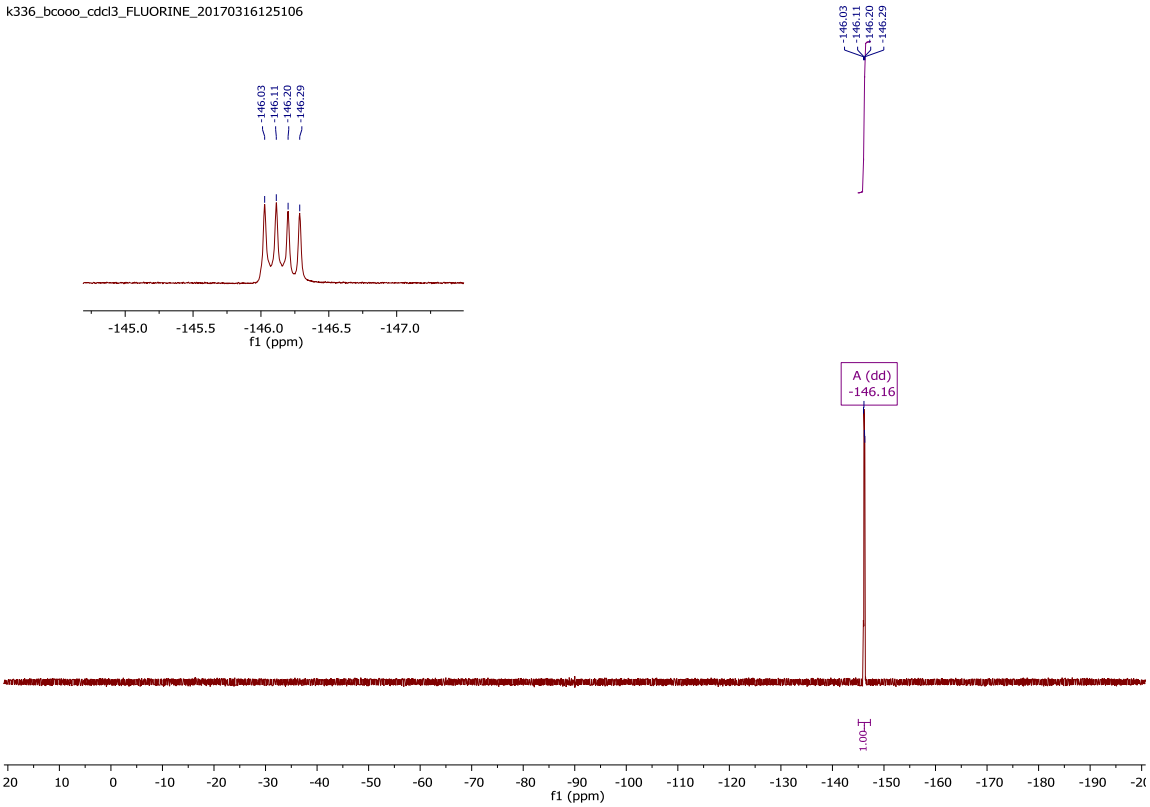

^{1}H COSY NMR

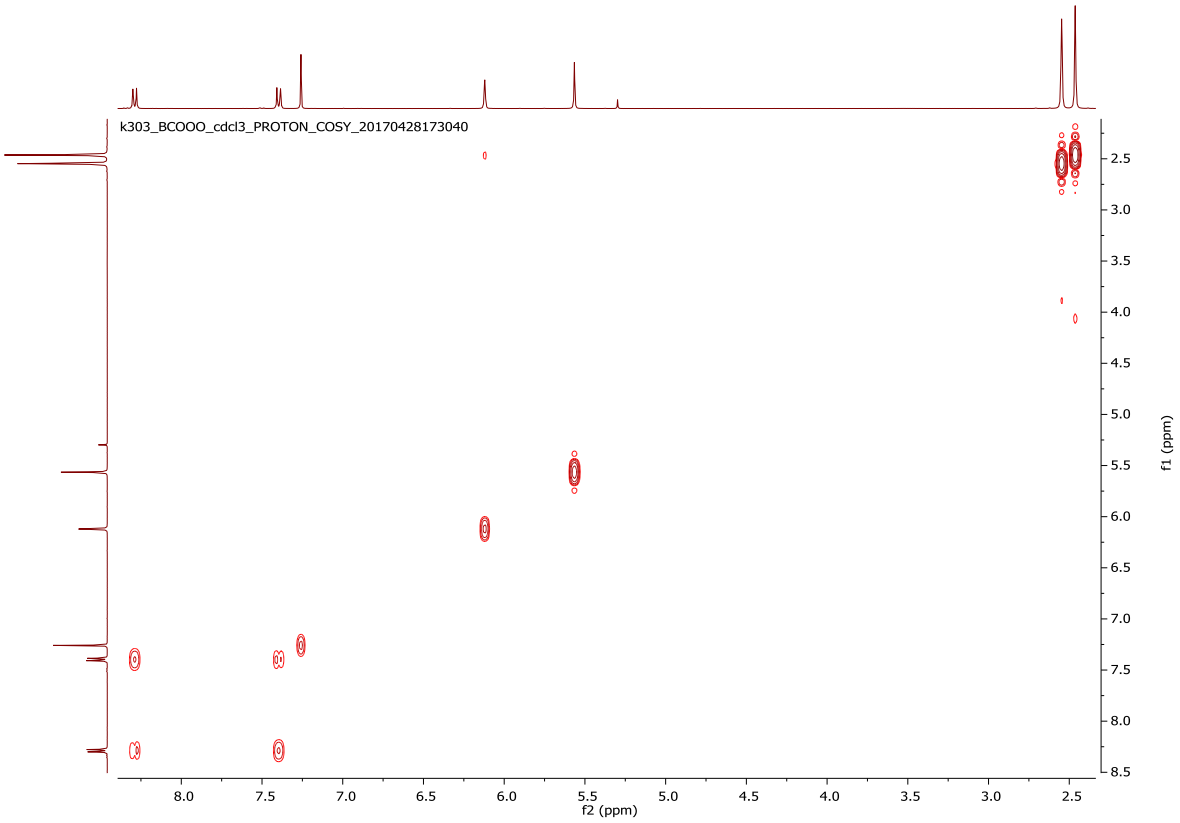

$^{1}H/^{13}C$ NMR ASAPHMQC

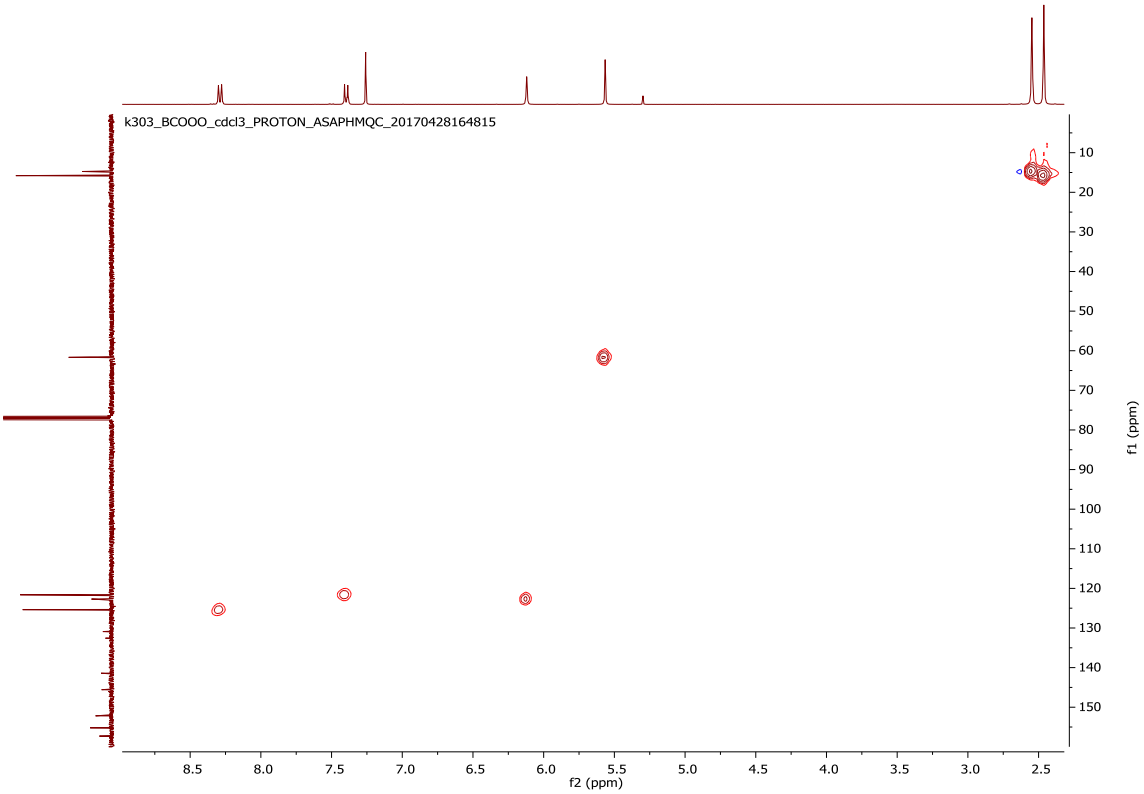

^{13}C NMR

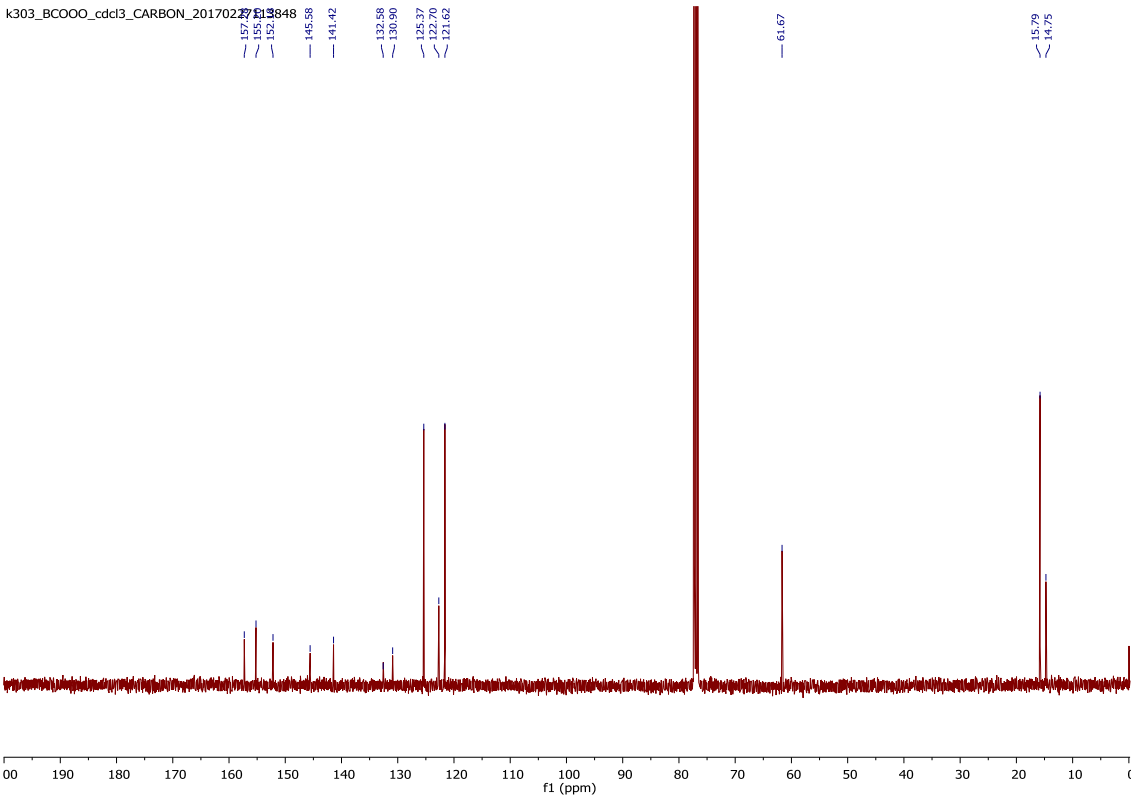

(5,5-difluoro-2,8-dichloro-1,3,7,9-tetramethyl-5H-4l4,5l4-dipyrrolo[1,2-c:2',1'-f][1,3,2]diazaborinin-10-yl)methyl(4-nitrophenyl) carbonate (**4**)

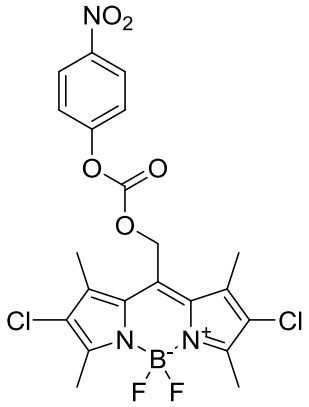

^{1}H NMR

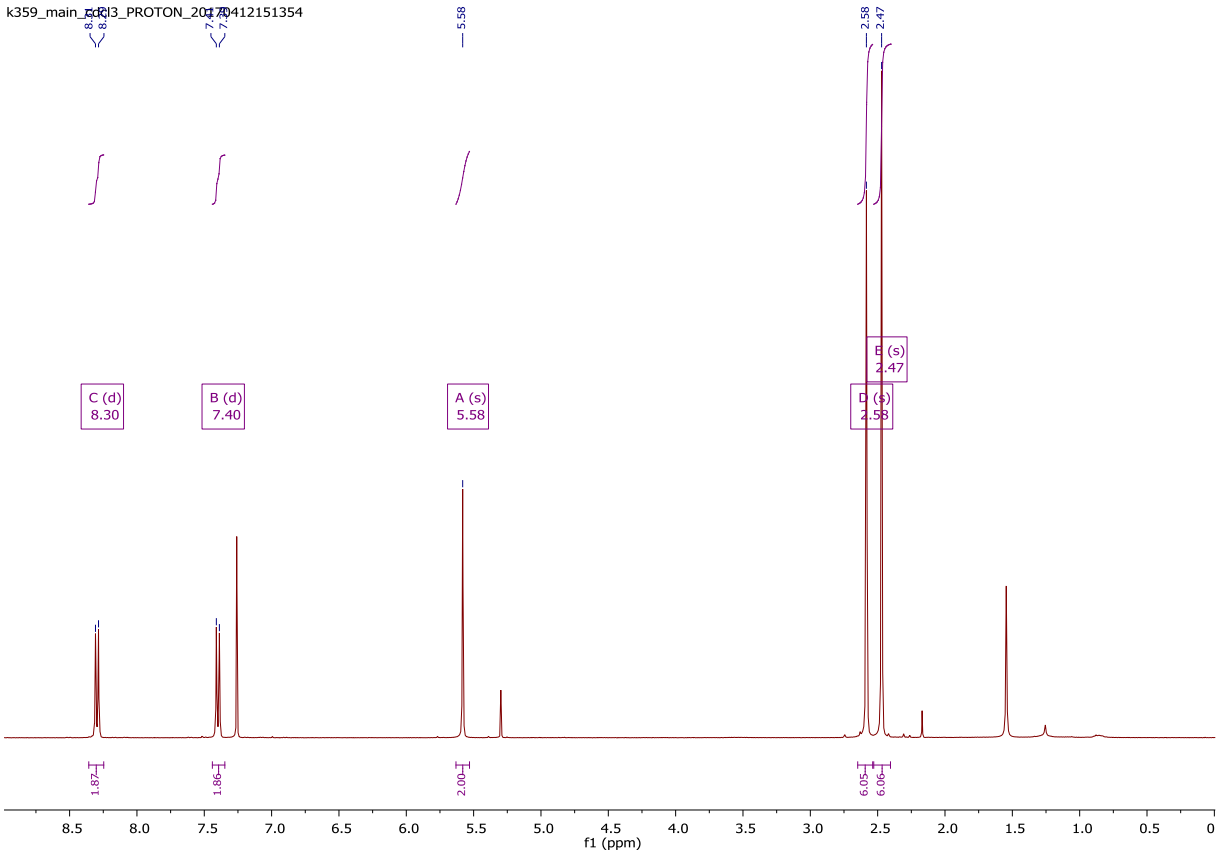

^{19}F NMR

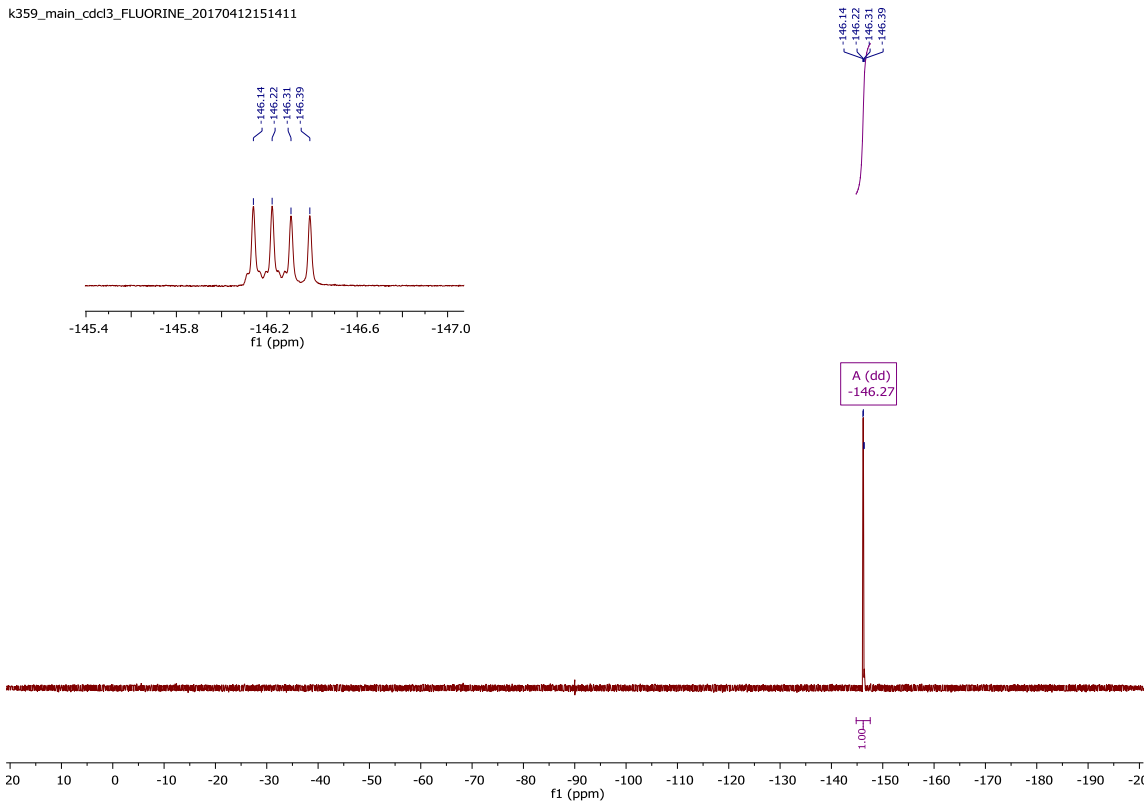

^{1}H COSY NMR

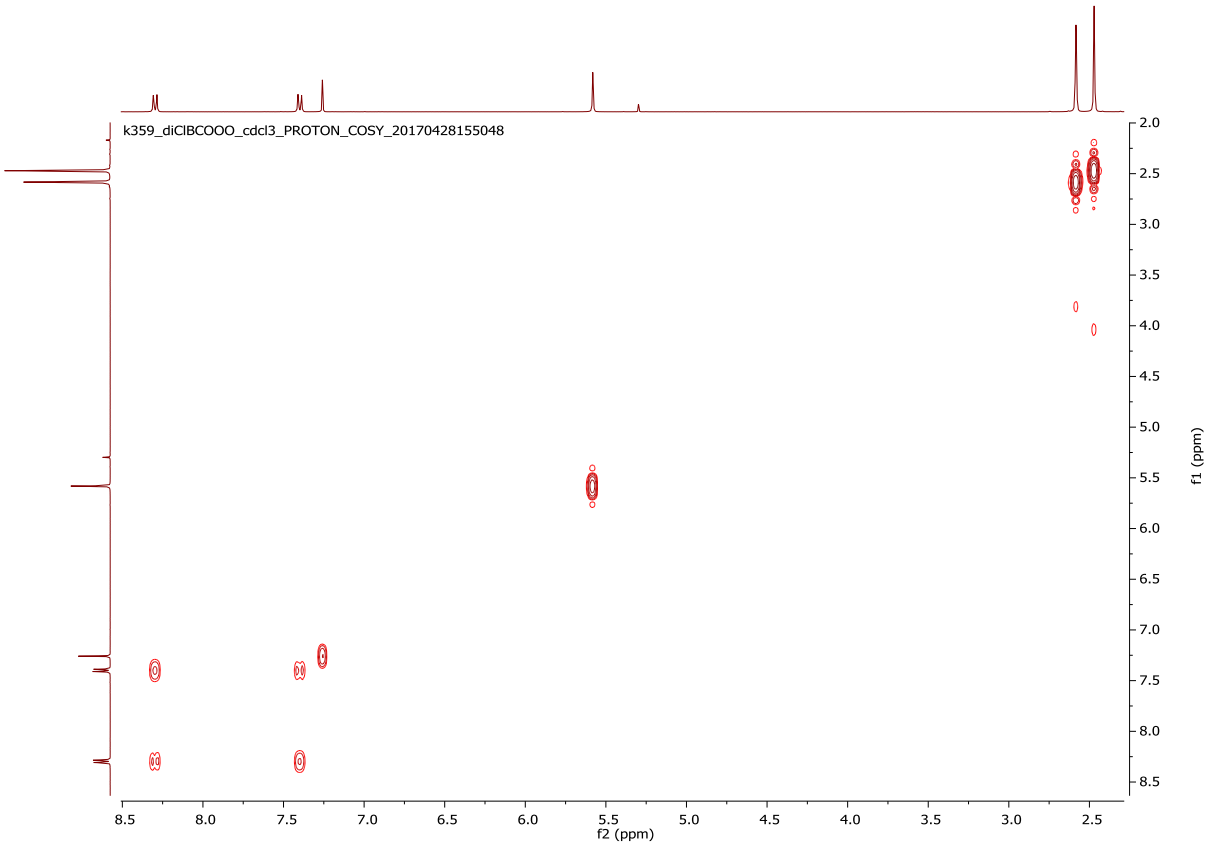

$^{1}H/^{13}C$ NMR ASAPHMQC

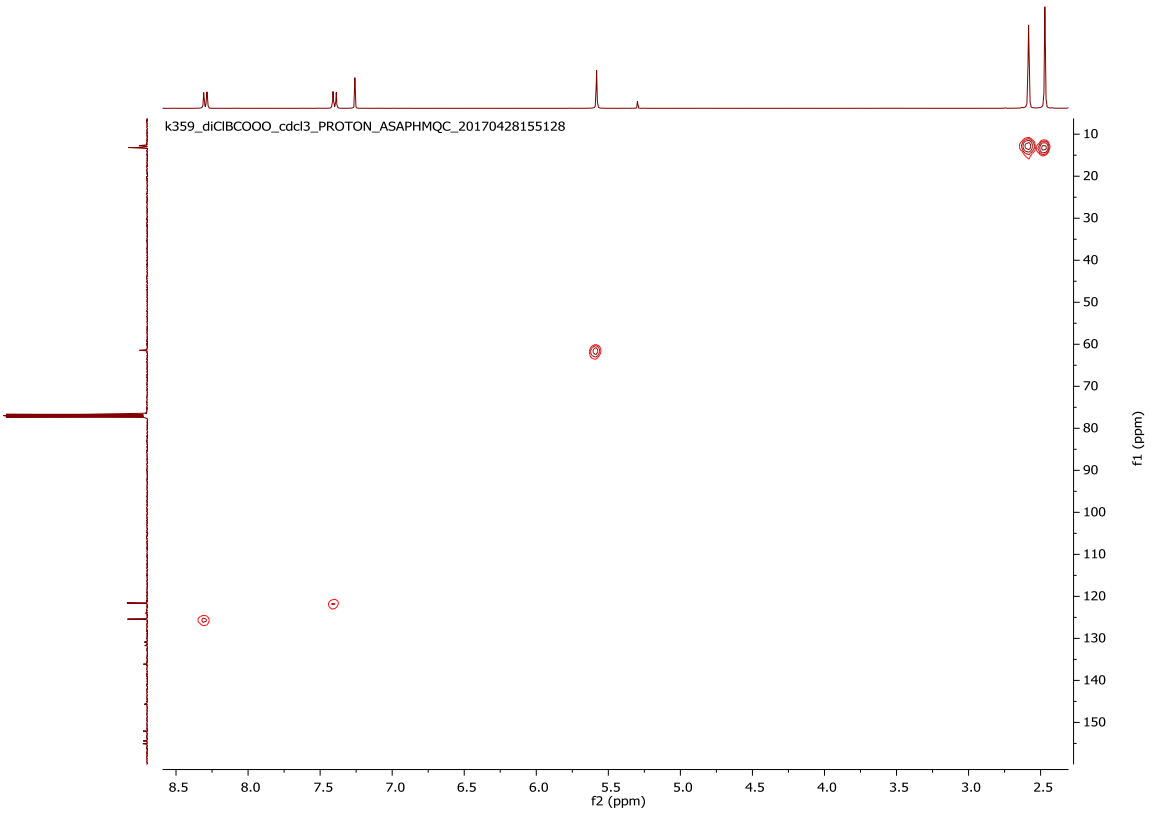

^{13}C NMR

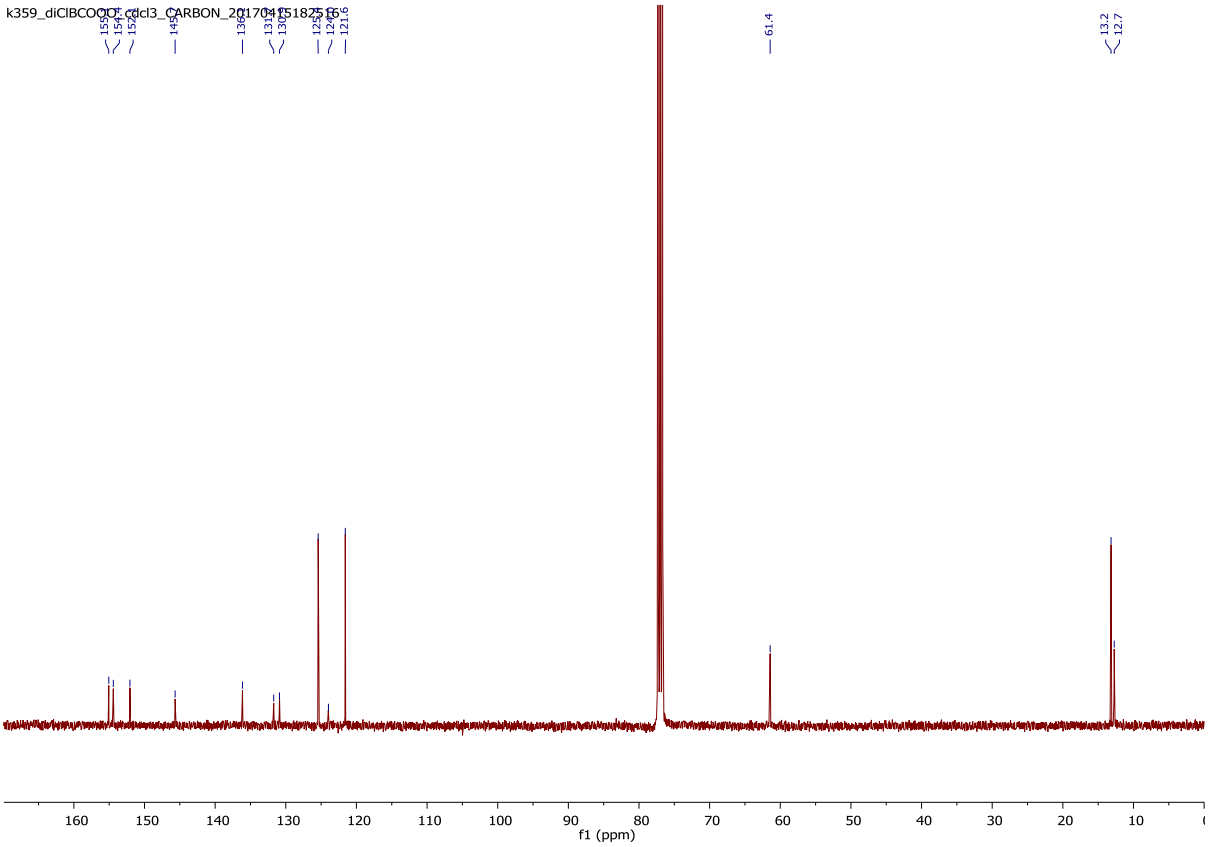

(5,5-difluoro-2,8-dibromo-1,3,7,9-tetramethyl-5H-4l4,5l4-dipyrrolo[1,2-c:2',1'-f][1,3,2]diazaborinin-10-yl)methyl (4-nitrophenyl) carbonate (**5**)

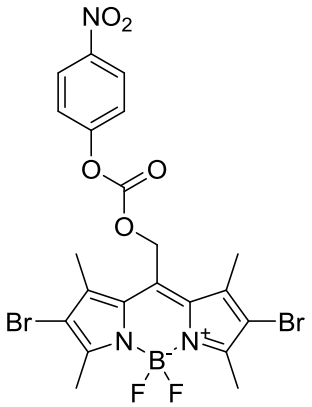

^{1}H NMR

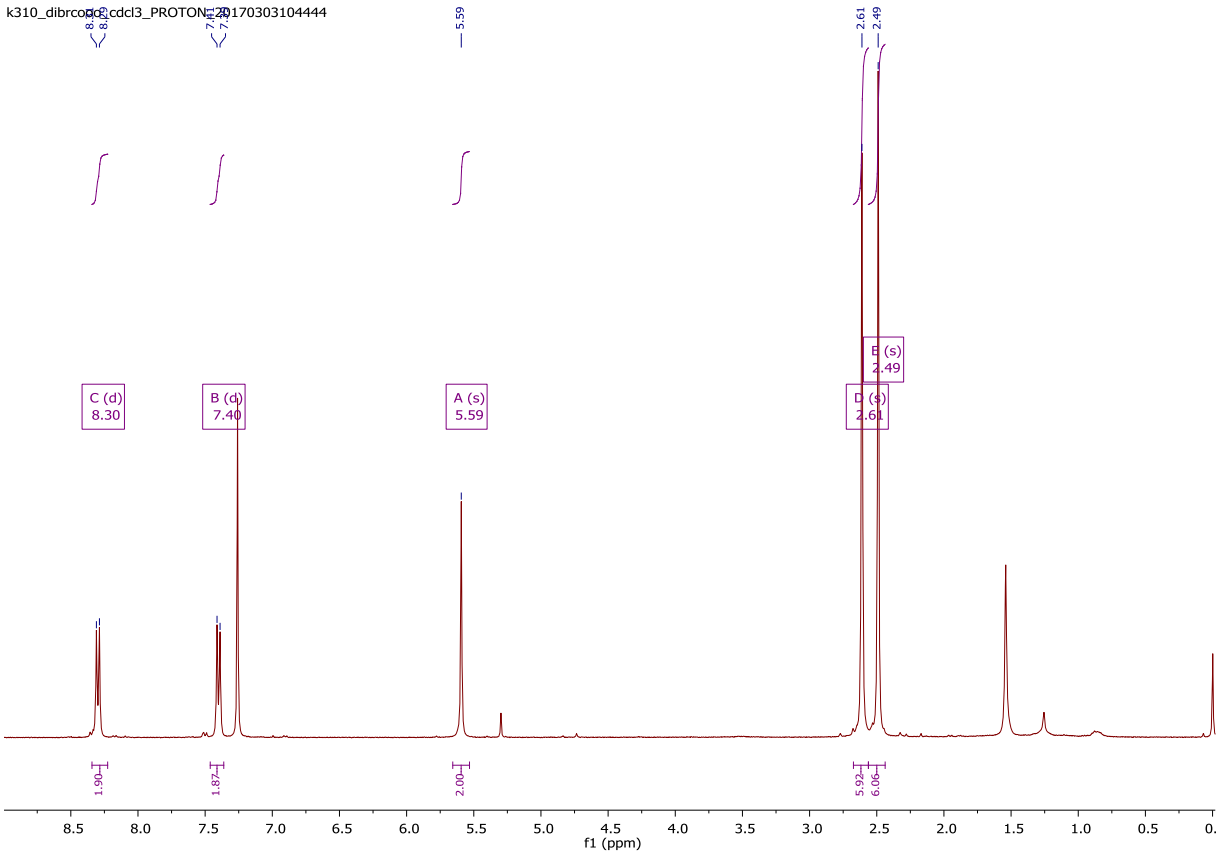

^{19}F NMR

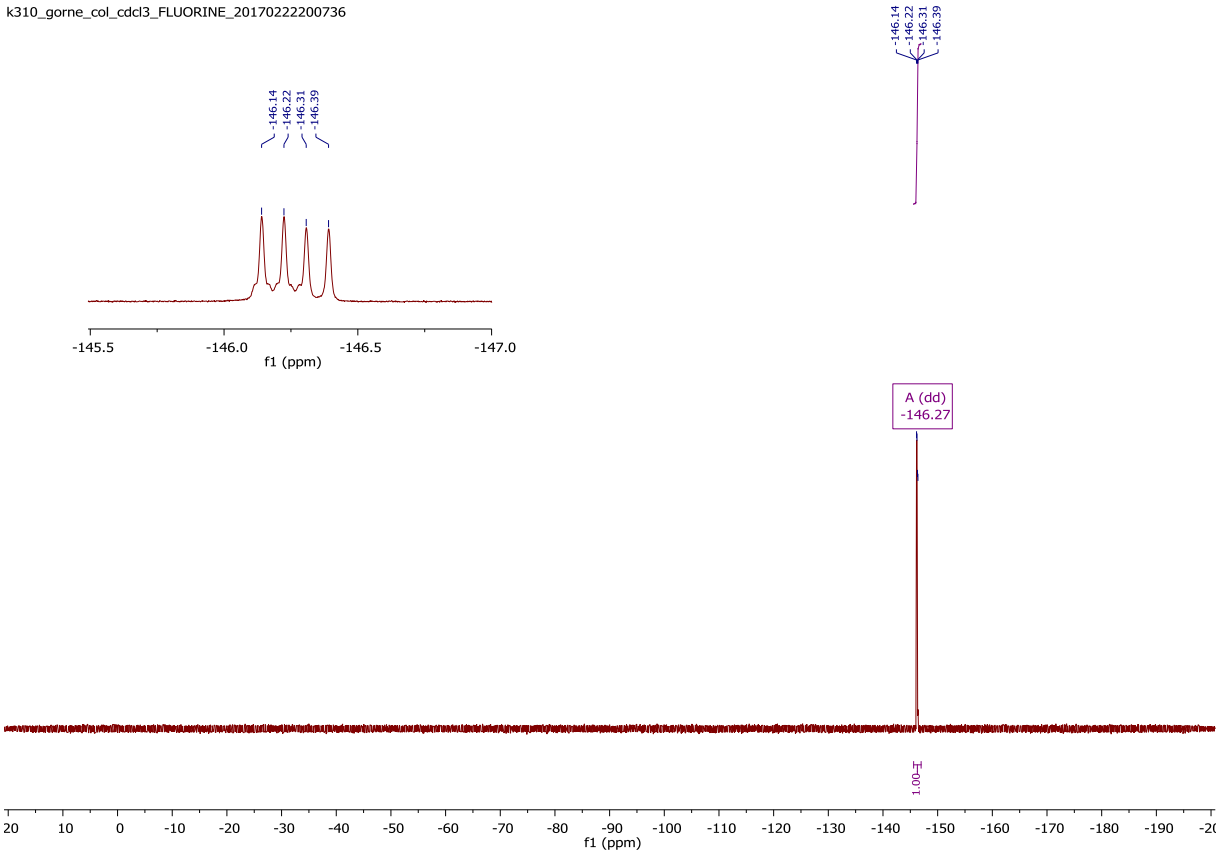

^{1}H COSY NMR

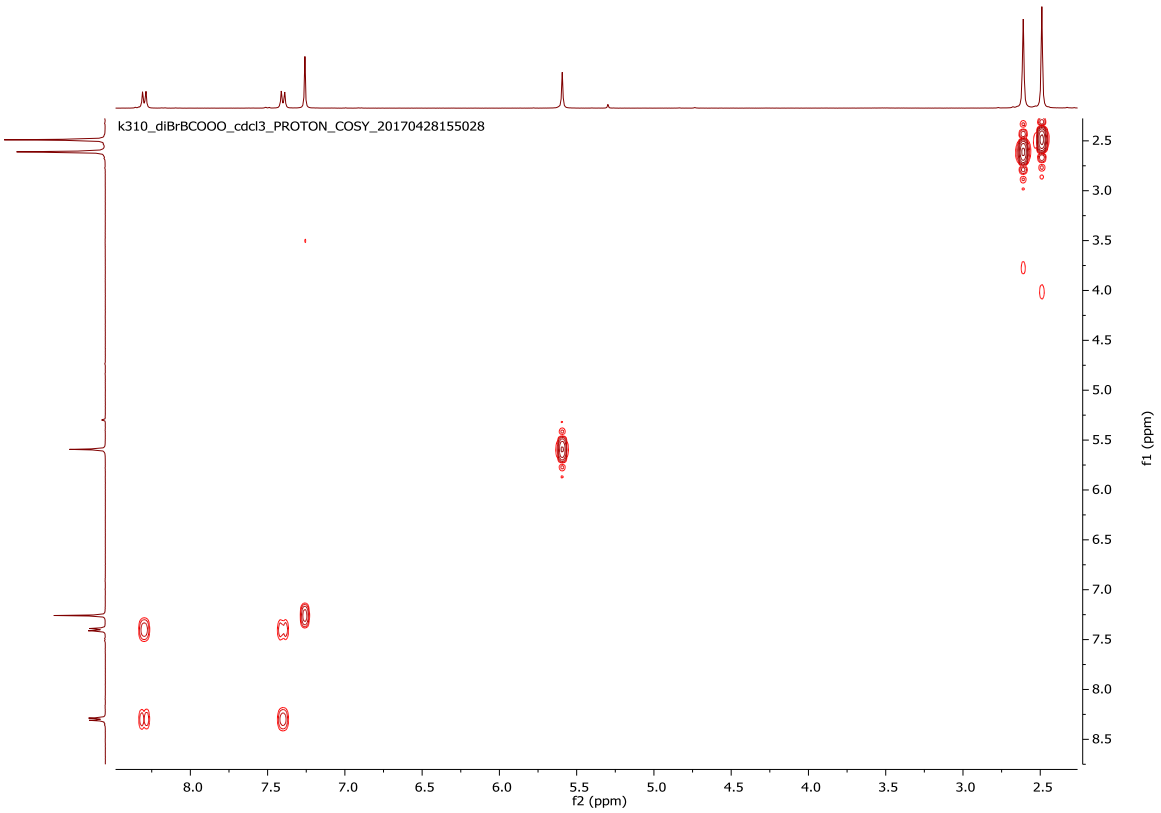

$^{1}H/^{13}C$ NMR ASAPHMQC

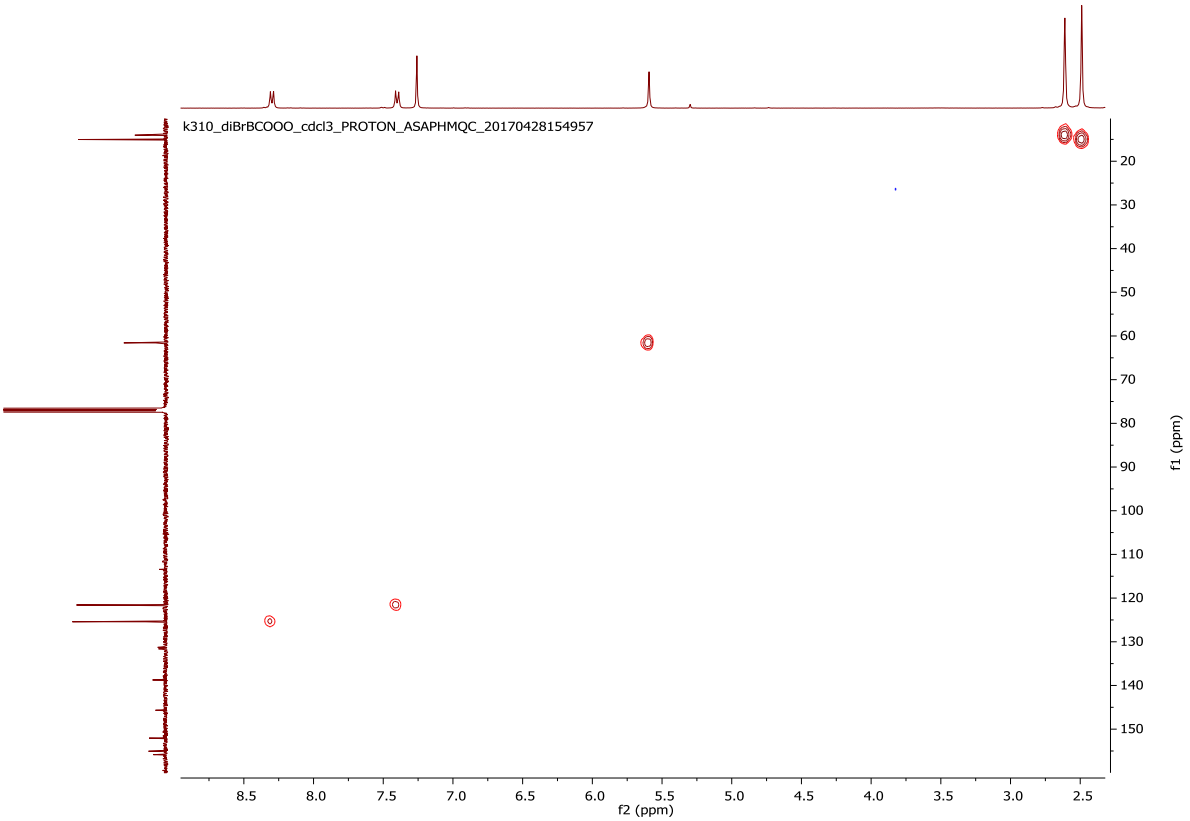

^{13}C NMR

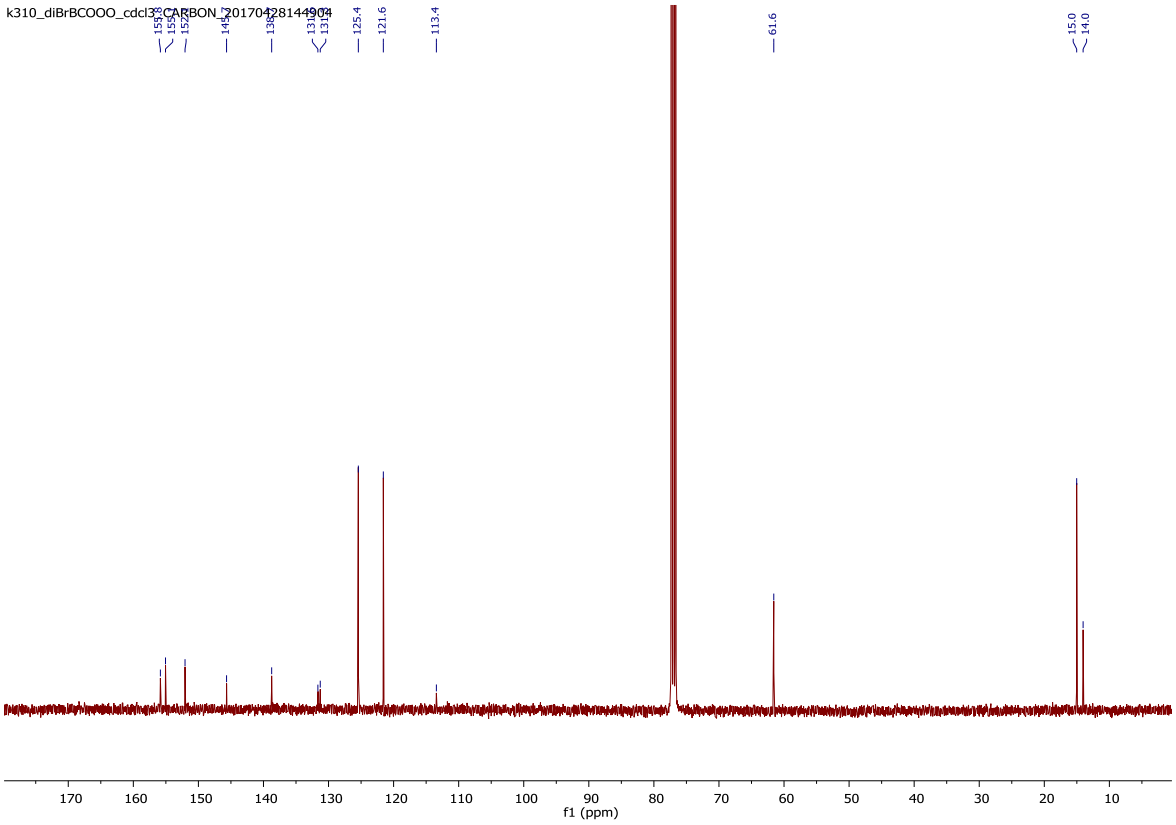

(5,5-difluoro-2,8-diiodo-1,3,7,9-tetramethyl-5H-4l4,5l4-dipyrrolo[1,2-c:2',1'-f][1,3,2]diazaborinin-10-yl)methyl (4-nitrophenyl) carbonate (**6**)

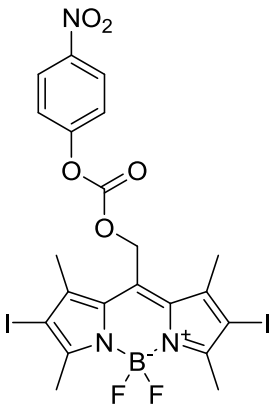

^{1}H NMR

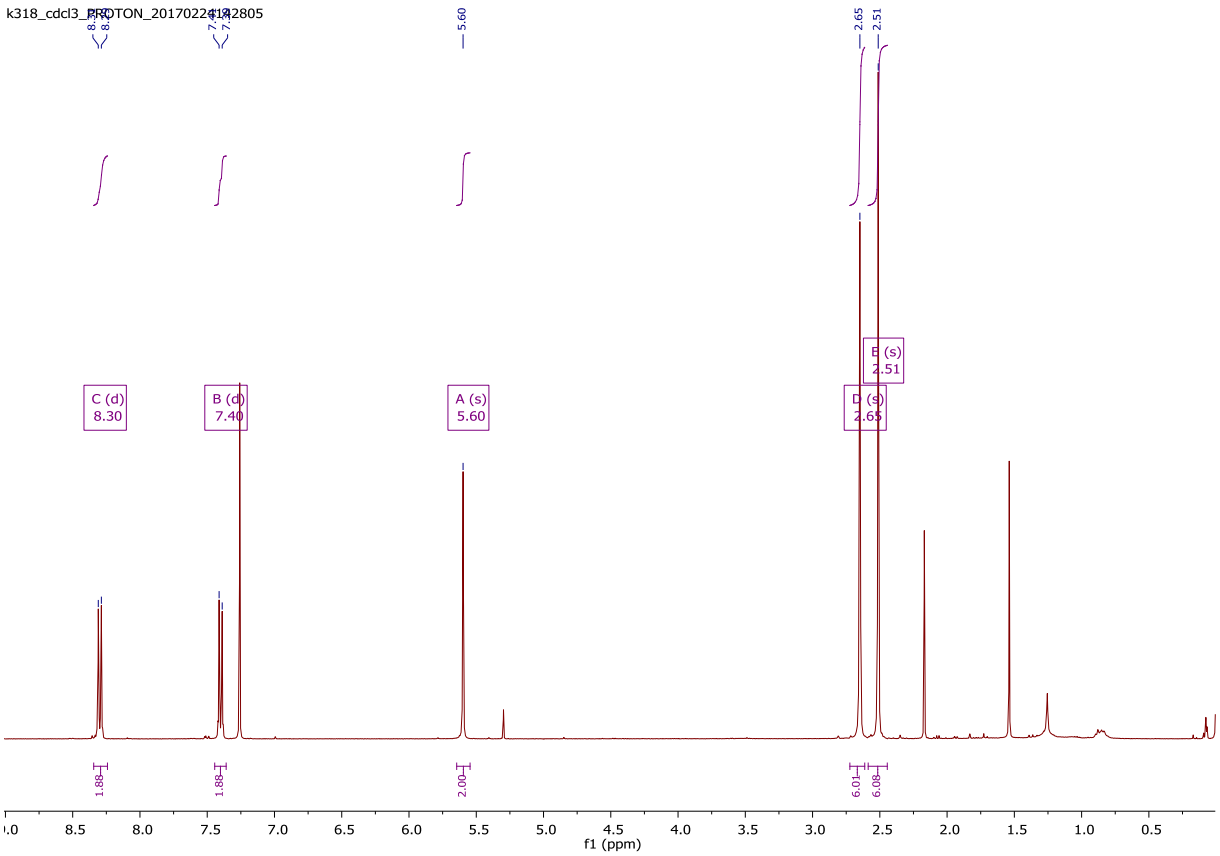

^{19}F NMR

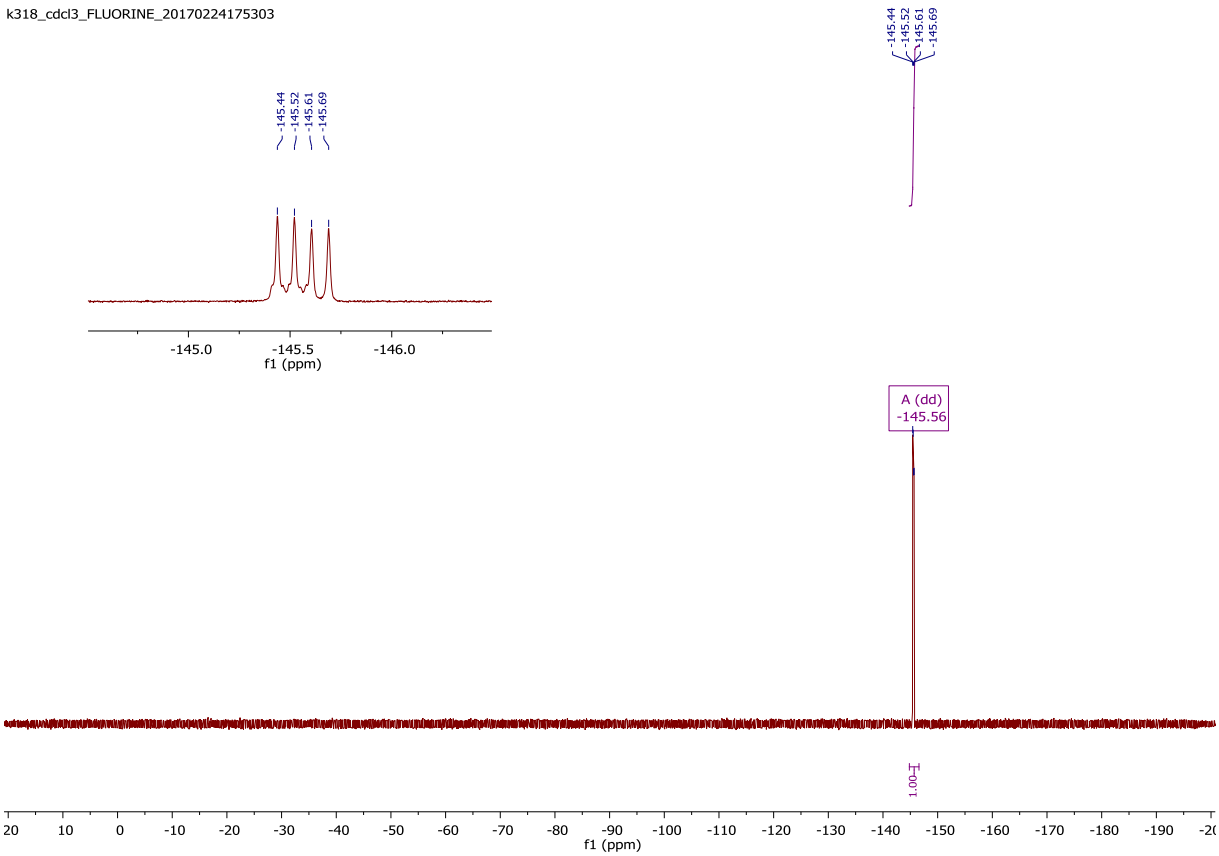

^{1}H COSY NMR

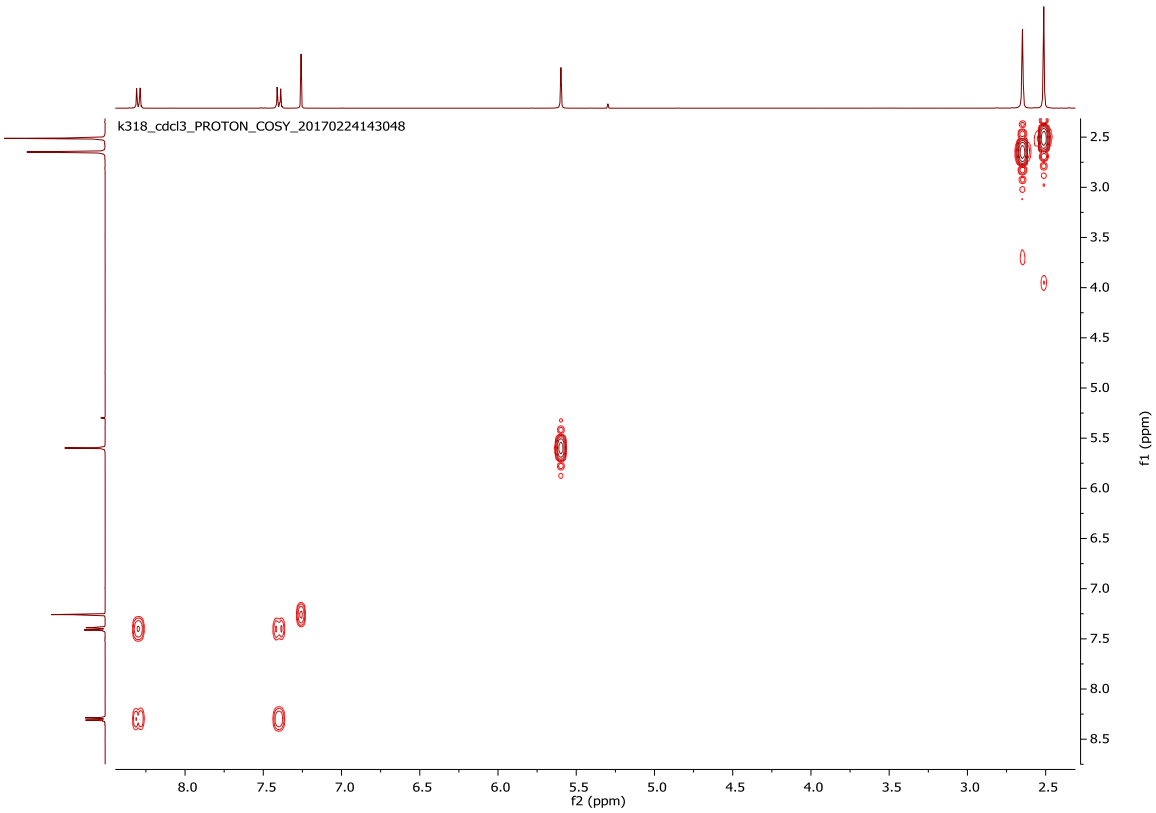

$^{1}H/^{13}C$ NMR ASAPHMQC

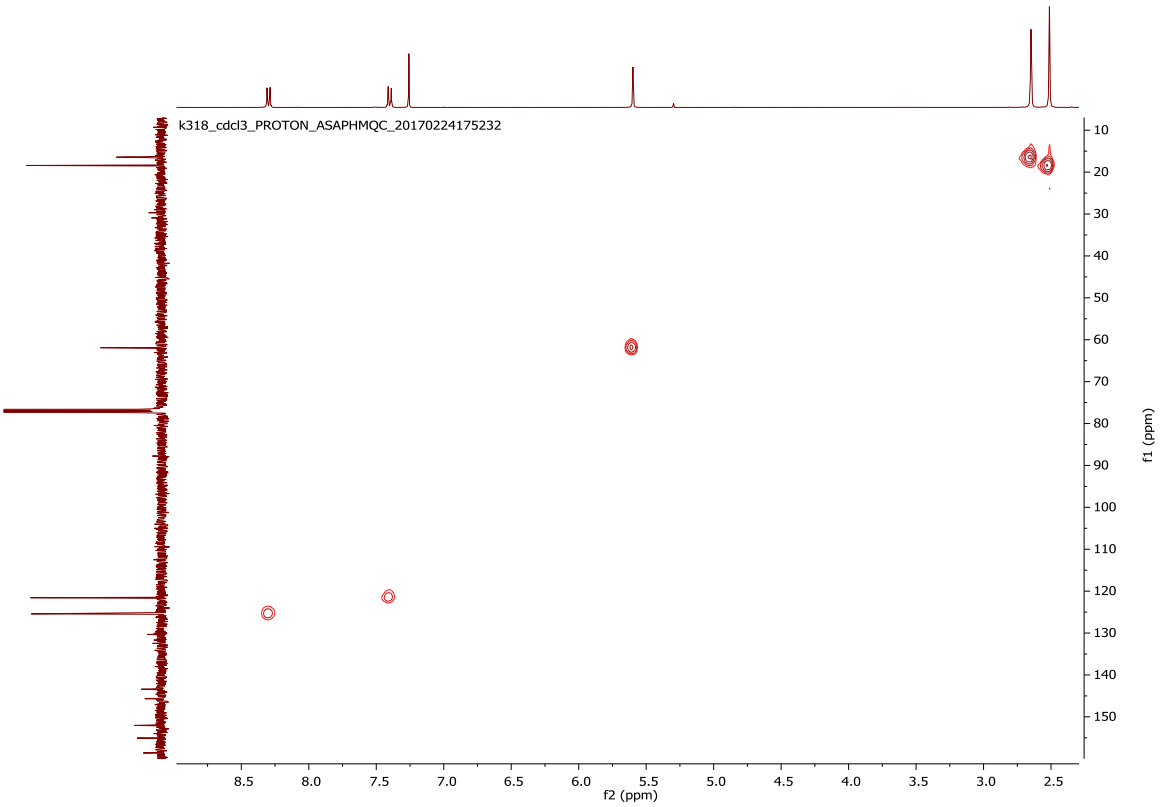

^{13}C NMR

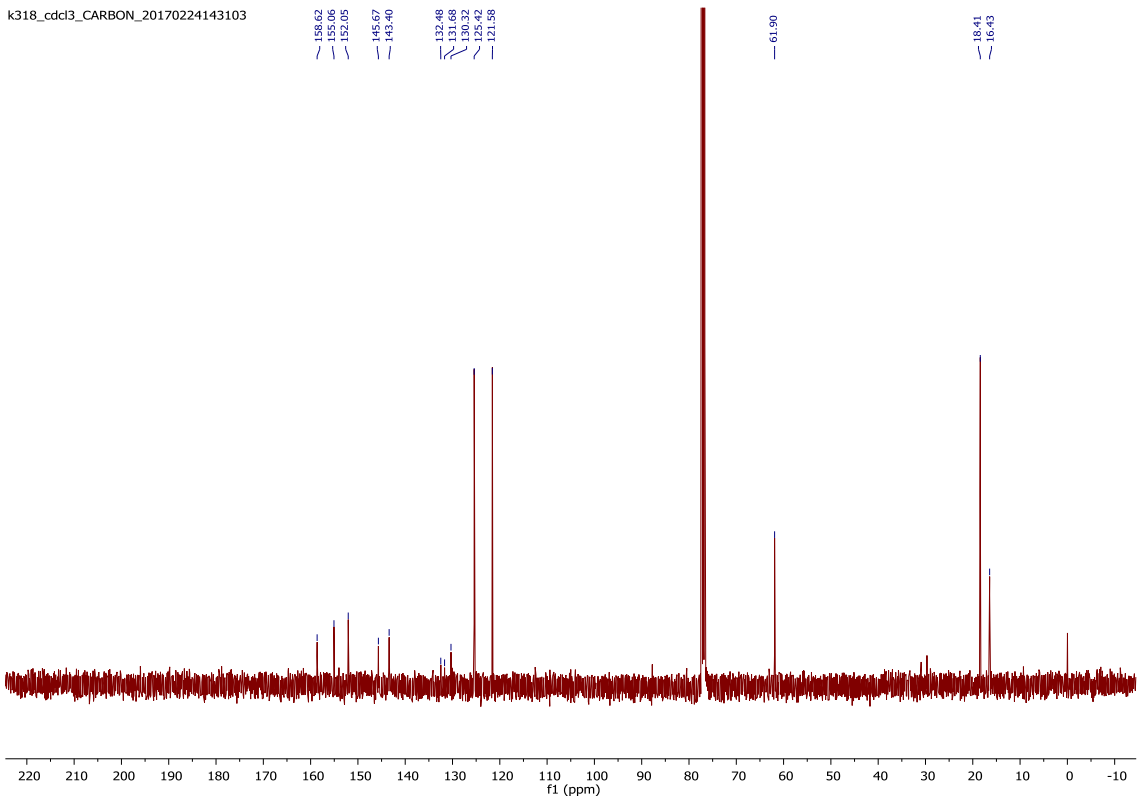

(5,5-difluoro-1,3,7,9-tetramethyl-5H-4l4,5l4-dipyrrolo[1,2-c:2',1'-f][1,3,2]diazaborinin-10-yl)methyl (4-fluorobenzyl)carbamate (**7**)

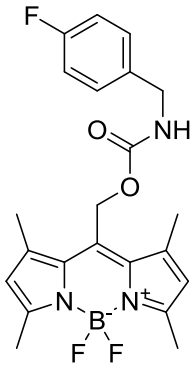

^{1}H NMR

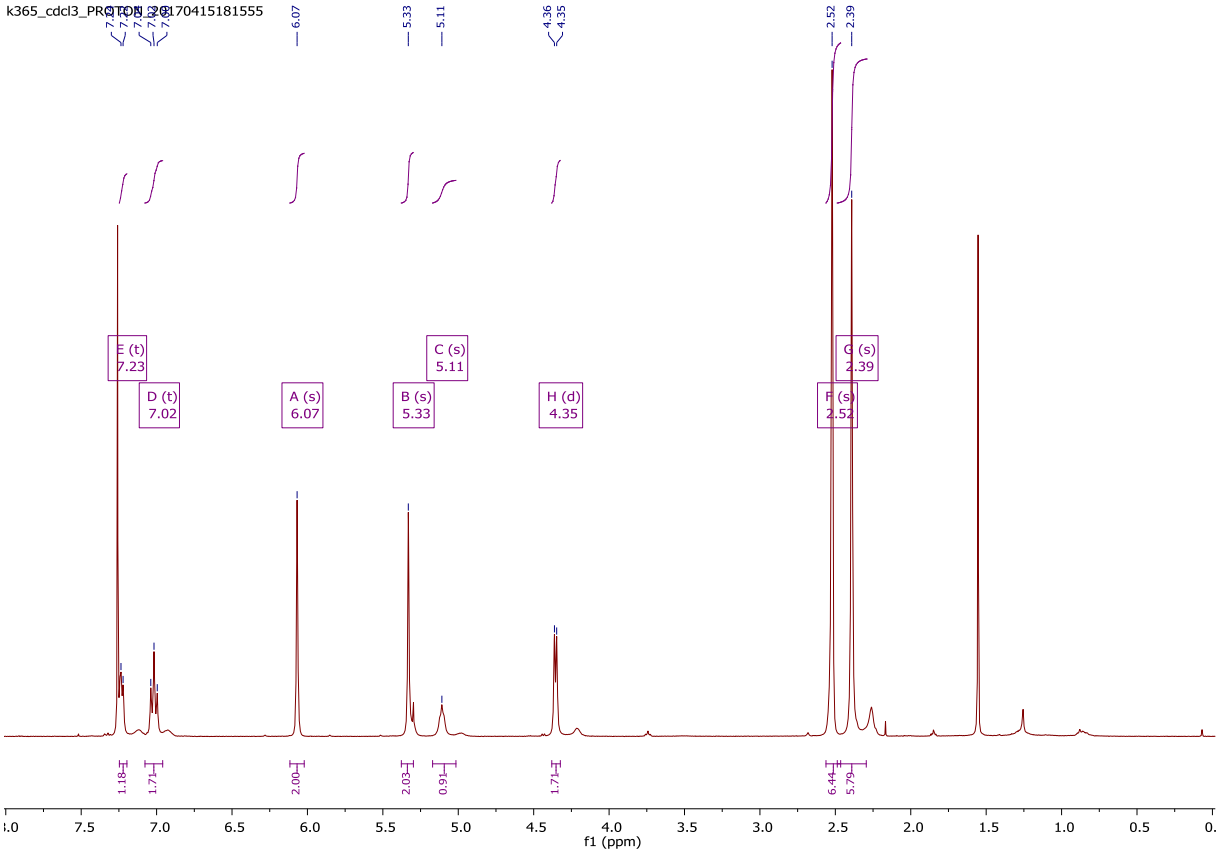

^{19}F NMR

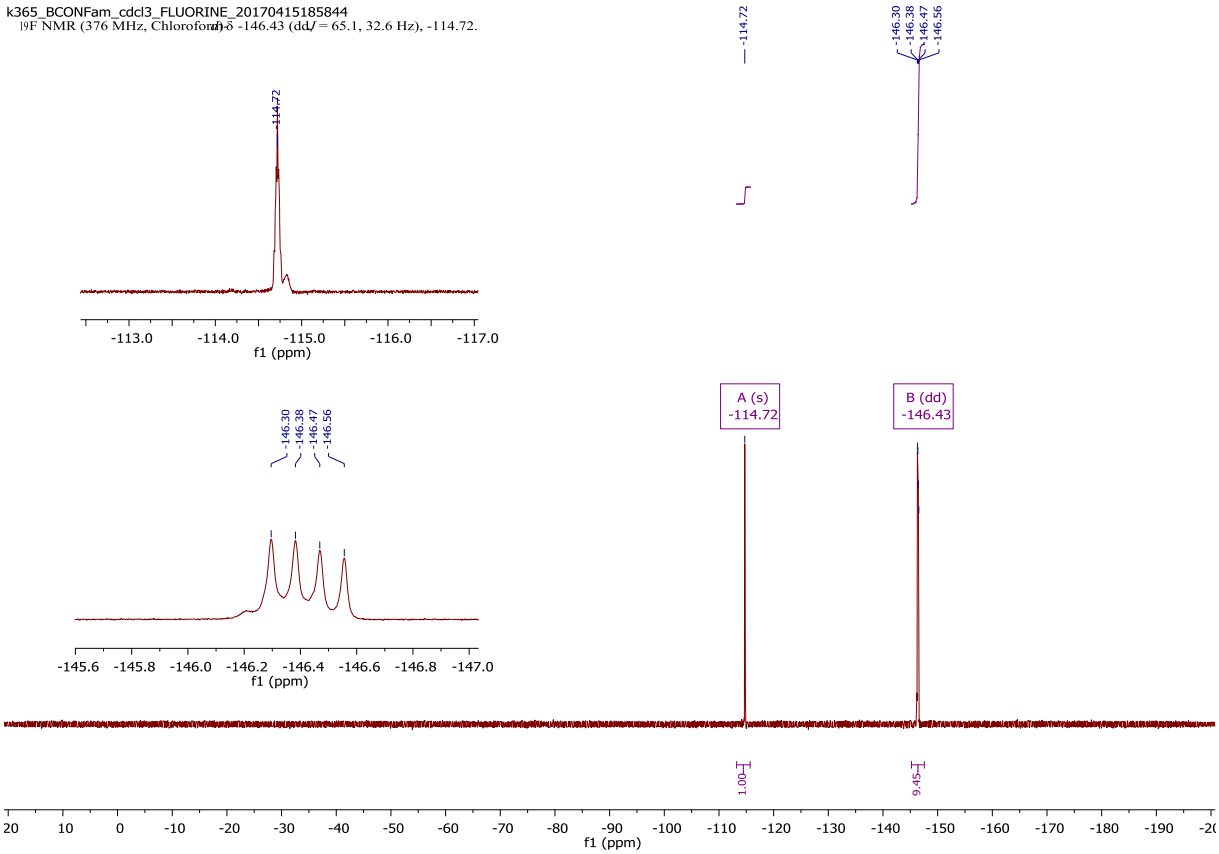

^{1}H COSY NMR

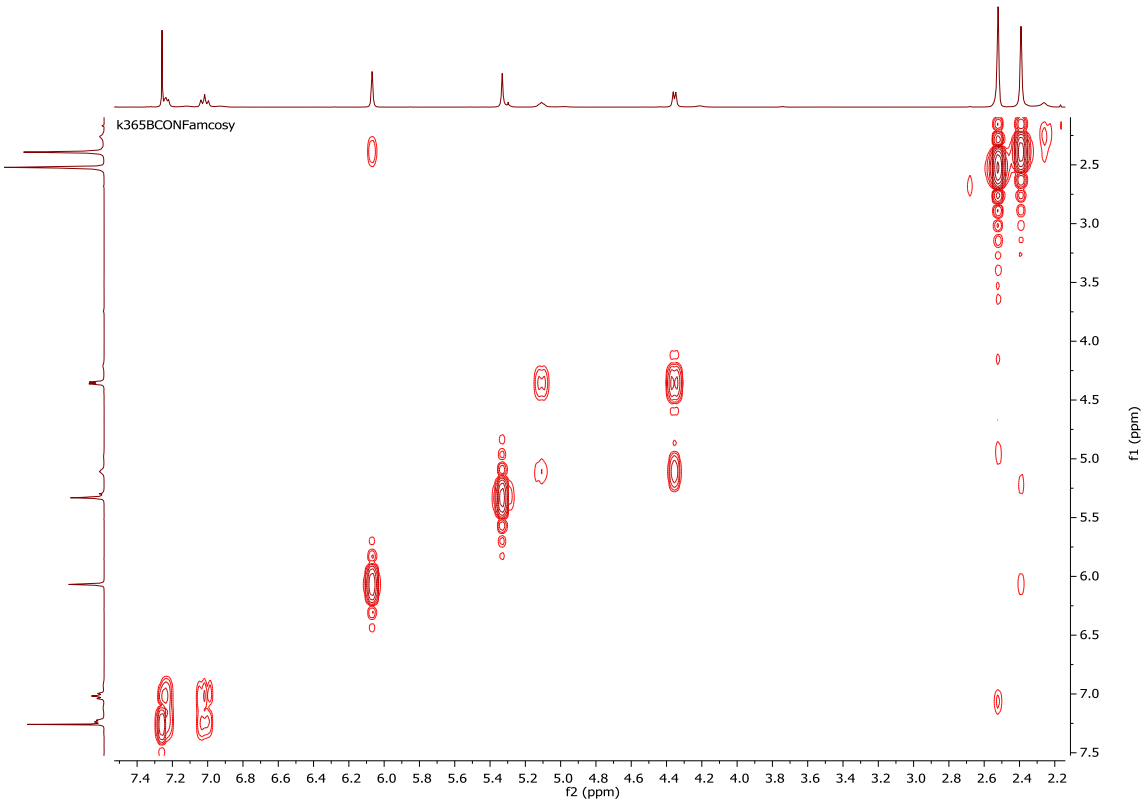

$^{1}H/^{13}C$ NMR ASAPHMQC

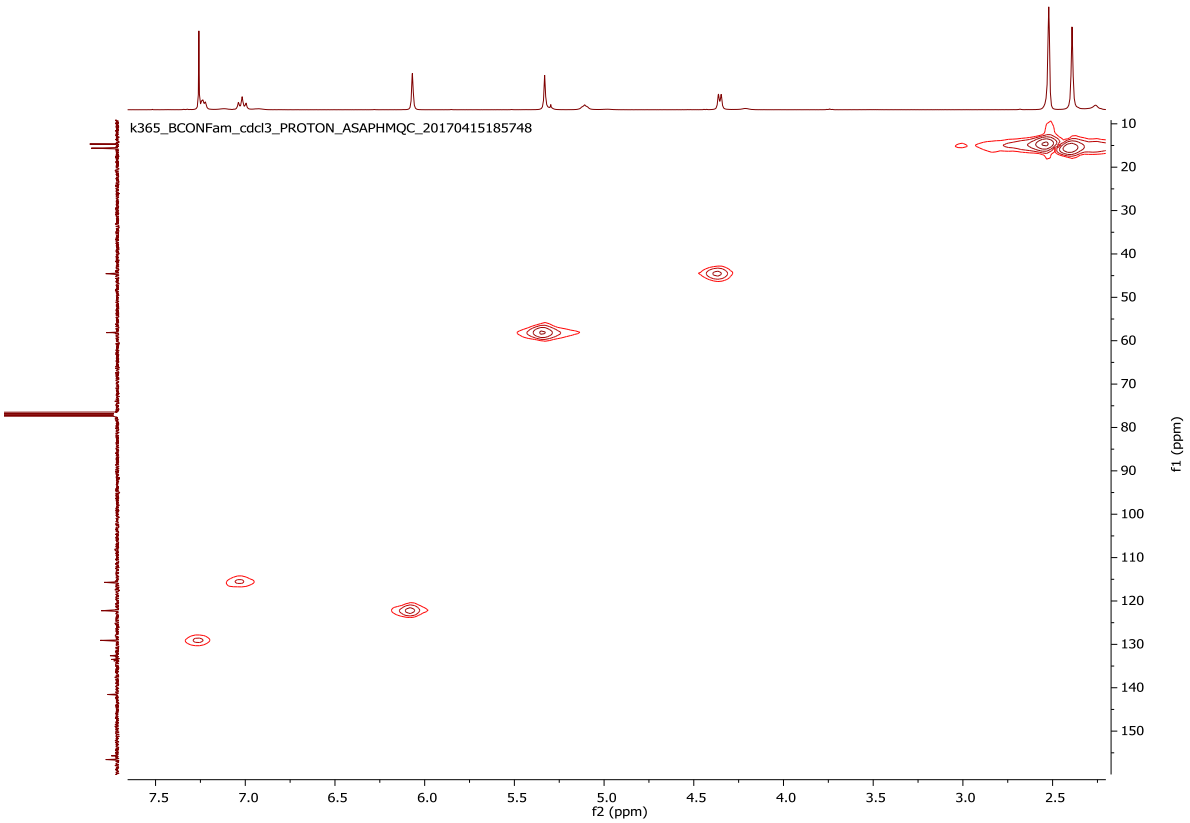

^{13}C NMR

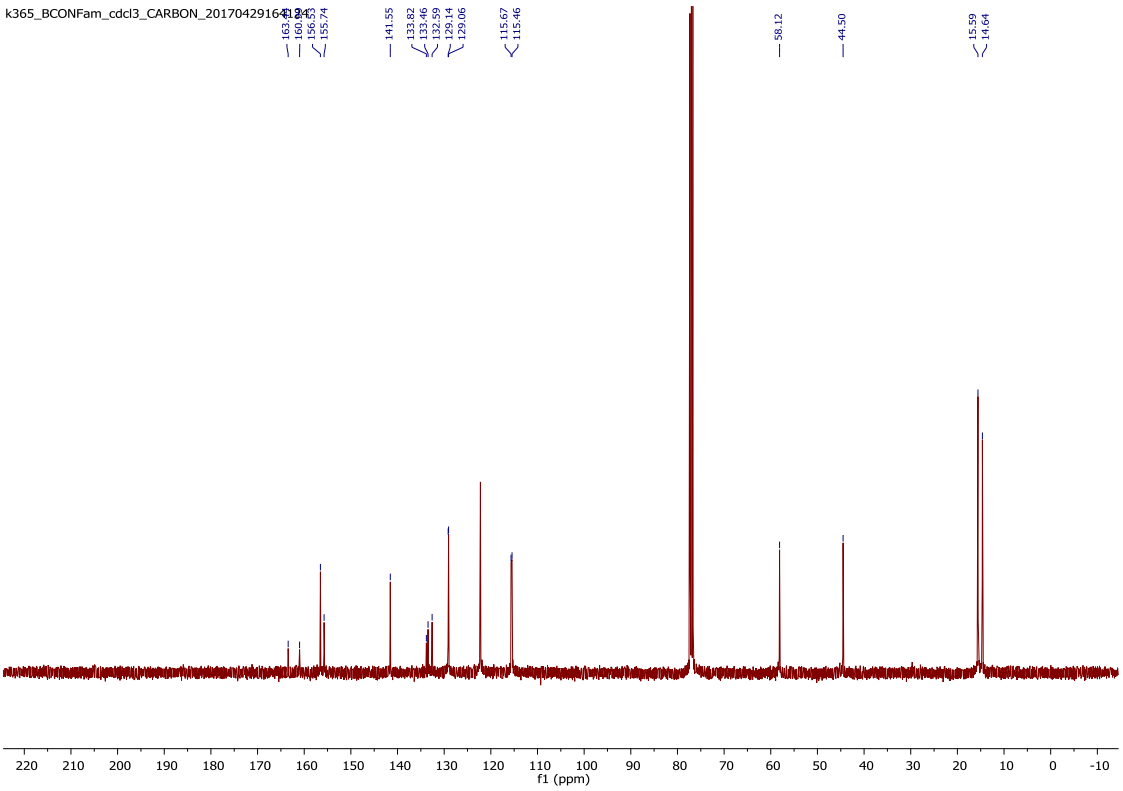

(2,8-dichloro-5,5-difluoro-1,3,7,9-tetramethyl-5H-4l4,5l4-dipyrrolo[1,2-c:2',1'-f][1,3,2]diazaborinin-10-yl)methyl (4-fluorobenzyl)carbamate (**8**)

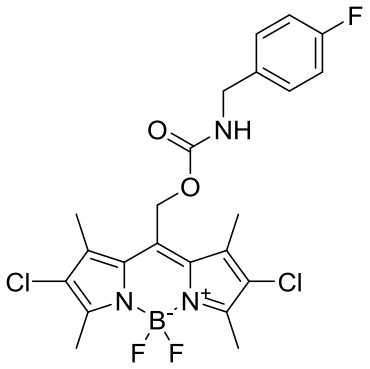

^{1}H NMR

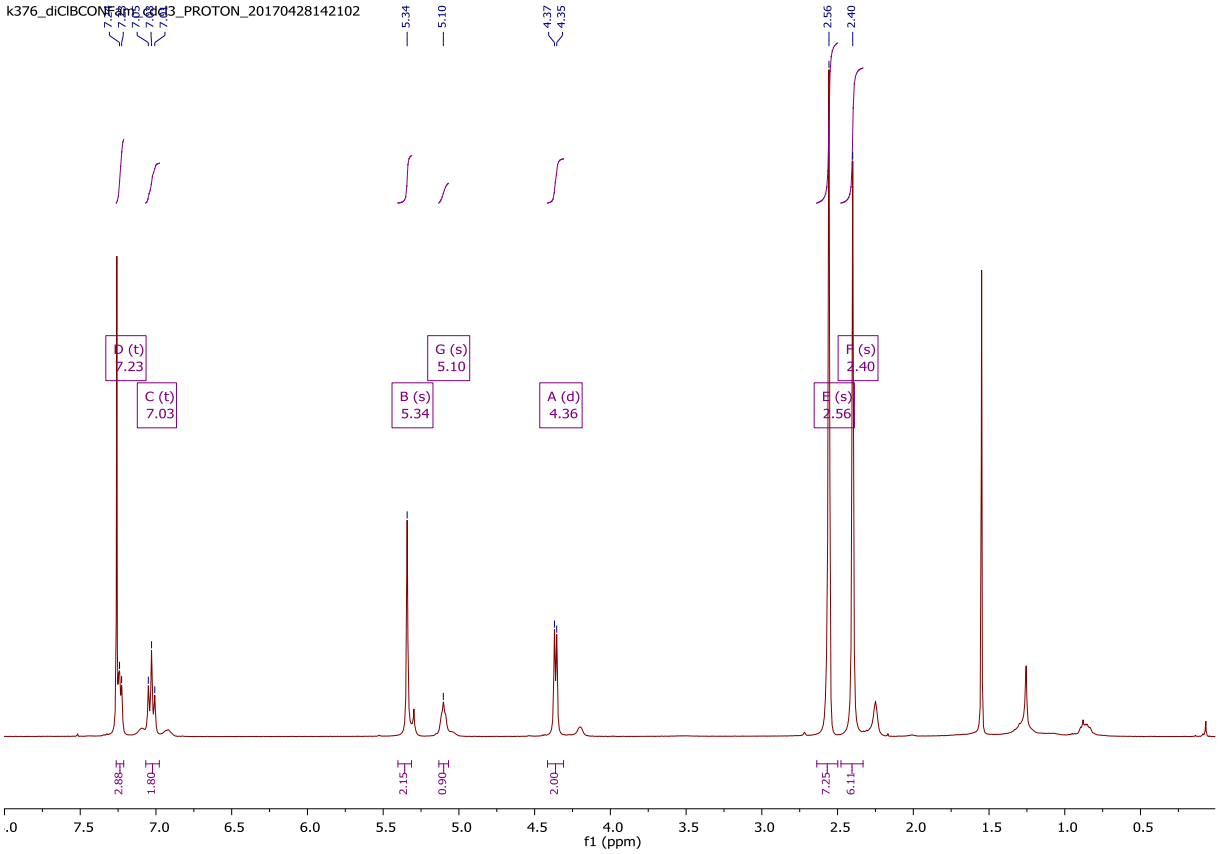

^{19}F NMR

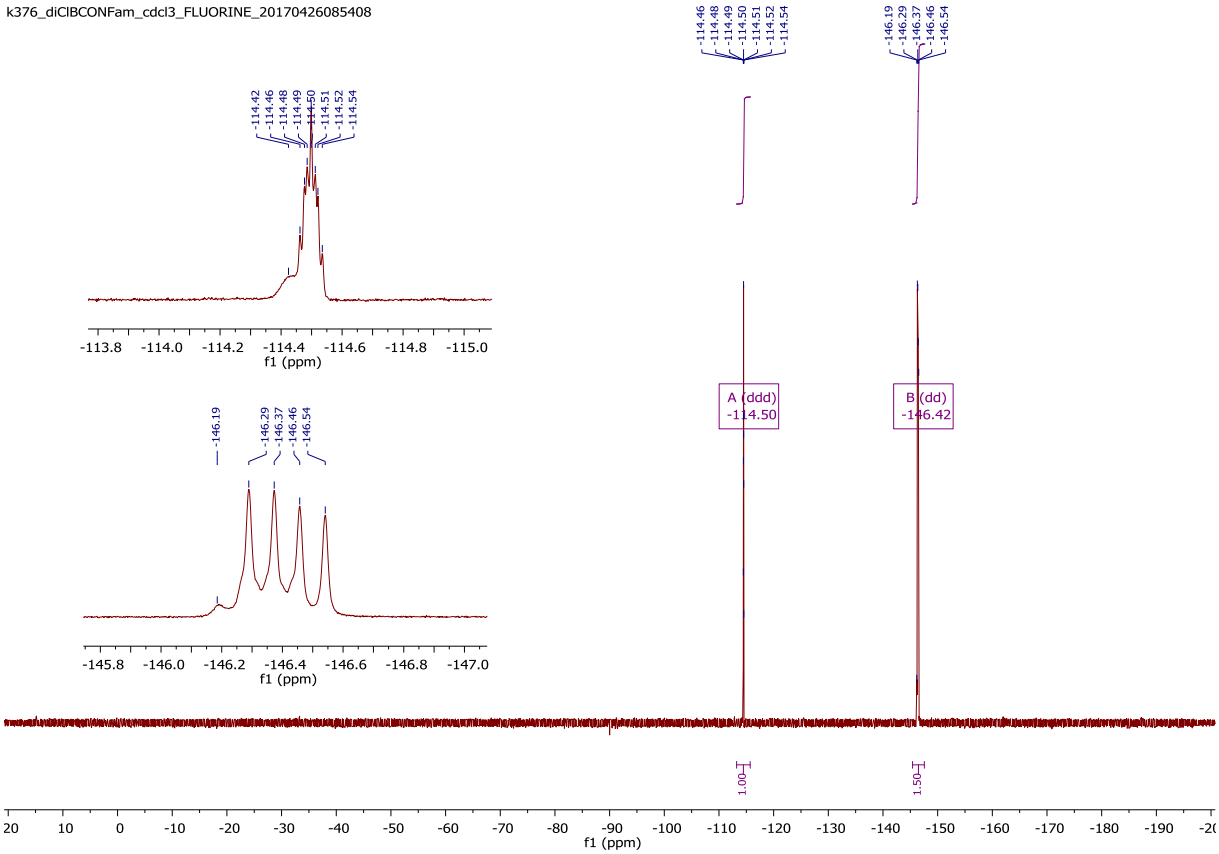

^{1}H COSY NMR

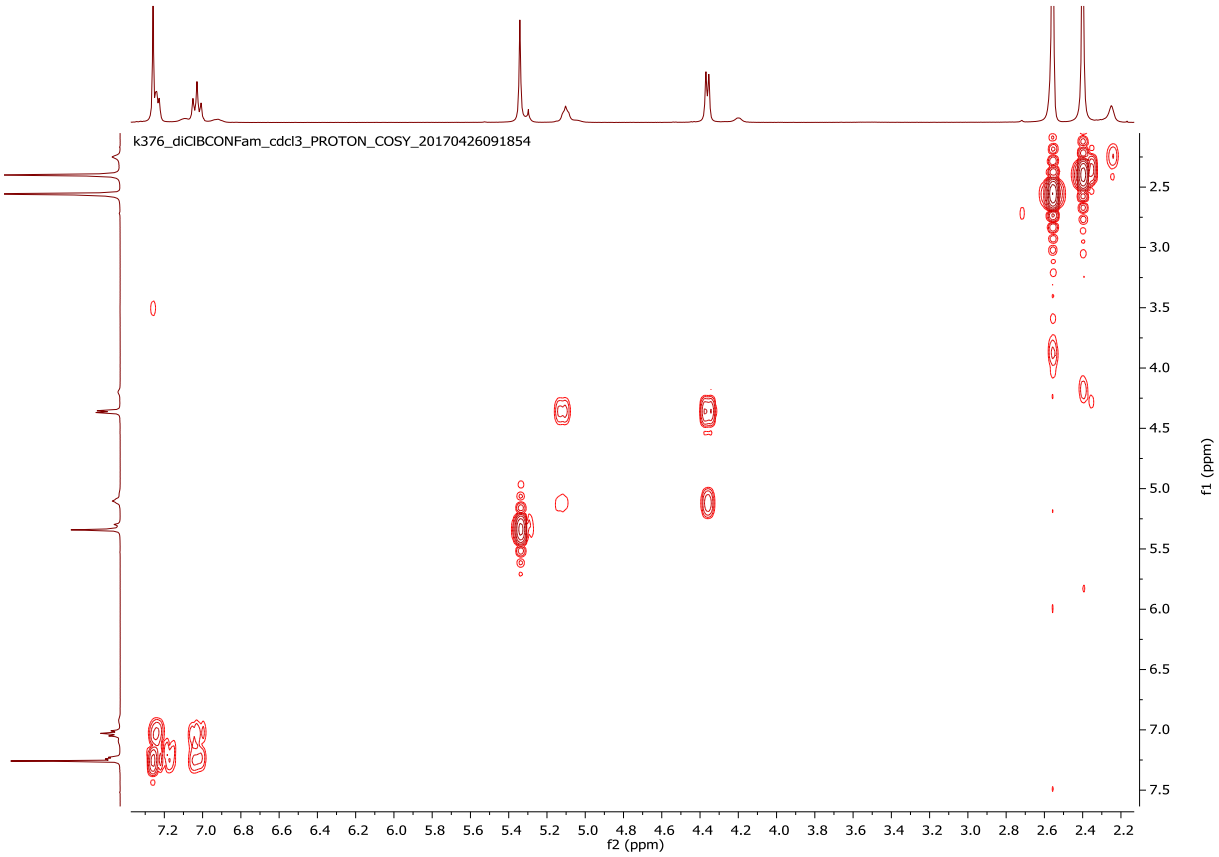

$^{1}H/^{13}C$ NMR ASAPHMQC

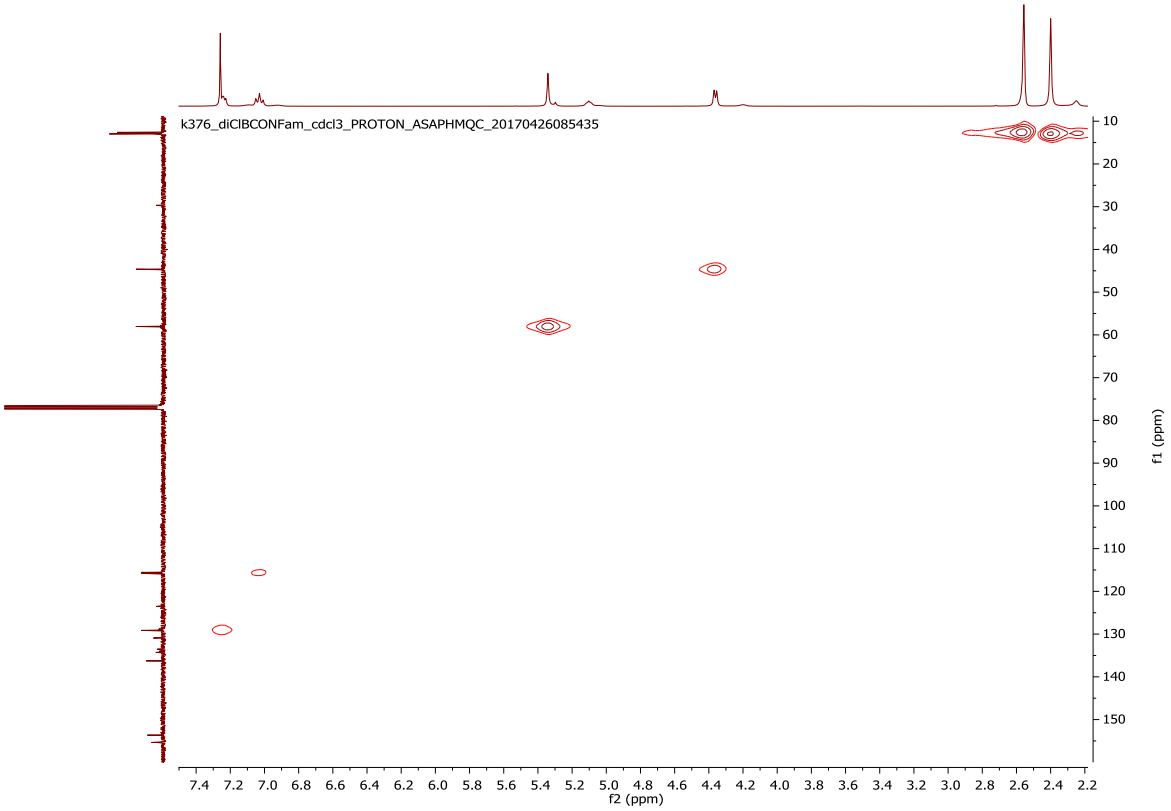

^{13}C NMR

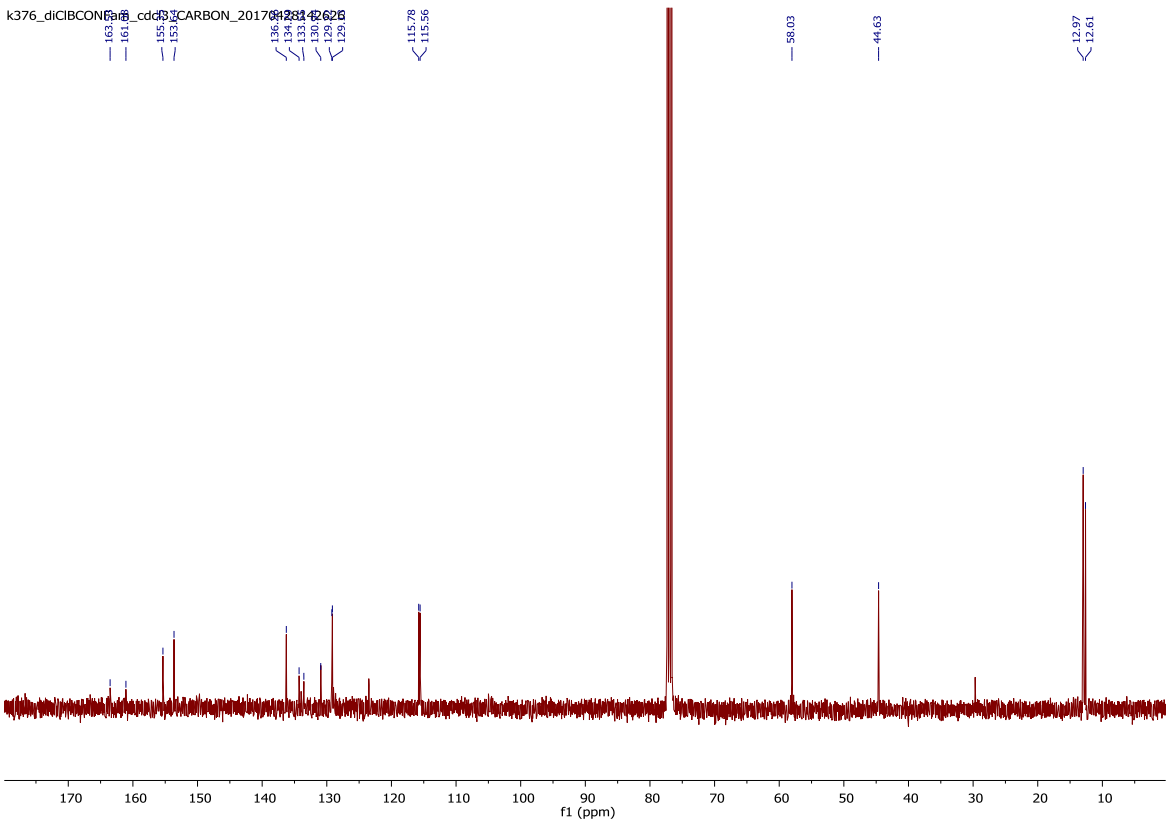

(2,8-dibromo-5,5-difluoro-1,3,7,9-tetramethyl-5H-4l4,5l4-dipyrrolo[1,2-c:2',1'-f][1,3,2]diazaborinin-10-yl)methyl (4-fluorobenzyl)carbamate (**9**)

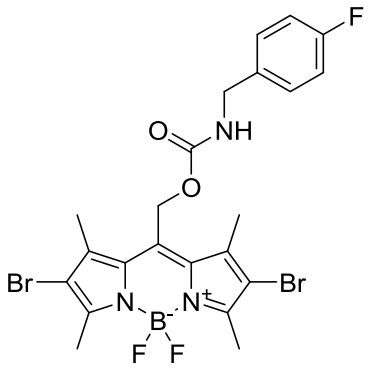

^{1}H NMR

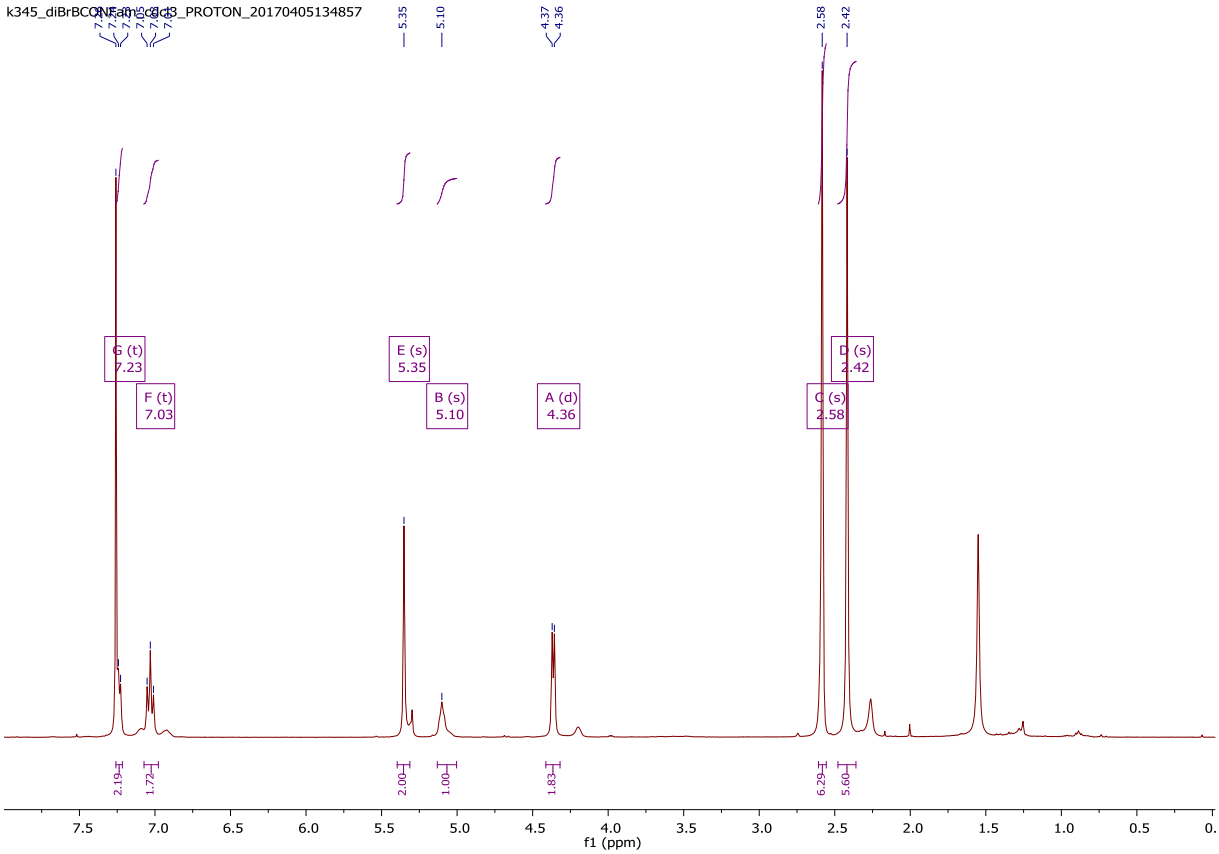

^{19}F NMR

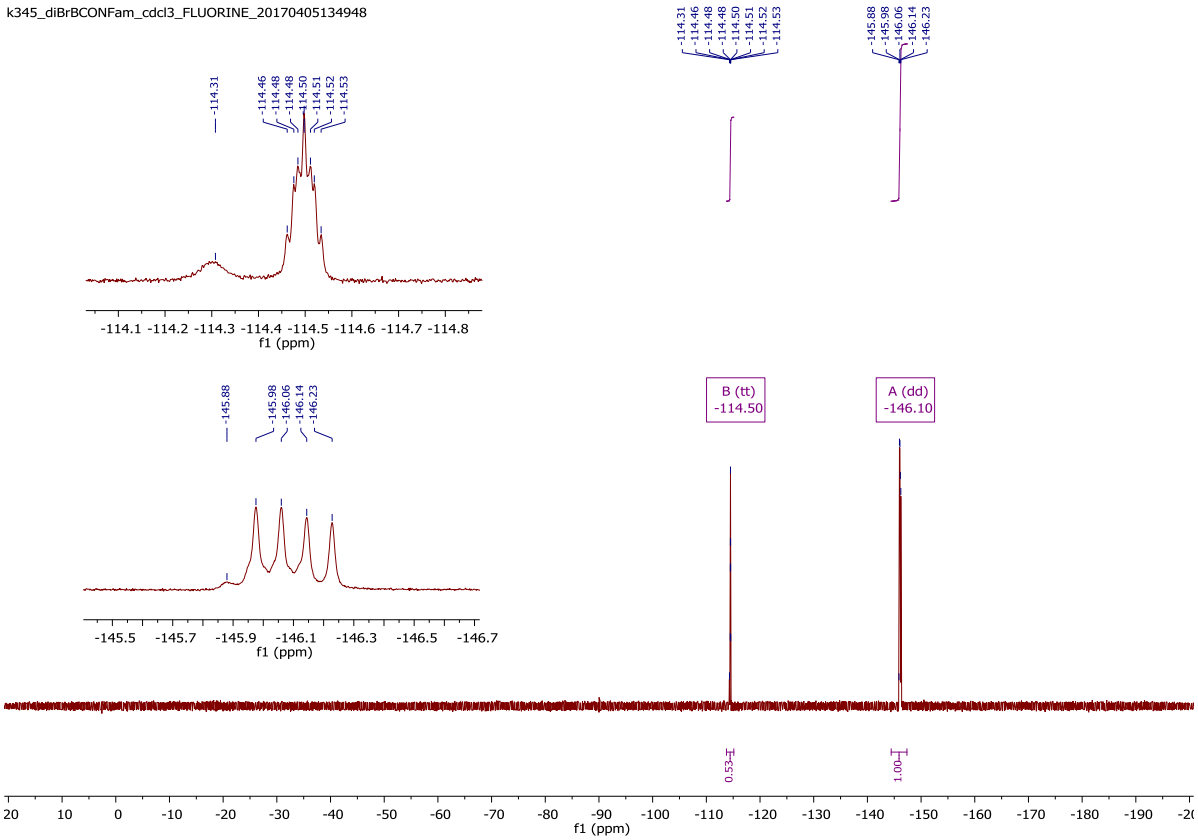

^{1}H COSY NMR

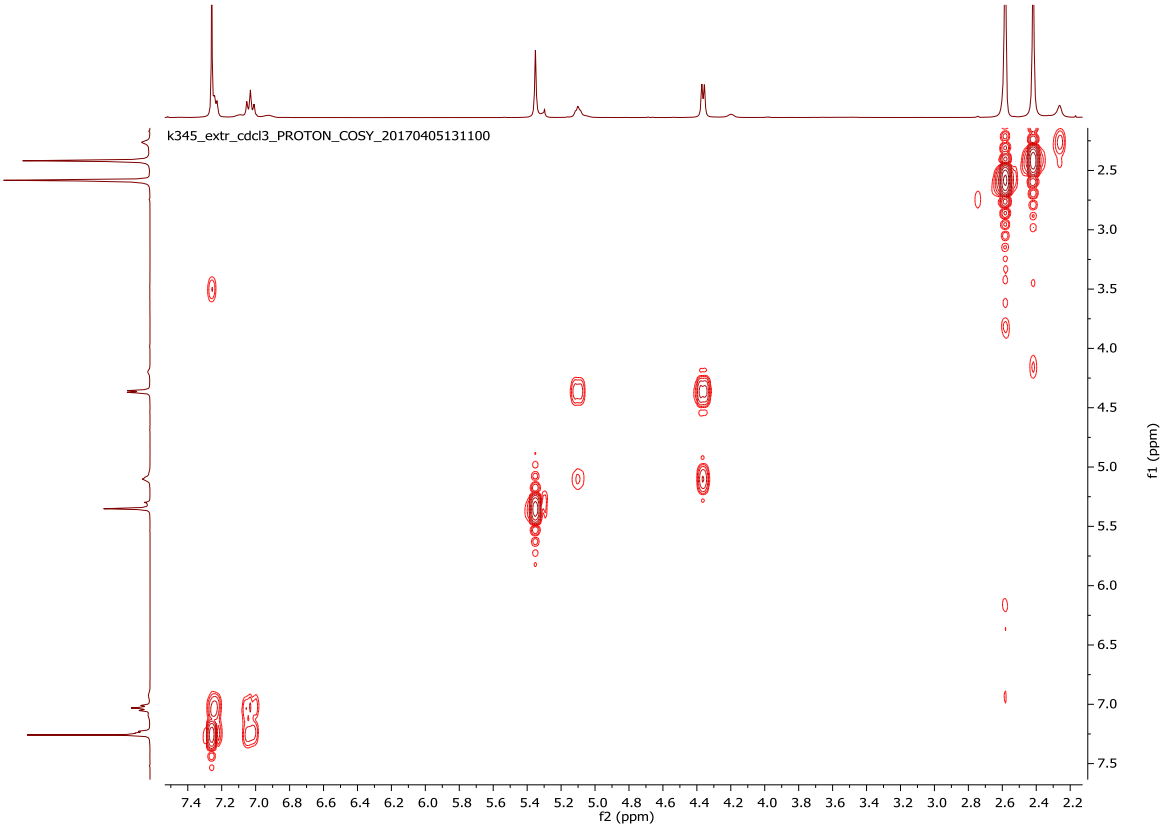

$^{1}H/^{13}C$ NMR ASAPHMQC

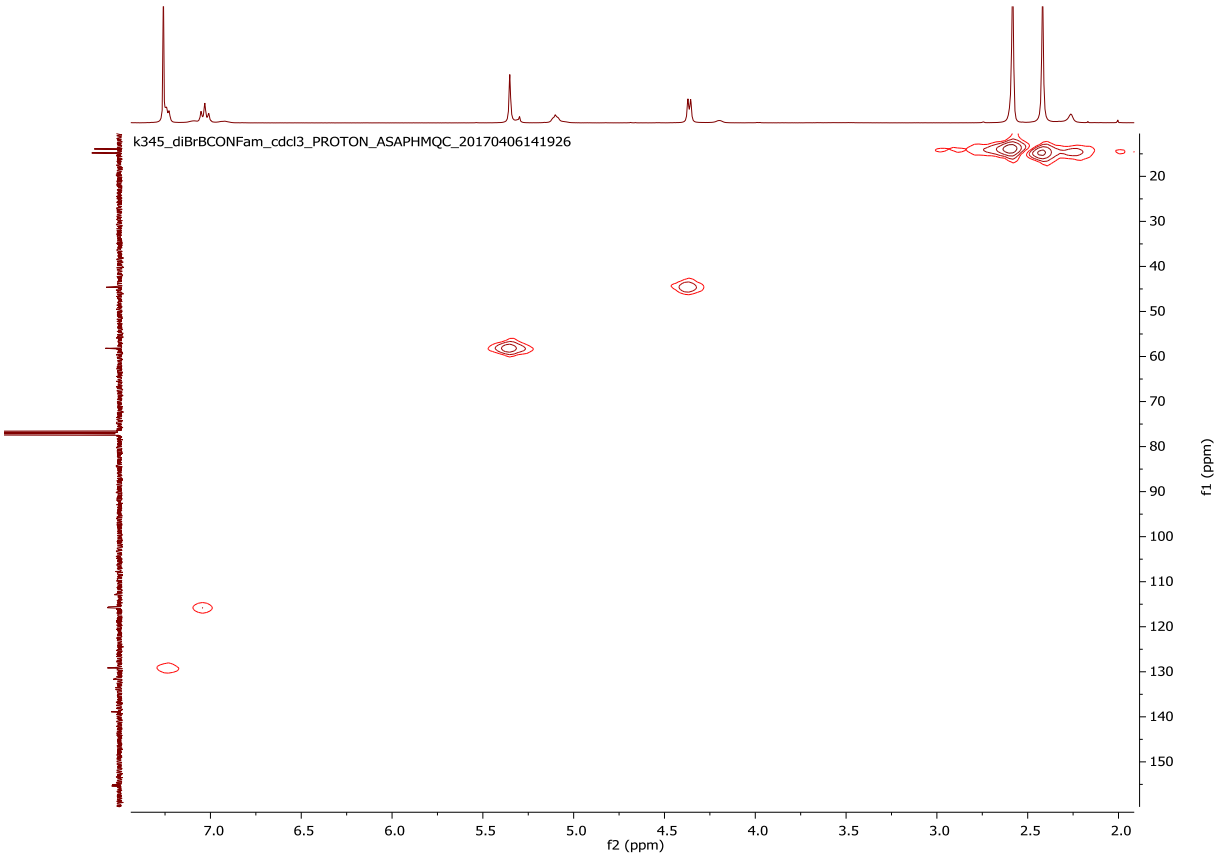

^{13}C NMR

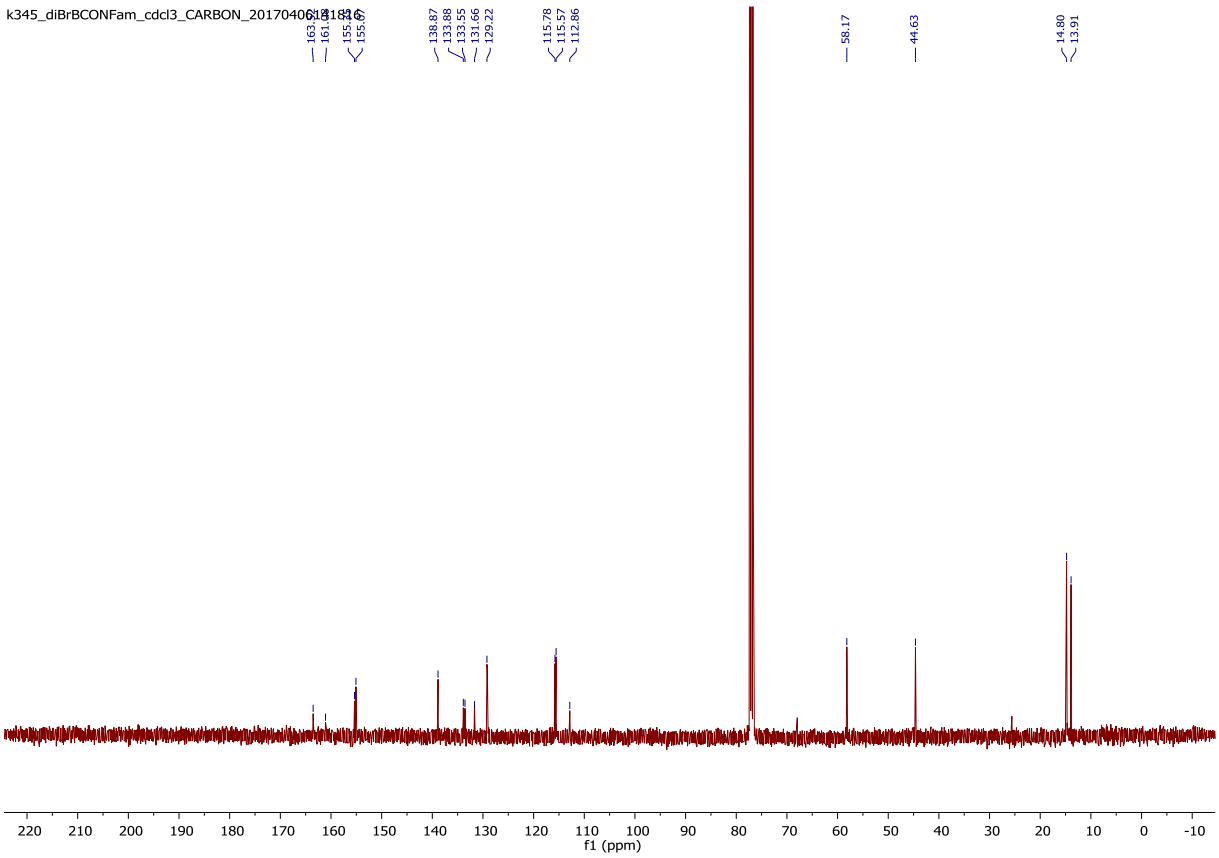

(2,8-diiodo-5,5-difluoro-1,3,7,9-tetramethyl-5H-4l4,5l4-dipyrrolo[1,2-c:2',1'-f][1,3,2]diazaborinin-10-yl)methyl (4-fluorobenzyl)carbamate (**10**)

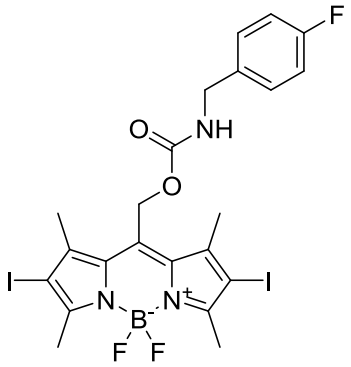

^{1}H NMR

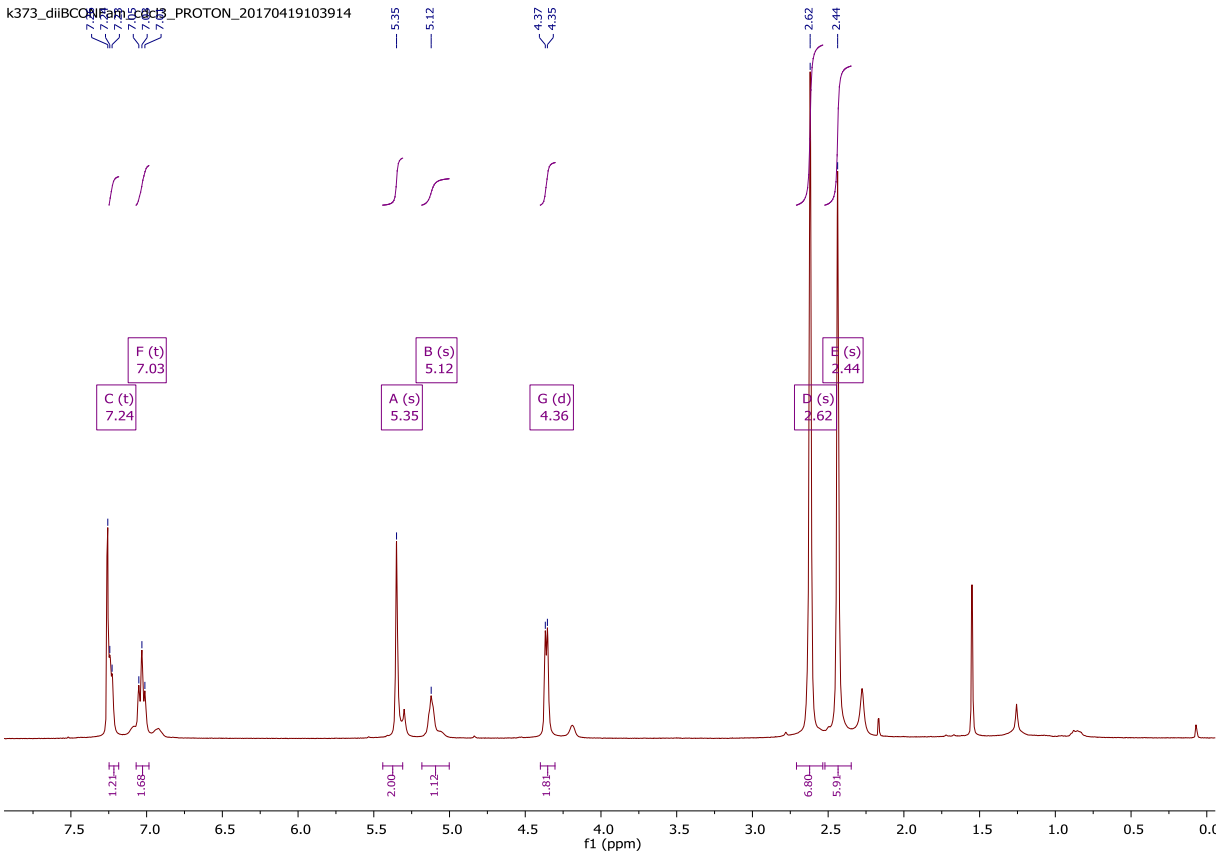

^{19}F NMR

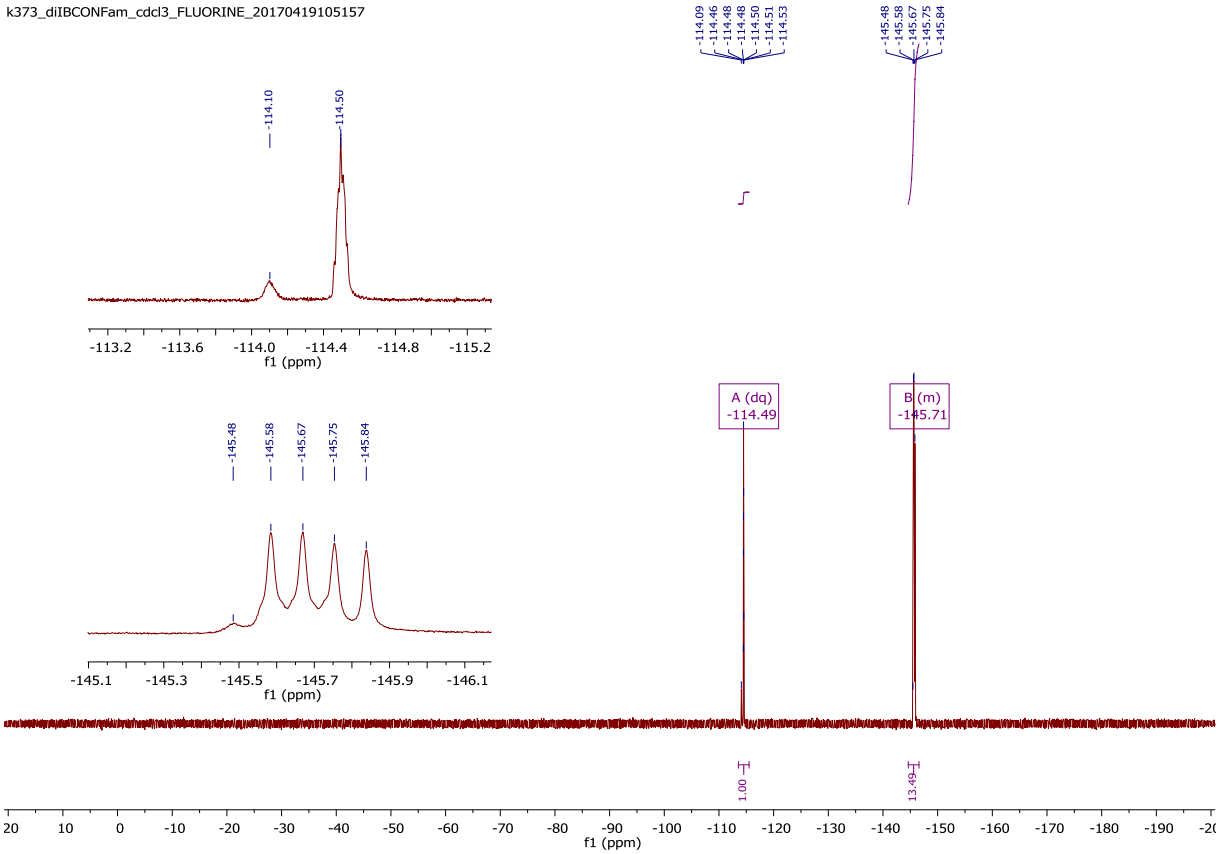

^{1}H COSY NMR

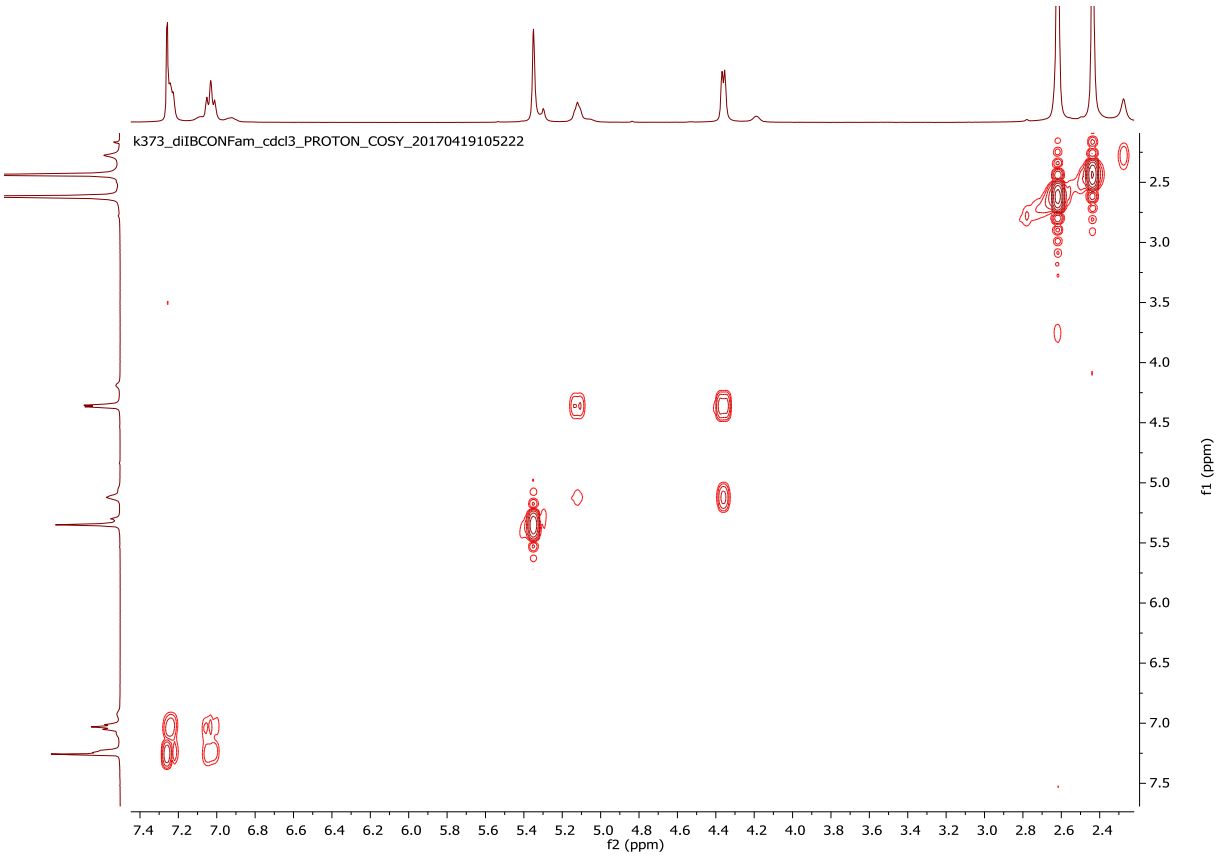

$^{1}H/^{13}C$ NMR ASAPHMQC

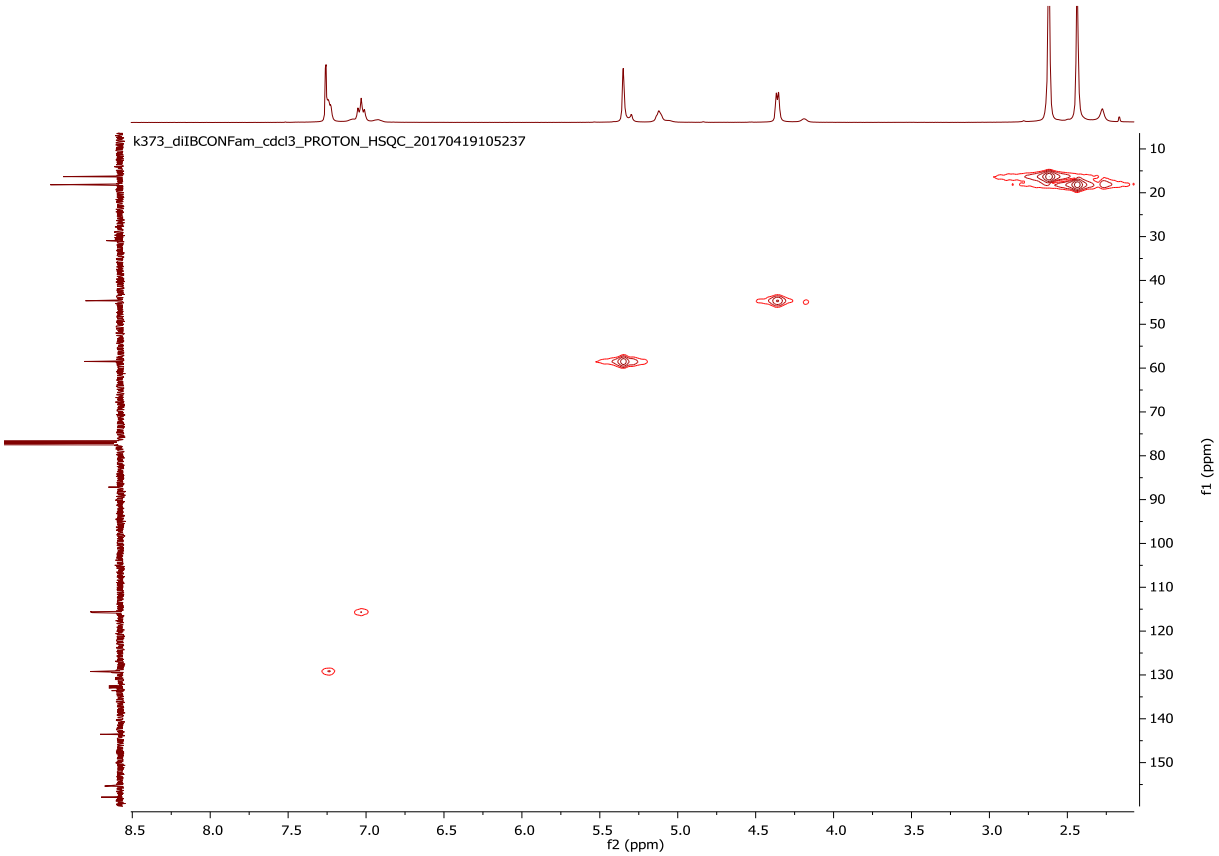

^{13}C NMR

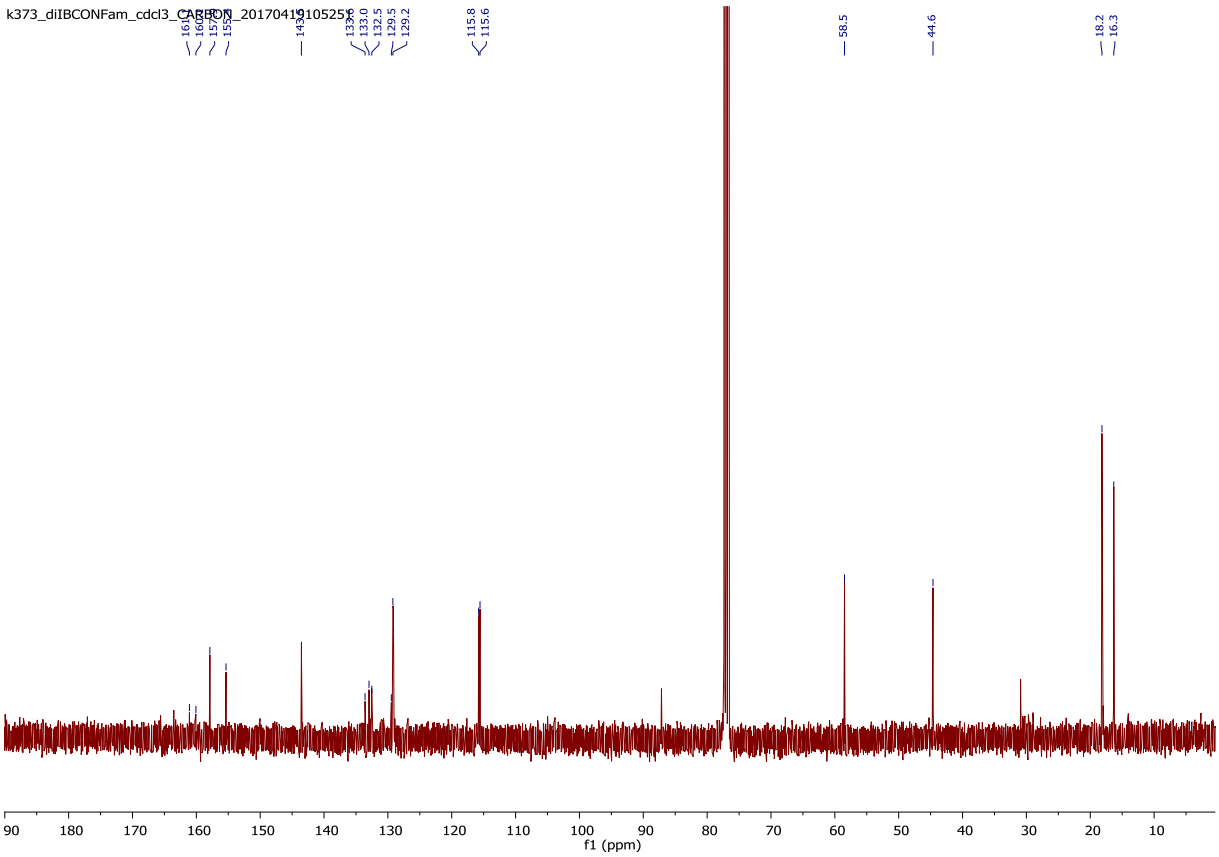

(5,5-difluoro-1,3,7,9-tetramethyl-5H-4l4,5l4-dipyrrolo[1,2-c:2',1'-f][1,3,2]diazaborinin-10-yl)methyl (4-fluorobenzyl)(methyl)carbamate (**11**)

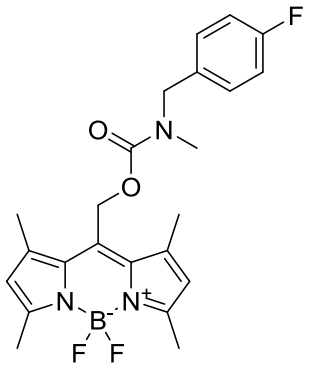

^{1}H NMR

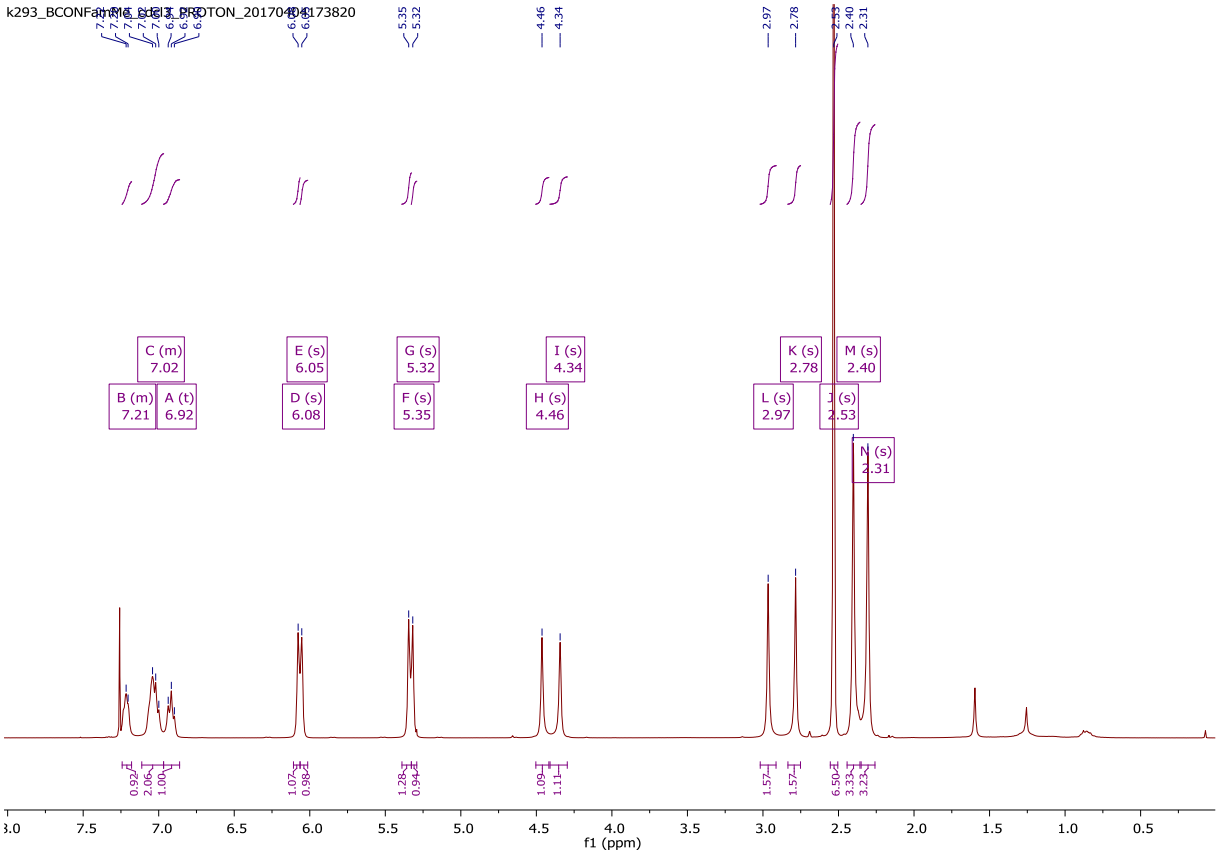

^{19}F NMR

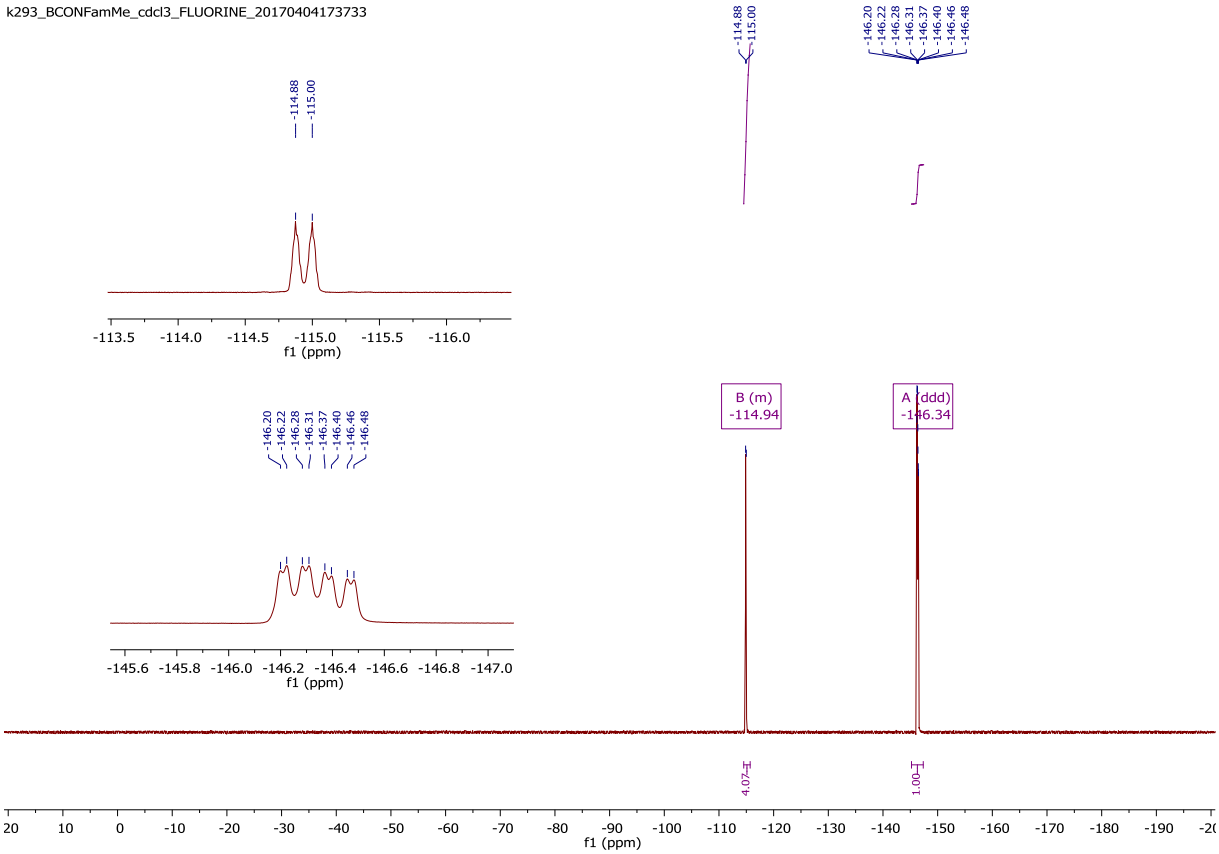

^{1}H COSY NMR

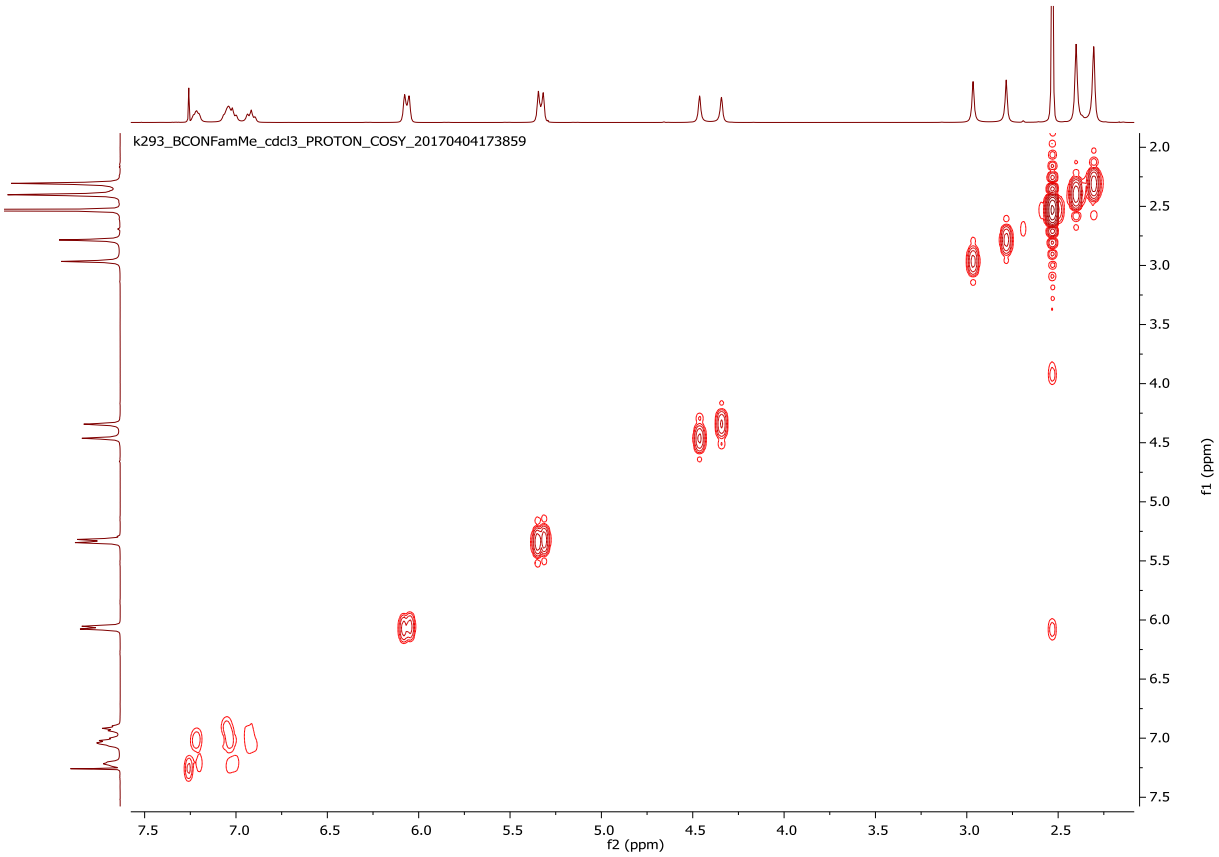

$^{1}H/^{13}C$ NMR ASAPHMQC

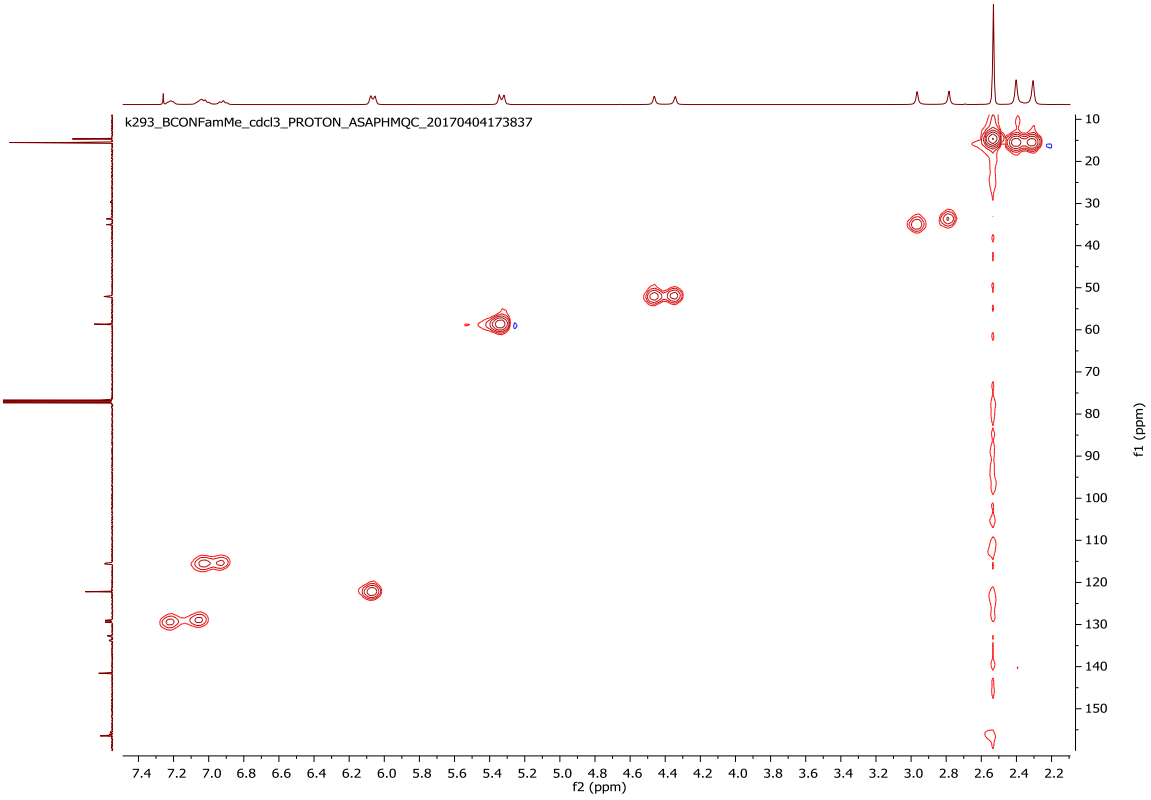

^{13}C NMR

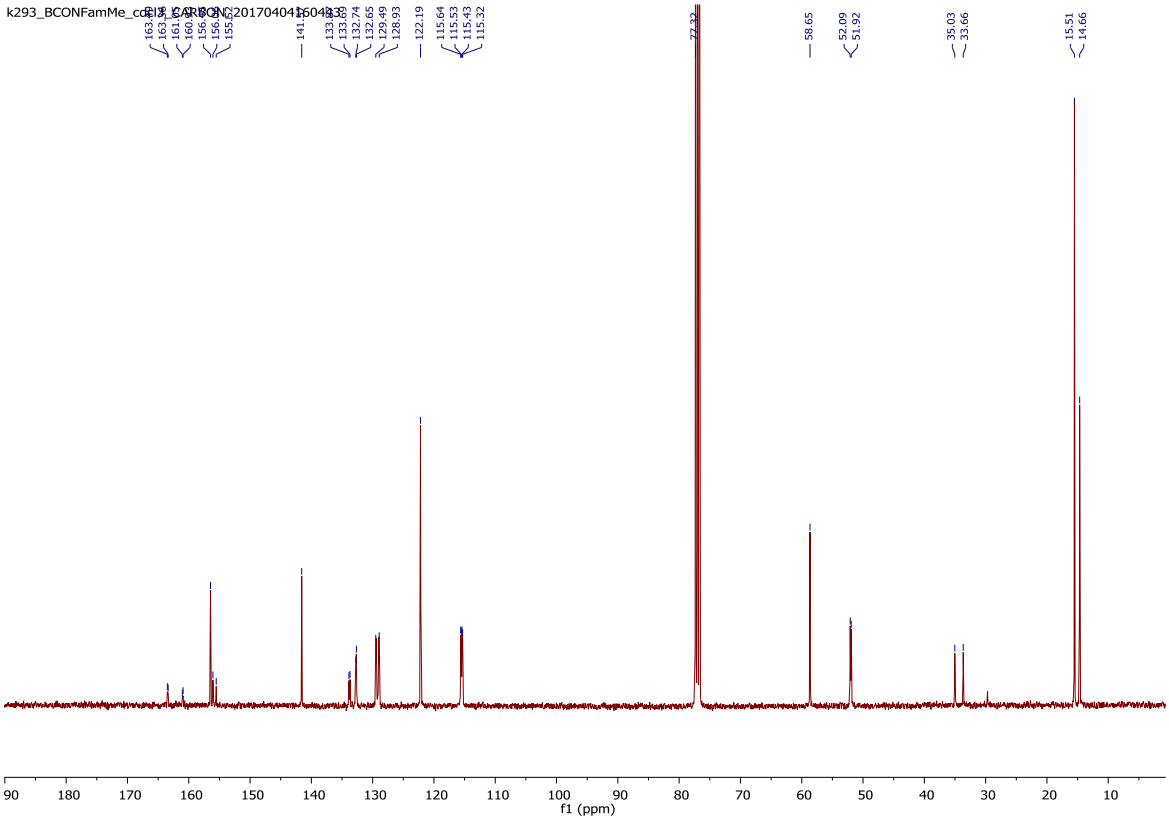

(2,8- dichloro-5,5-difluoro-1,3,7,9-tetramethyl-5H-4l4,5l4-dipyrrolo[1,2-c:2',1'-f][1,3,2]diazaborinin-10-yl)methyl (4-fluorobenzyl)(methyl)carbamate (**12**)

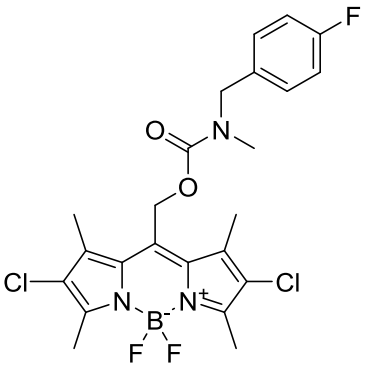

^{1}H NMR

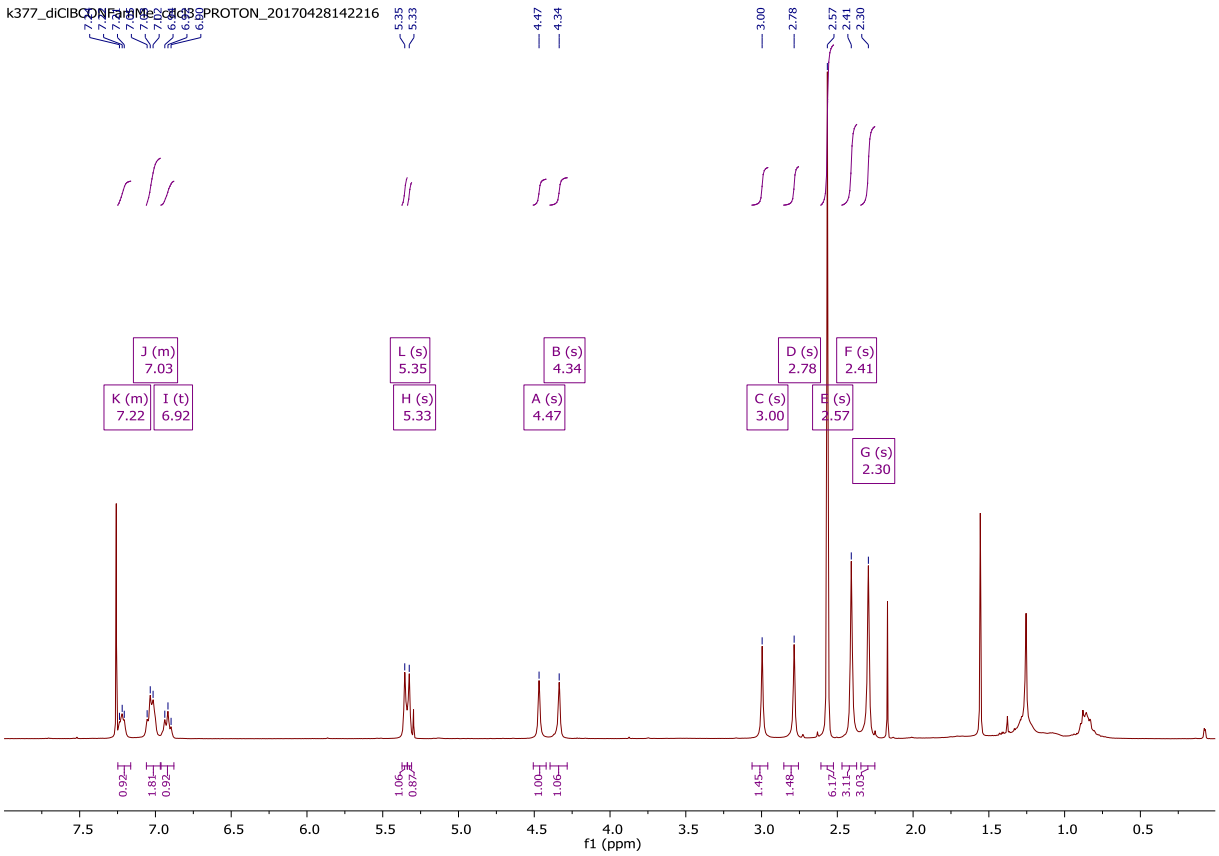

^{19}F NMR

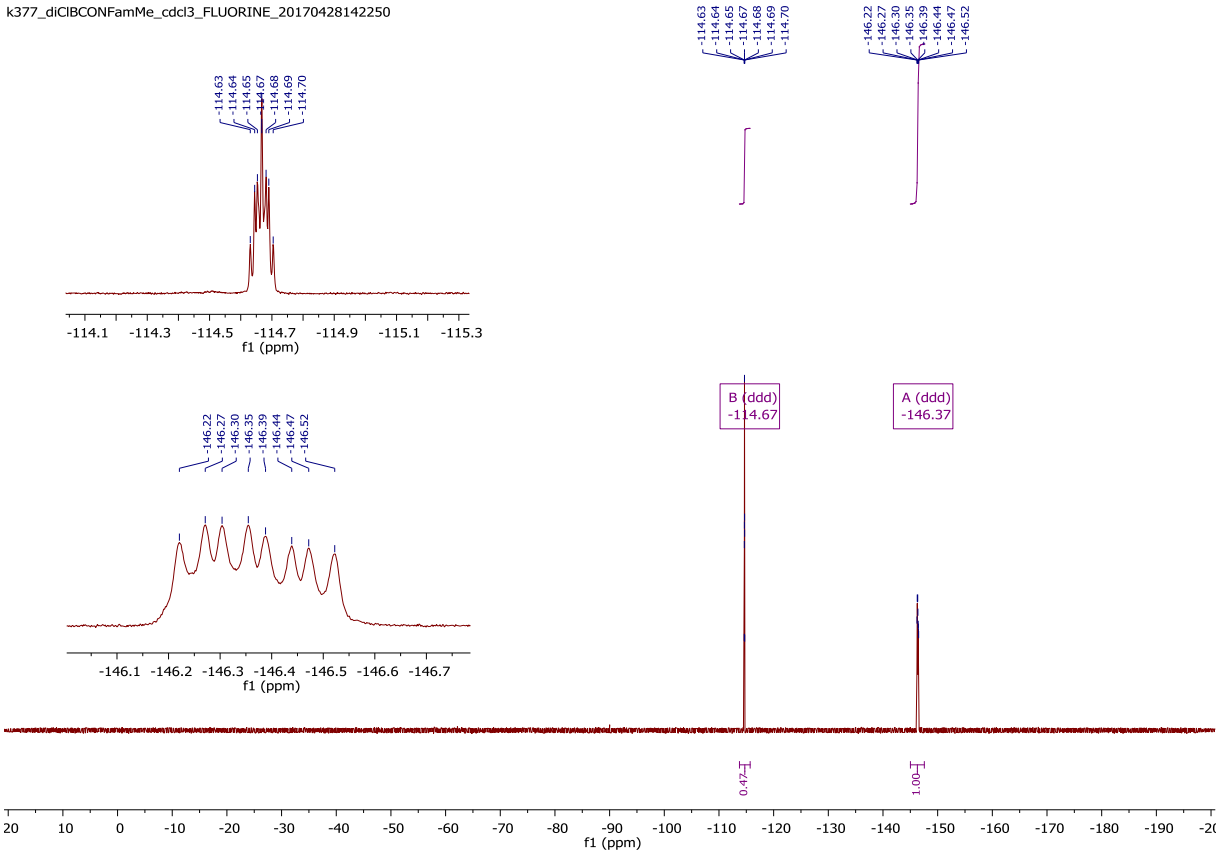

^{1}H COSY NMR

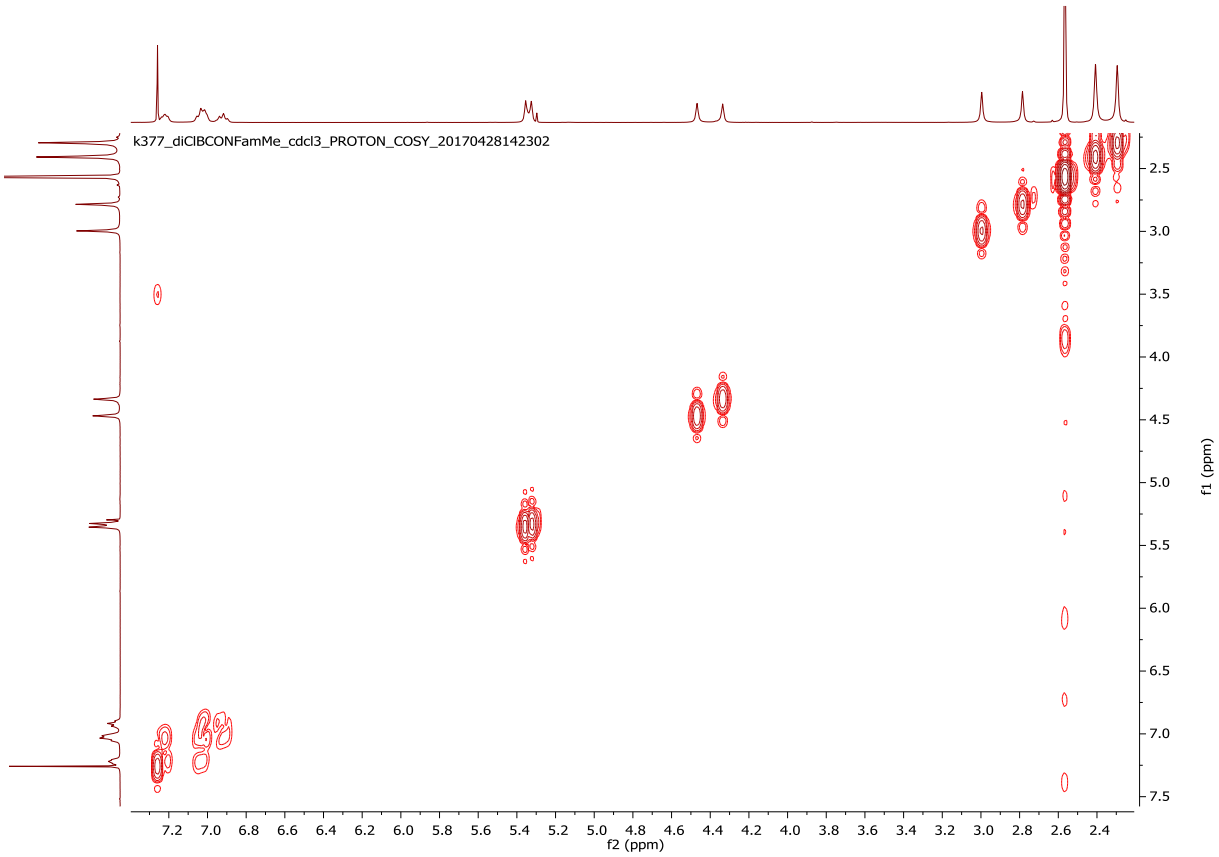

$^{1}H/^{13}C$ NMR ASAPHMQC

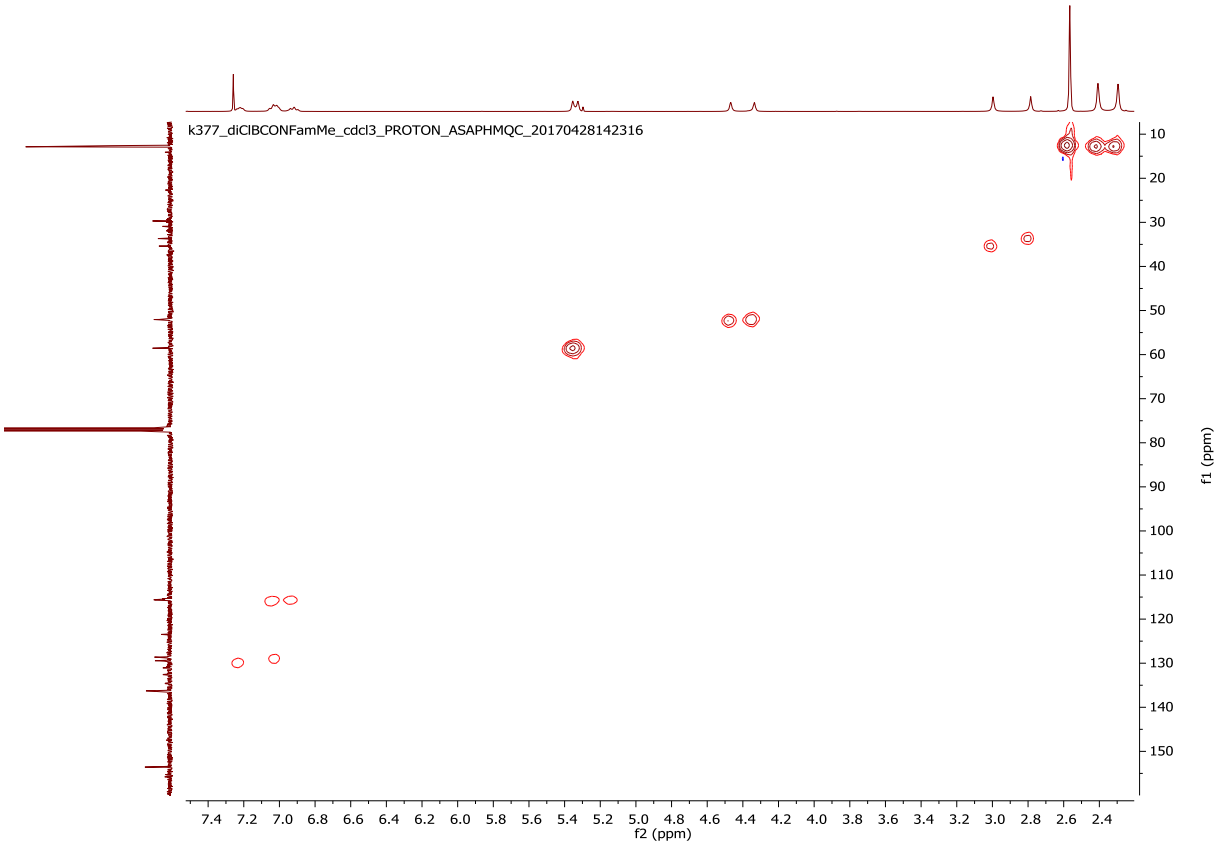

^{13}C NMR

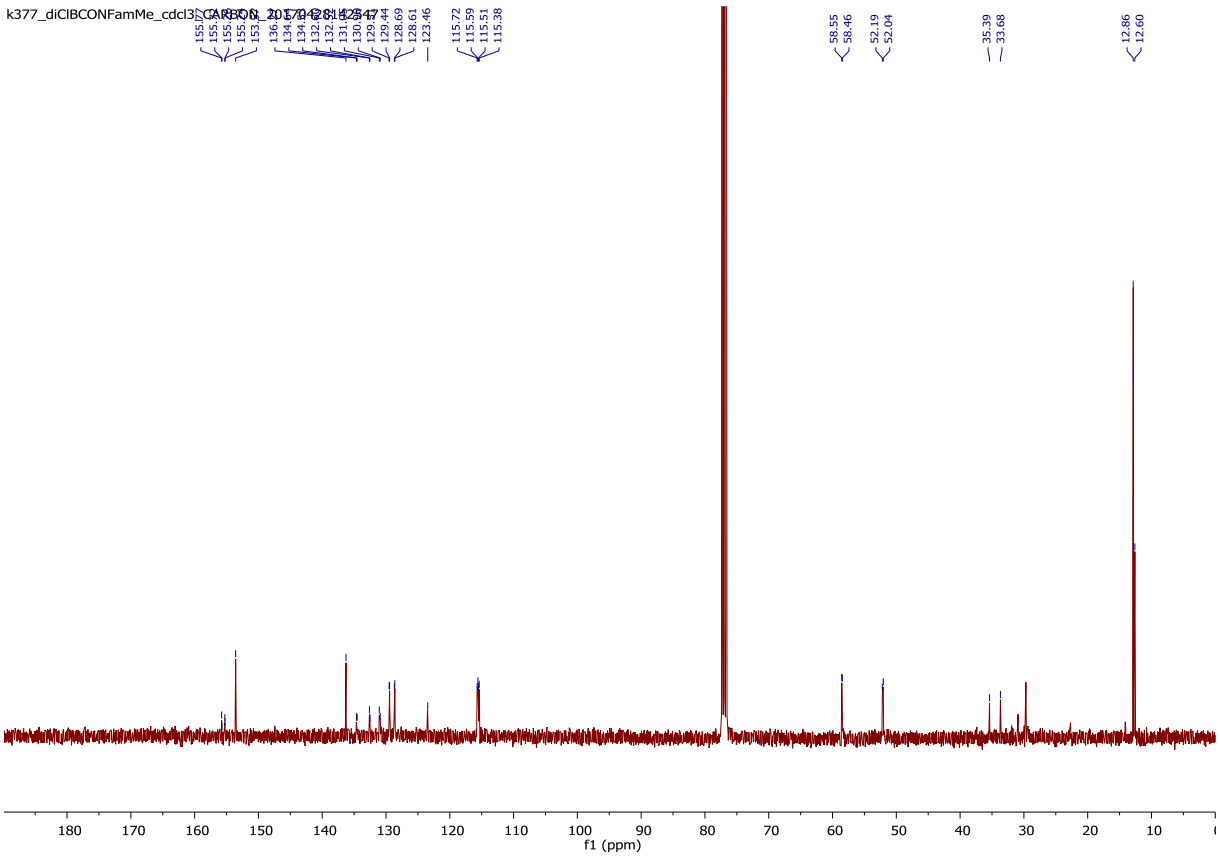

(2,8-dibromo-5,5-difluoro-1,3,7,9-tetramethyl-5H-4l4,5l4-dipyrrolo[1,2-c:2',1'-f][1,3,2]diazaborinin-10-yl)methyl (4-fluorobenzyl)(methyl)carbamate (**13**)

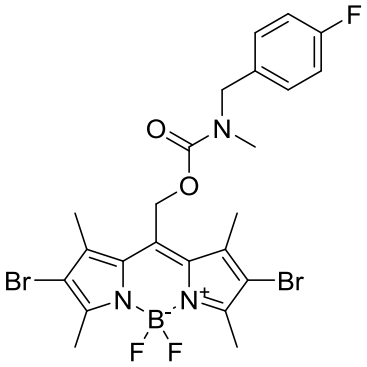

^{1}H NMR

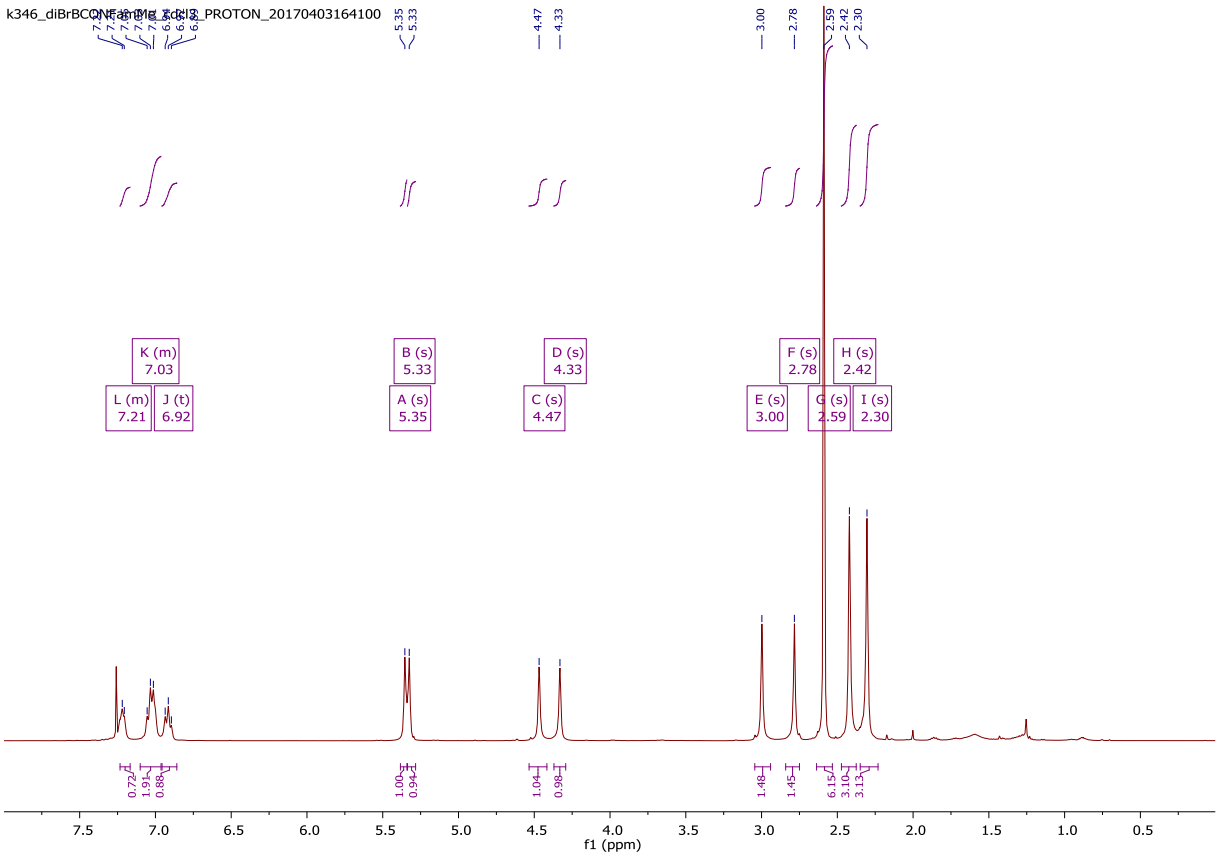

^{19}F NMR

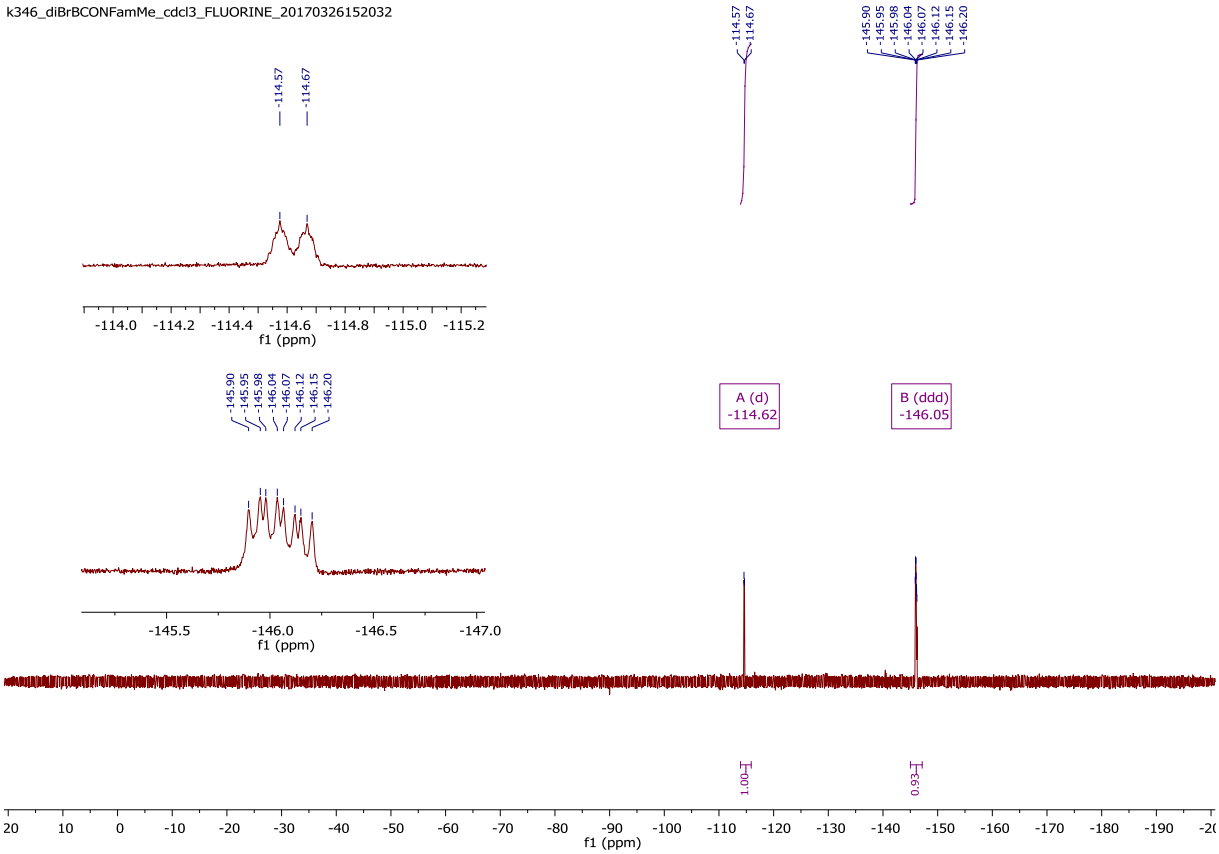

^{1}H COSY NMR

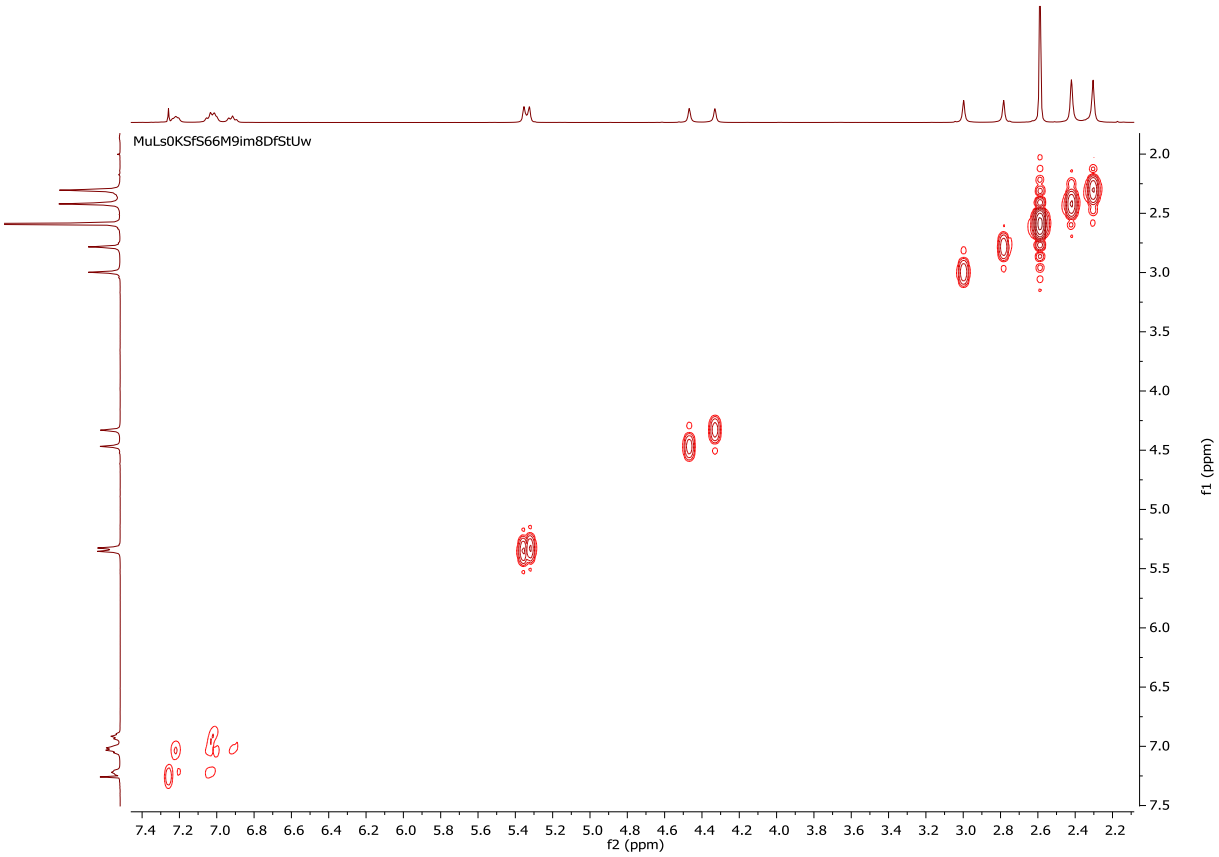

$^{1}H/^{13}C$ NMR ASAPHMQC

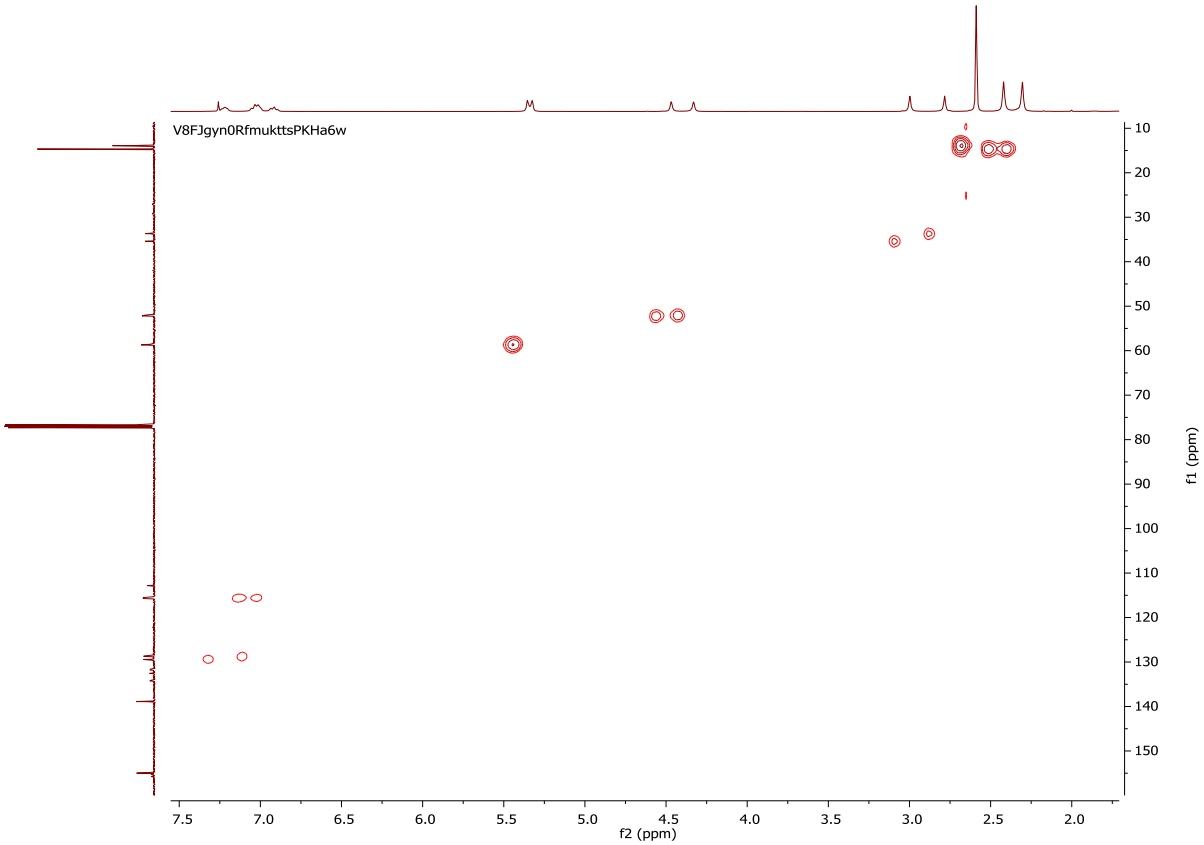

^{13}C NMR

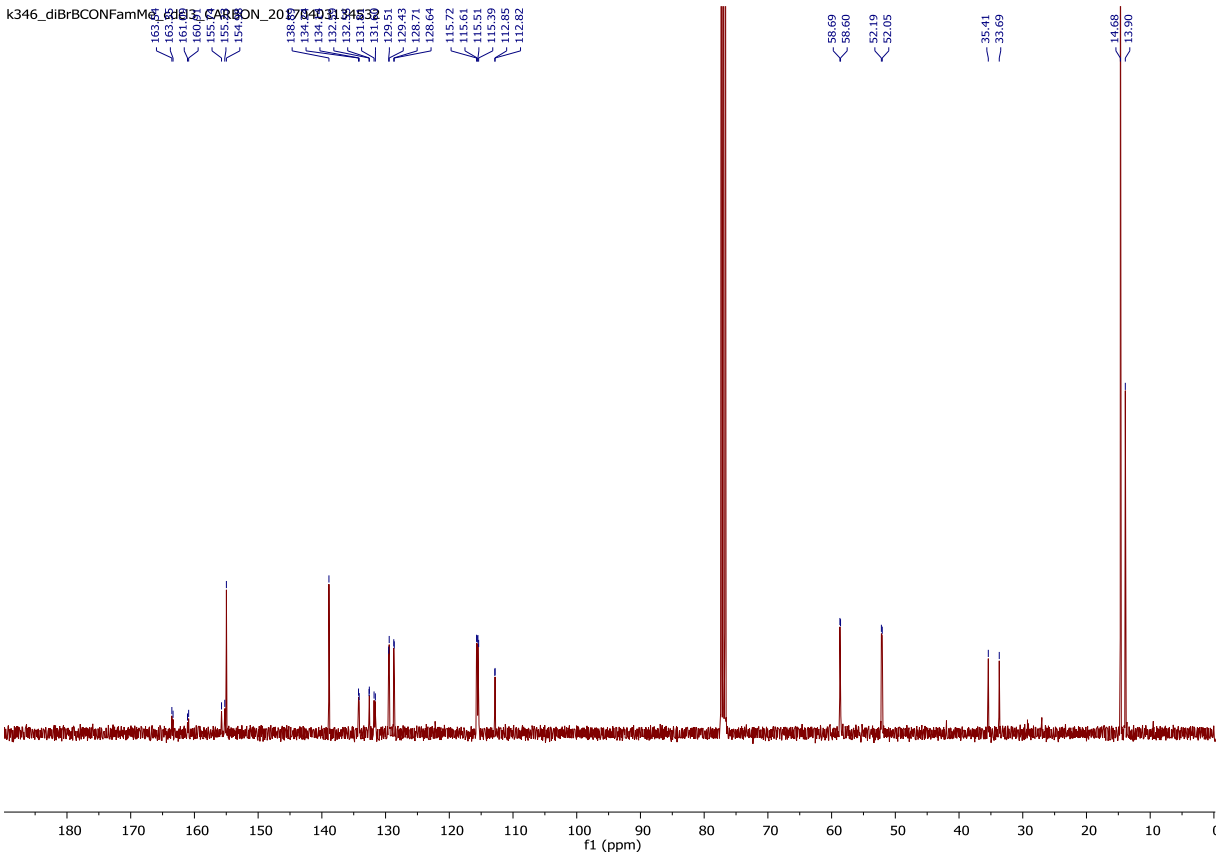

(2,8-diiodo-5,5-difluoro-1,3,7,9-tetramethyl-5H-4l4,5l4-dipyrrolo[1,2-c:2',1'-f][1,3,2]diazaborinin-10-yl)methyl (4-fluorobenzyl)(methyl)carbamate (**14**)

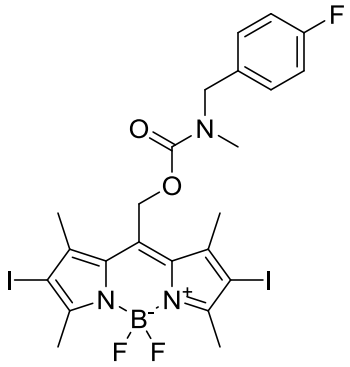

^{1}H NMR

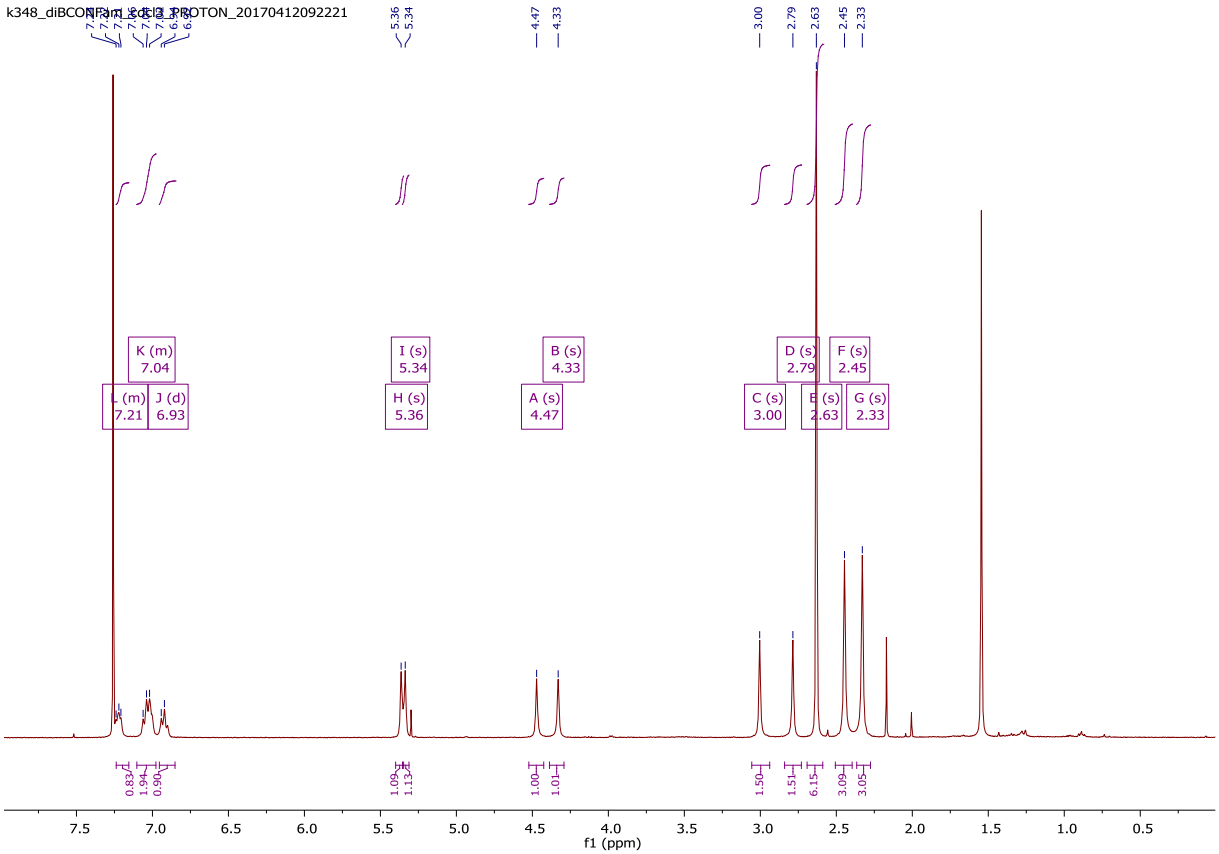

^{19}F NMR

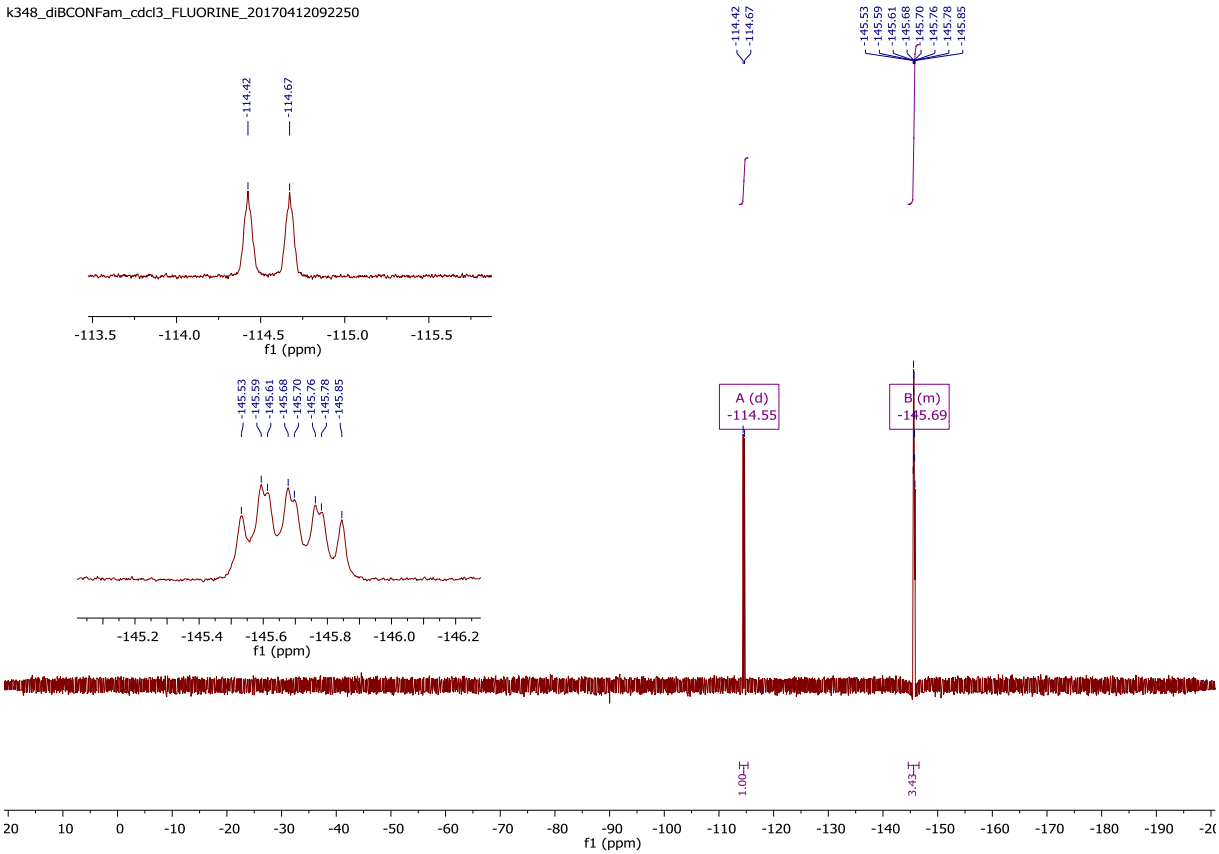

^{1}H COSY NMR

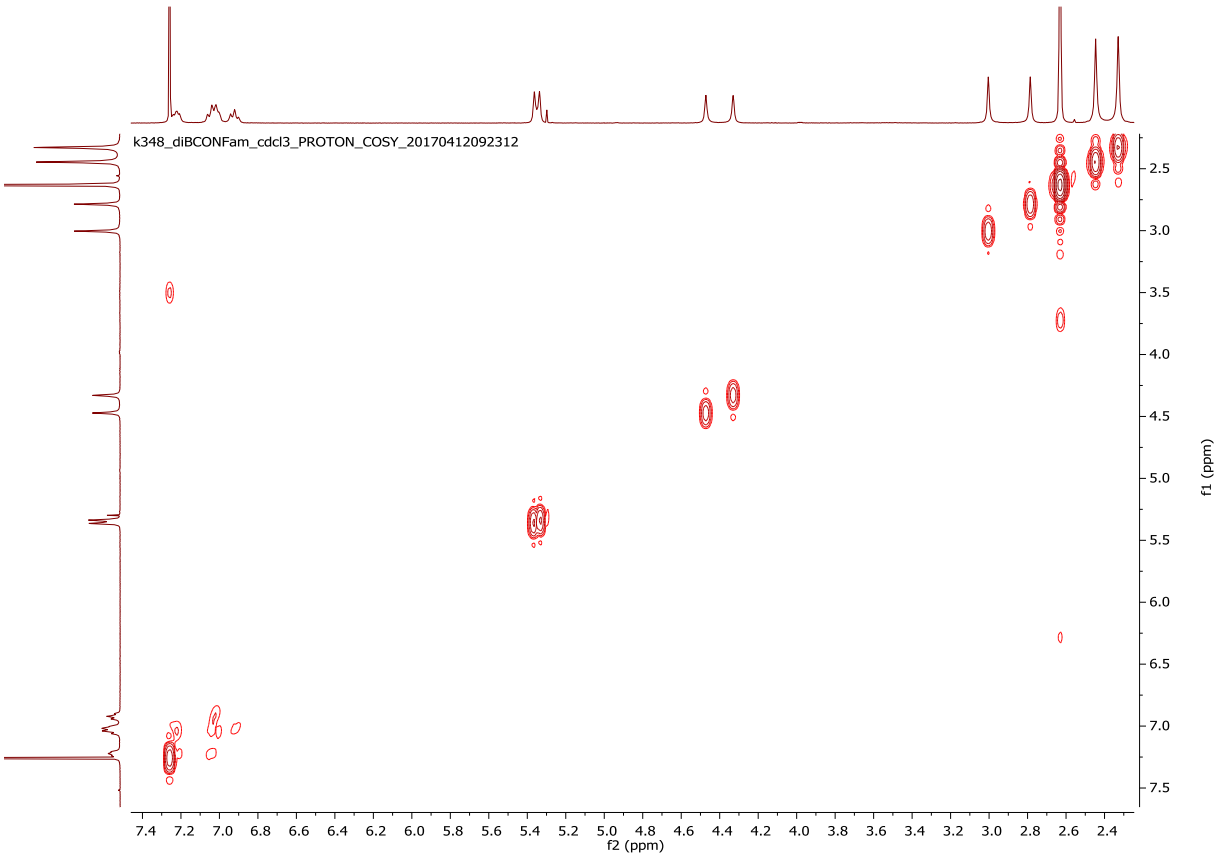

$^{1}H/^{13}C$ NMR ASAPHMQC

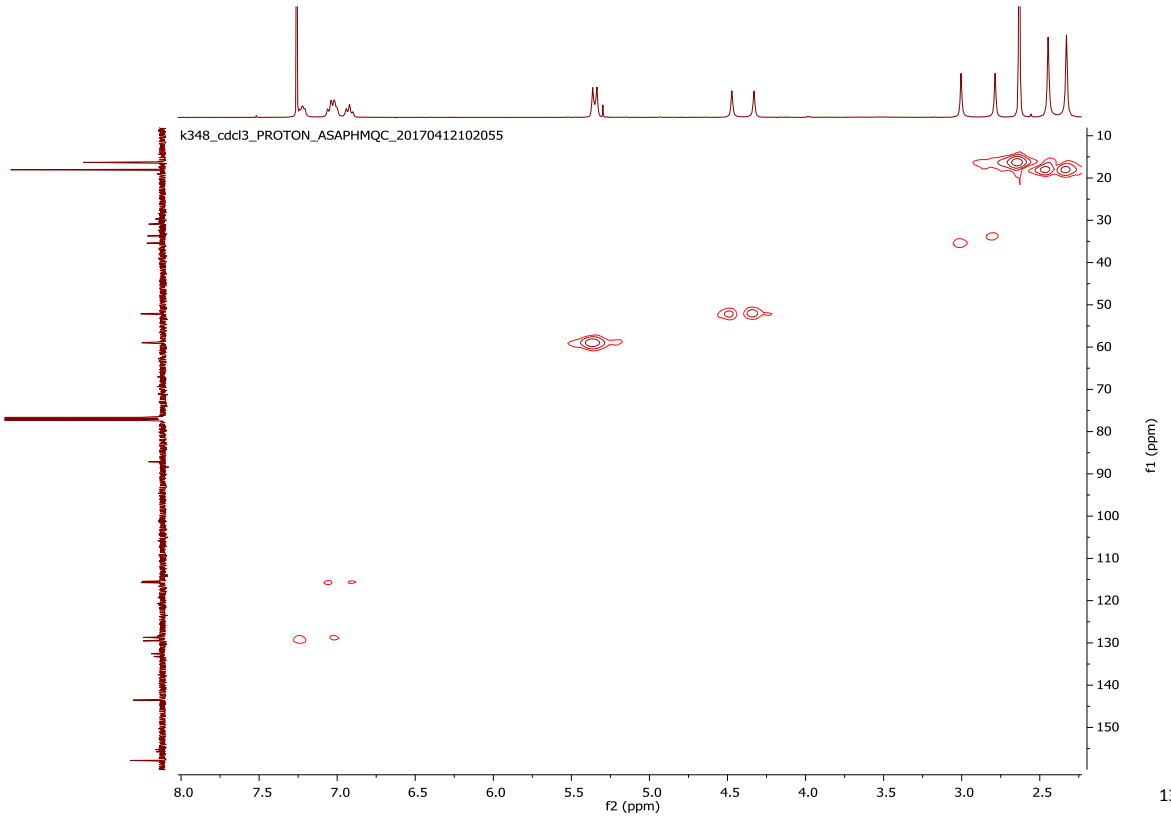

^{13}C NMR

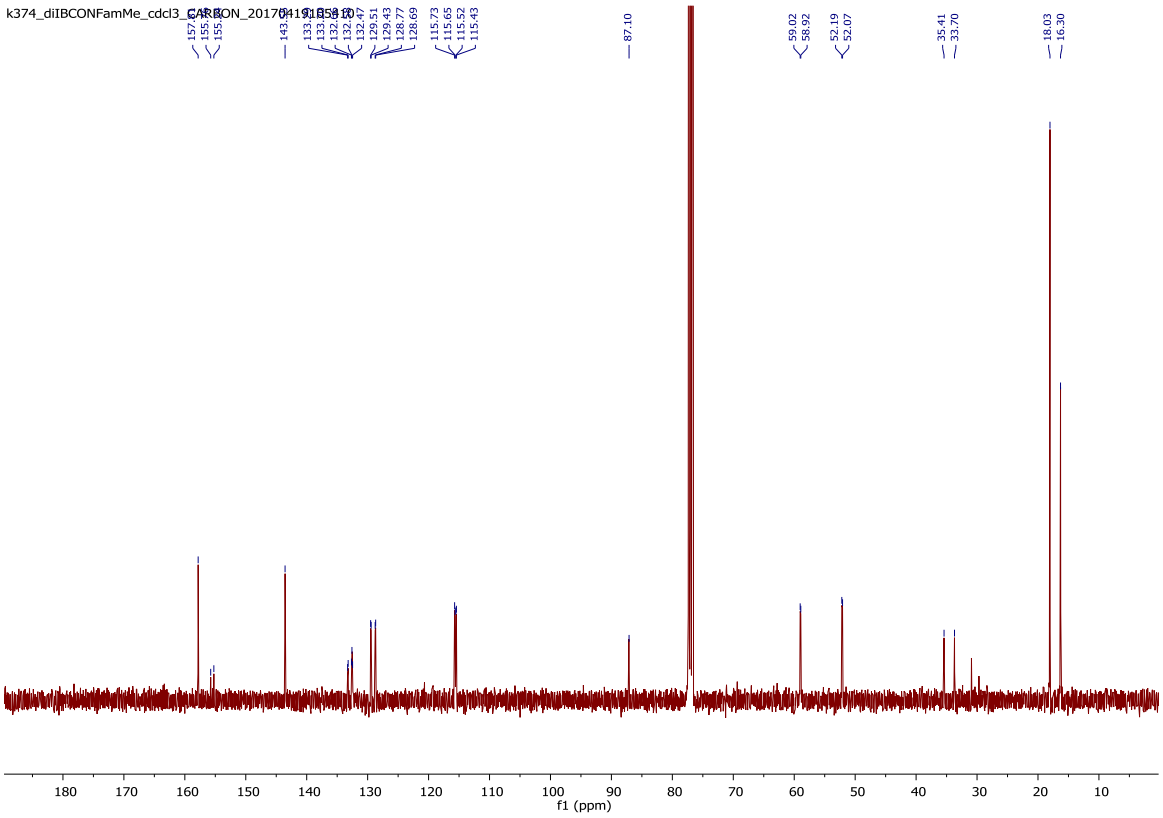

4. Quantum yields measurements

Chemical actinometry and quantum yield determination[1]

An aqueous 0.05 M H_2SO_4 solution containing 150 mM $K_3[Fe(C_2O_4)_3]$ (3 mL, 1 cm quartz cuvette), was irradiated at 20 °C for a given period of time in the dark with the respective wavelength. A volume of 20 µL was taken and diluted to 2.0 mL with an aqueous 0.5 M H_2SO_4 solution containing phenanthroline (1 g/L) and NaOAc (122.5 g/L). The absorption at λ = 517 nm was measured and compared to an identically prepared, non-irradiated sample. The concentration of $[Fe(phenanthroline)_3]^{2+}$ complex was calculated using its molar absorptivity ($\mathcal{E}$ = 11100 m^{-1} cm^{-1}).REF This concentration corresponded to the concentration of Fe^{2+} ions that had formed upon irradiation, divided by 100 (due to the dilution). The probabililty factor at = 527 nm was taken into account

[1] and the theoretical concentration of Fe^{2+} formed upon irradiation at all given time-points was calculated (probability factor = $1-10^{-Abs(527nm)}$). The Fe^{2+} ion concentration was plotted versus time and the following slope, obtained by linear fitting to the equation y = ax+b using Origin software, represents the rate of formation for the given wavelengths at standardized conditions. These rates can be converted in light doses by taking into account the quantum yield and area of irradiation which was 3 cm^2. Subsequently, the energy per moles of photons at a given wavelength ($E_{mole\ of\ photons} = N_A \times h \times \nu = N_A \times h \times c / \lambda$) is taken to convert the obtained values into J s^{-1} cm^{-2}.

Solutions of compounds **9** and **13** were irradiated with the Sahlmanns Photochemical Solutions 3xLXML PM01 high-power LEDs under identical standardized conditions as with the actinometry at concentrations high enough to absorb all incident light (absorbance at 530 nm ≥ 2). The absorbance decrease at λ = 560 nm for compound **9** and λ = 480 for compound **13** was monitored over time by UV-vis spectroscopy. The molar absorptivities λ_{max} [**9**, $\mathcal{E}_{max}$ = 19000 m^{-1} cm^{-1}; for **13**, $\mathcal{E}_{max}$ = 30000 m^{-1} cm^{-1}] were used to calculate the concentration decrease of compounds **9** and **13** respectively using the equation $\Delta c = \Delta abs/\mathcal{E}$. The initial concentration increase was plotted versus time and the slope, the rate of formation of *cis* isomer over time, was obtained by linear fitting to the equation y = ax+b using Origin software. The photochemical quantum yield for **9** and **13** were calculated by comparison of the rate of decomposition of these compounds with the rate of Fe^{2+} ion formation at identical conditions upon 527 nm irradiation from potassium ferrioxalate using the known quantum yield for the ferrioxalate at the given wavelength (ϕ= 0.53).

[2] Calculation of the quantum yield for the photorelease reaction at 527 nm can be performed following $\phi_r = \phi_{fer} \times \mathcal{E}_{BODIPY} \times [BODIPY]/(\mathcal{E}_{fer} \times [fer])$ equation.

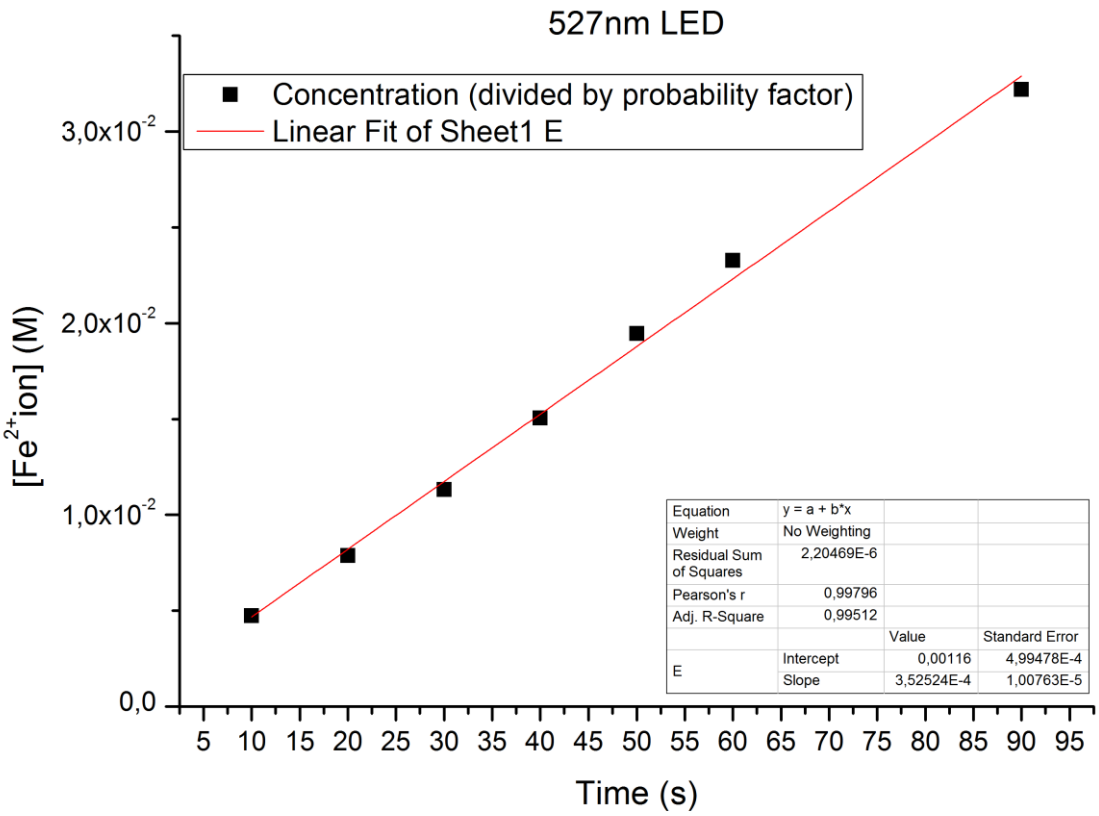

Fig. 33. Concentration of Fe^{2+} ions measured after seven different irradiation times (10, 20, 30, 40, 50, 60, 90 s) with 527 nm light. The slope of the plot corresponds to the rate of Fe^{2+} ion formation: 3.52×10^{-4} M s^{-1} ± 1.00×10^{-5} M s^{-1} = 1.05 x 10^{-6} mole s^{-1} ± 3 x 10^{-8} mole s^{-1}. Following ϕ(ferrioxalate at 527 nm)= 0.53 and the area of irradiation = 3 cm^2 and $E_{(\text{mole of photons at 527 nm})}$ = 2.27 x 10^5 this gives the light dose at 527 nm of 1.49 x 10^{-1} J s^{-1} cm^{-2}.

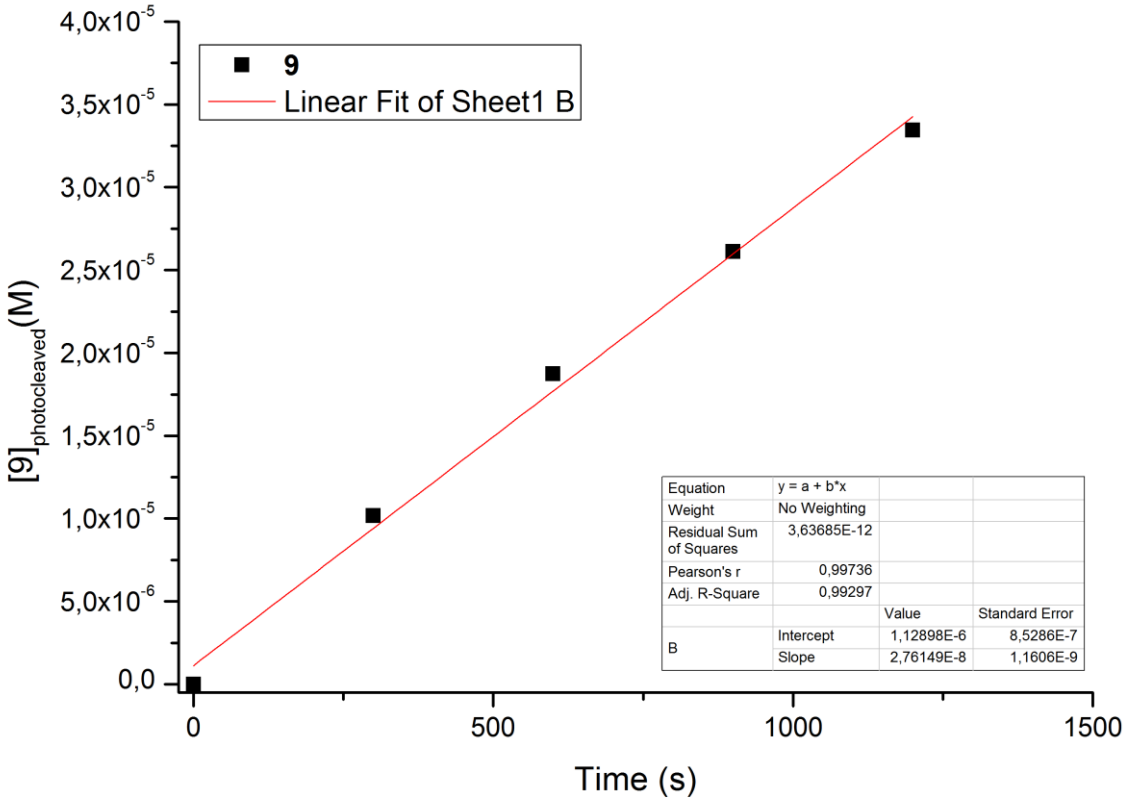

Fig. 34. Plot of the concentration of **9** as a function of time during λ_{max} = 527 nm irradiation of a solution of **9** in 20 % DMSO in phosphate buffer pH = 7.5 (c = 1.25 × 10^{-4} M, 1 cm quartz cuvette) obtained by monitoring the absorption decrease at λ = 560 nm. The slope of the plot corresponds to the compounds decomposition rate: 2.76 × 10^{-8} M s^{-1} ± 1.16 × 10^{-9} M s^{-1} = 5.52 x 10^{-10} mole s^{-1} ± 2.58 x 10^{-11} mole s^{-1}. Correlation of this rate to the rate of ferrioxalate consumption at these standardized conditions with 527 nm and the ferrioxalate quantum yield at the given wavelength gives a quantum yield of 4.2 x 10^{-5}.

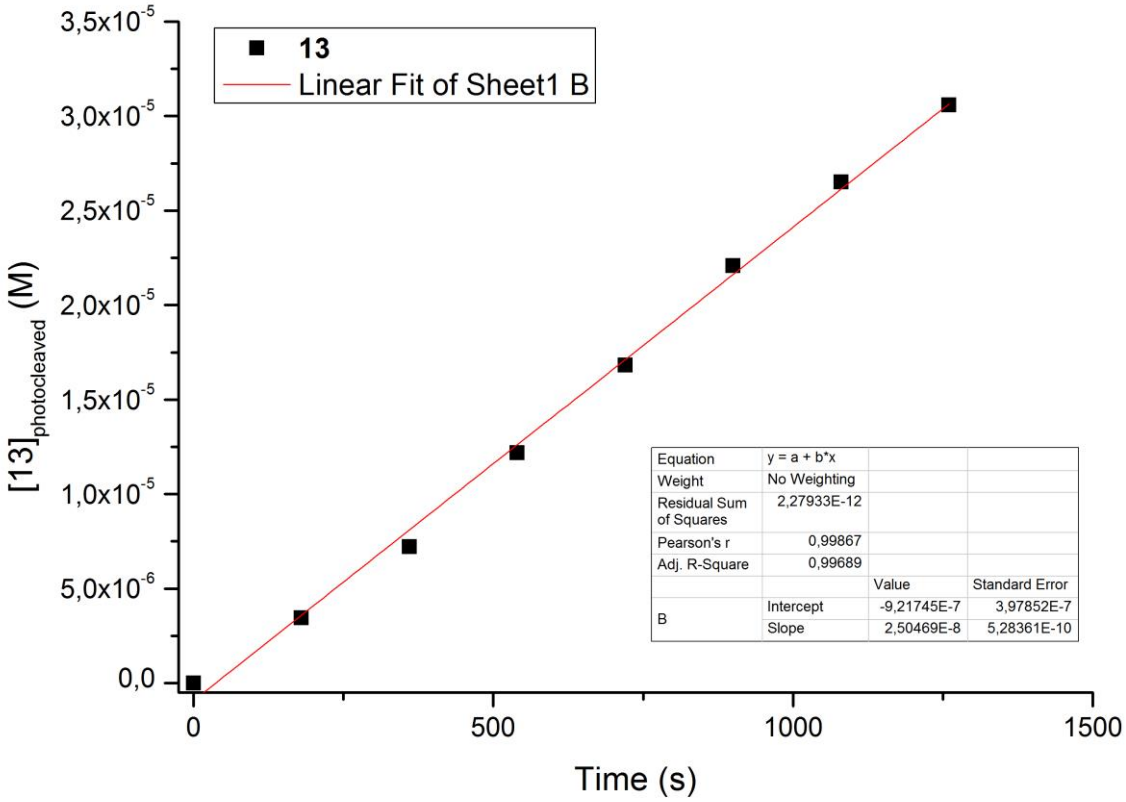

Fig. 35. Plot of the concentration of **13** as a function of time during λ_{max} = 527 nm irradiation of a solution of **13** in 20 % DMSO in phosphate buffer pH = 7.5 (c = 1.25 × 10^{-4} M, 1 cm quartz cuvette) obtained by monitoring the absorption decrease at λ = 480 nm. The slope of the plot corresponds to the compounds decomposition rate: 2.50 × 10^{-8} M s^{-1} ± 5.28 × 10^{-10} M s^{-1} = 5.00 x 10^{-10} mole s^{-1} ± 1.06 x 10^{-11} mole s^{-1}. Correlation of this rate to the rate of ferrioxalate consumption at these standardized conditions with 527 nm and the ferrioxalate quantum yield at the given wavelength gives a quantum yield of 3.8 x 10^{-5}.

5. 19F NMR of crude carbamate formation reaction mixtures

Compound **8** with side product (see manuscript, Scheme 1, final reaction)

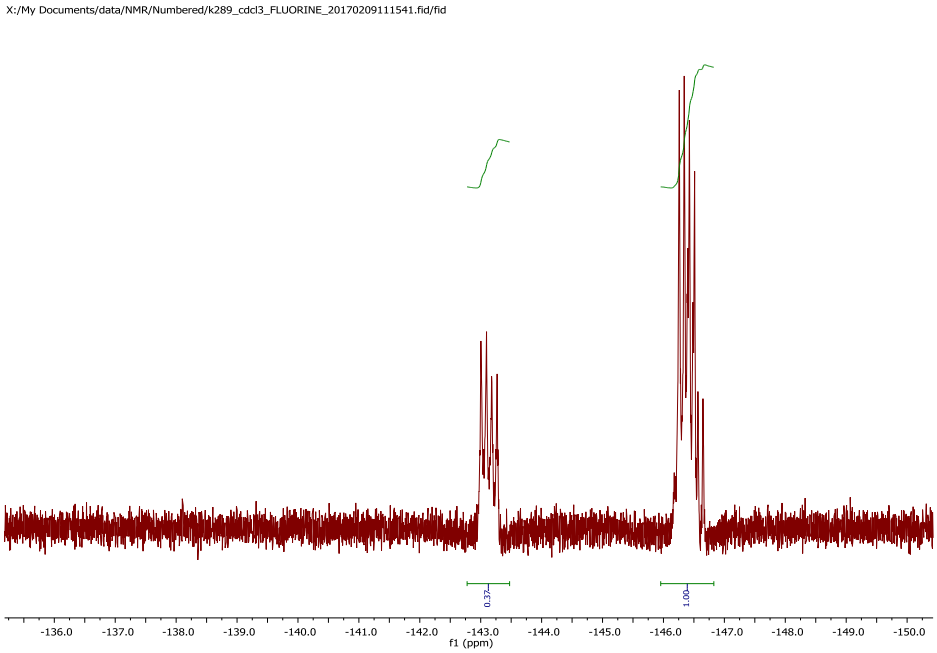

Compound **13** with side product (see manuscript, Scheme 1, final reaction)

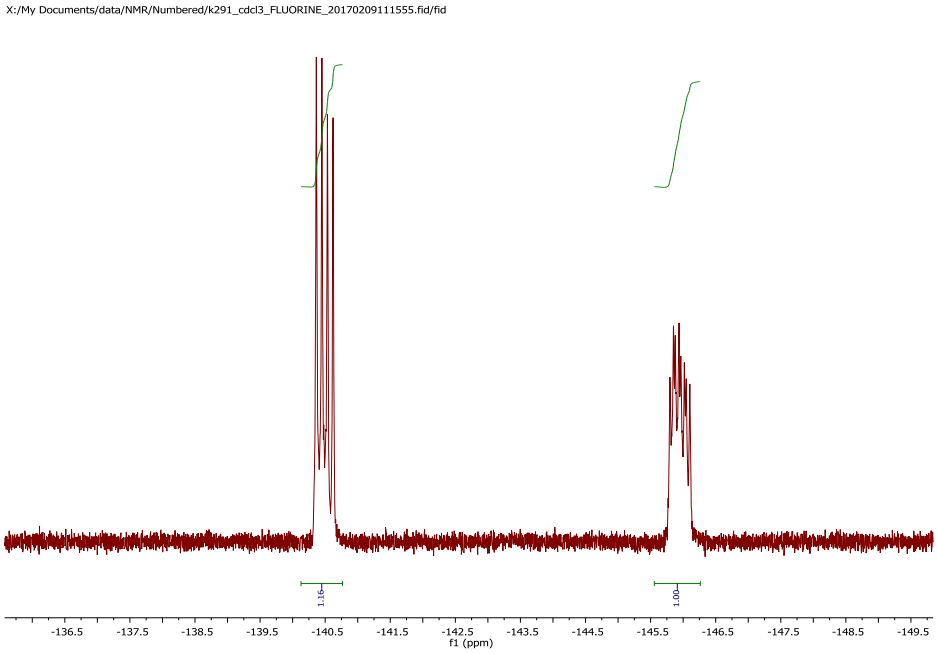

6. Characterization of side product **15**

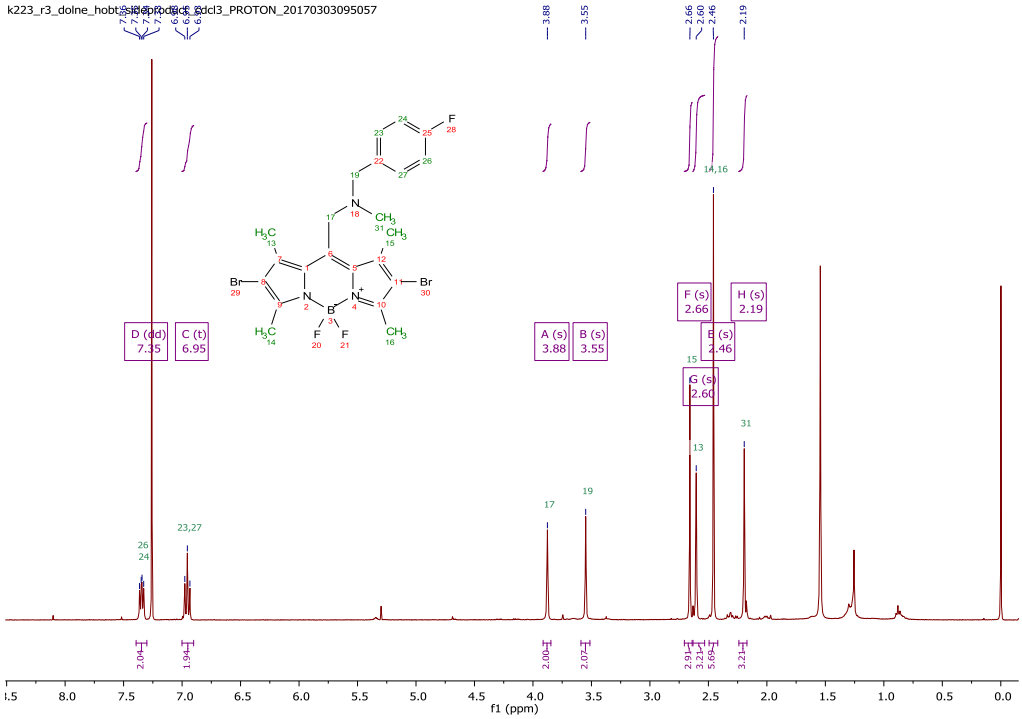

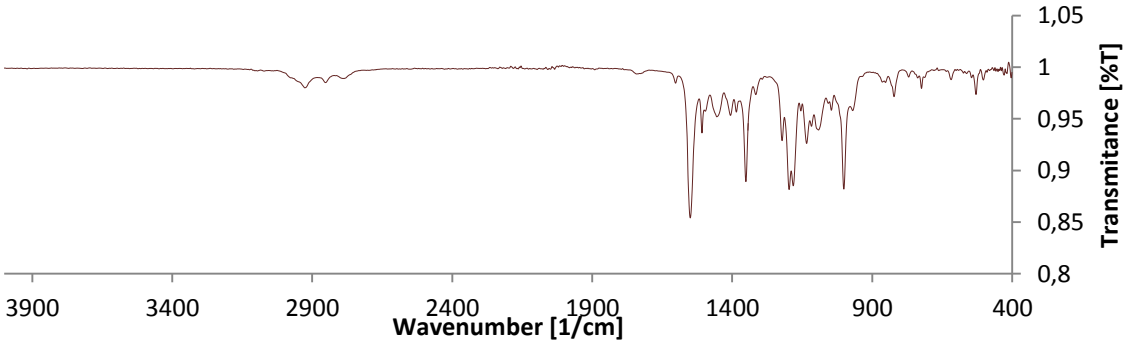

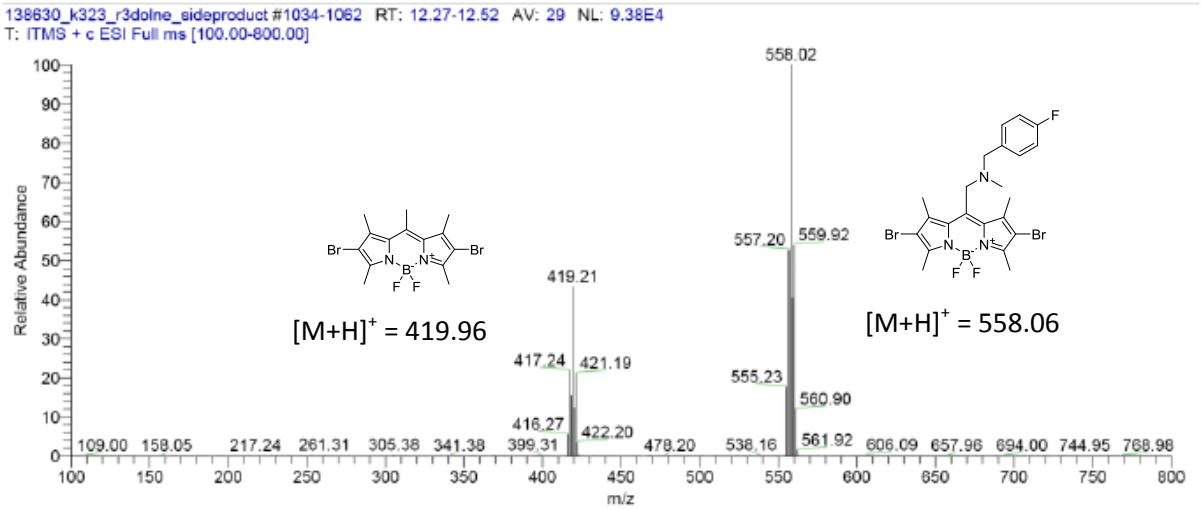

7. LED light source specification

Sahlmann Photochemical Solutions

LED light source 3x 530 nm

LED type: 3x LXML PM01
rank: 0100
typ. optical power: 810 mW

emission characteristics:
spectrometer: Ocean Optics USB 4000
peak wavelenght: 526 nm
FWHM: 35.1 nm

spectral distribution:

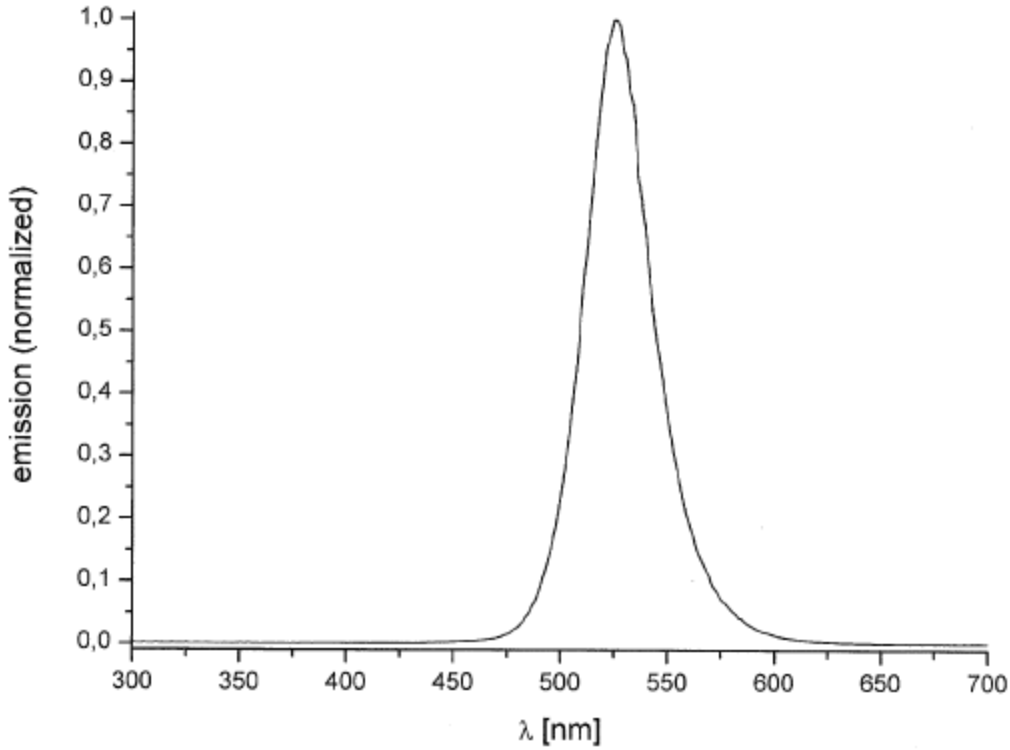

8. References

[1] Hopkins, S. L.; Siewert, B.; Askes, S. H. C.; Veldhuizen, P.; Zwier, R.; Hegerc, M.; Bonnet, S.; *Photochem. Photobiol. Sci.*, **2016**, *15*, 644-653

[2] a) Hatchard, C. G.; Parker, C. A.; *Proc. R Soc. Lond. A Math. Phys. Eng. Sci.,* **1956**, *235*, 518–536. b) Montalti, M.; Credi, A; Prodi, L.; Gandolfi, M.T.; Handbook of Photochemistry, Third Edition, (CRC Press, 2006).